UNIVERSITÀ DI PARMA

UNIVERSITA' DEGLI STUDI DI PARMA

DOTTORATO DI RICERCA IN SCIENZA E TECNOLOGIA DEI MATERIALI

CICLO XXXIII

FUNCTIONALIZED BIOMIMETIC HYBRID SCAFFOLDS FOR BONE TISSUE REGENERATION AND PREVENCTION OF INFECTIOUS DESEASES

Coordinatore:
Chiar.mo Prof. Enrico DalCanale

Tutore:
Dott.ssa Monica Sandri

Co-Tutori:
Dott.ssa Elisabetta Campodoni

Dott.ssa Marisela Vélez

Dottorando: Mulazzi Manuela

Anni 2017/2020

"...ο δὲ ανεξέταστος βίος ου βιωτός ανθρώπω"

Da "Apologia di Socrate" parte V capitolo XXVIII, 38a

THE AIM

During these three years, the aim of my PhD thesis was focused on the study of functionalization processes, performed on hybrid scaffolds for bone tissue regeneration and aimed to develop new devices useful to face new important challenges. Different methods were applied such as physical absorption through soaking technique of pharmaceutical molecules and chemical linking by the use of covalent bond formation with biomimetic molecules.

The hybrid scaffolds consist in magnesium doped hydroxyapatite nucleated on type I collagen fibers (MgHA/Coll) obtained by means of a nature-inspired biomineralization process, suitable to recreate hybrid materials very similar with natural bone and excellent candidates for bone regeneration due to their biomimicry of extracellular matrix and biocompatibility.

Through this synthesis, 3D porous bioceramic scaffolds are possible to obtain, providing, after *in vivo* implantation, the suitable microenvironment to generate a smart host tissue-biomaterial interface capable of triggering favourable biochemical events that positively influence the cellular response and promote bone tissue regeneration.

In particular, the research activity was focused on the study of the interaction between hybrid scaffold and different active molecules in order to obtain medicated scaffolds exploit them in different applications such as local therapies for osteomyelitis and osteosarcomas, as well as for the creation of a 3D cancer model.

Firstly, hybrid scaffolds were functionalized with antibiotics in order to prevent or reduce osteomyelitis and simultaneously regenerate bone damage tissue.

Infected bone defects are normally intractable and considered a huge issue for bone grafting. The development of medicated osteoinductive bone substitutes to control

in situ drug release would be an ideal approach to simultaneously eradicate or prevent infections, and repair bone defects.

The challenge is to modulate local antibiotics release suitable to reduce systemic dosing and thereby effectively decrease any systemic toxicity.

An antibacterial bone graft was designed by loading different antibiotics in MgHA/Coll scaffold. Vancomycin and gentamicin were considered for testing since their large spectra against Gram-positive and negative bacteria.

Medicated hybrid scaffolds, different for the amounts of MgHA (from 0 to 70 wt%), were prepared by loading gentamicin and vancomycin through a simple soaking method selected because easy to be reproduce in surgery room just before implant, in order to evaluate the drug interaction with the scaffold and how the release kinetics change by diversifying the amount of the mineral component. UV spectroscopy was used to examine the delivery profile of Vancomycin and Gentamicin released from the scaffolds and Kirby-Bauer disc diffusion method to assess the antimicrobial activity of drugs post-releasing.

Finally, was developed a method to create a coupling between MgHA/Coll scaffold and Alginate polymer, selected as mimetic of hyaluronic acid, exploiting the typical oxidation of carbohydrates with periodate. I performed this activity in collaboration with ICP-CSIC (Institute of Catalysis and Petrochemistry of Madrid, Dr Marisela Velèz) and CIALS-CSIC (Institute of Food Science Research, Dr Oswaldo Hernandez)

The need of innovative mimetic biomaterials, suitable to promote bone tissue regeneration, is strongly increasing due to the raising of bone pathologies related to life styles and the progressive aging population.

The challenge leads to better mimic the chemistry of tumor bone niche and obtain a 3D system enable the design of an *in vitro* cancer model for the prediction of new and targeted cancer therapy. Nowadays 3D cell culture models are becoming increasingly important for the study of cancer biology because these models recapitulate developmental dynamics and tumor progression observed *in vivo*, better than standard monolayer cultures. Moreover, those *in vivo* models are important for the achievement of novel and targeted cancer therapies.

CHAPTER 1

1. INTRODUCTION

Tissue engineering involves in the recreation of tissue and organs by developing biological substitutes that restore, maintain or improve tissue features.

Materials must have complex and smart characteristics in order to interact with cells and initiate the biological response. In tissue engineering we have three important tools: the cell, the scaffold and the growth factor. The scaffold is considered the environment in which cells can proliferate. Thereby, the cells synthesize matrices of new tissue and promote the regeneration, assisted by growth factors.[1]

In these years, tissue engineering holds the promise of revolutionizing healthcare by providing artificially developed biological substitutes on demand (tissues and organs), that can be employed in the regenerative medicine through the design of innovative 3D biomaterial. [2-3] The designed biological substitute supplies to cells the suitable microenvironment for regenerative processes, supporting cell attachment, proliferation, differentiation, and neo tissue genesis.[4-5-6]

Different parameters have to be considered for the development of a device suitable for tissue engineering such as chemical composition, physical structure and biologically functional moieties playing an important role in the control of the new tissue formation. [7]

For instance, the porosity supports cell proliferation because an adequate pores size and interconnection promote cell growth and proliferation, as well as the permeation of nutrients and oxygen from the surface towards the core of the

scaffold and the elimination of CO_2 and other metabolites from the core towards the surface.[8]

Furthermore, materials used for the development of the devices must be biocompatible, non-toxic and bioresorbable with a rate of bio-resorption and degradation compatible with the neo bio-tissue formation. Besides, the mechanical properties must be comparable with the natural tissue to favor the correct integration with the surrounding tissue. A substitute endowed with the suitable stiffness (evaluated by stress-strain curves) is able to avoid its damage and to slow down the degradation process favoring the integration with the surrounding tissue.[9-10]

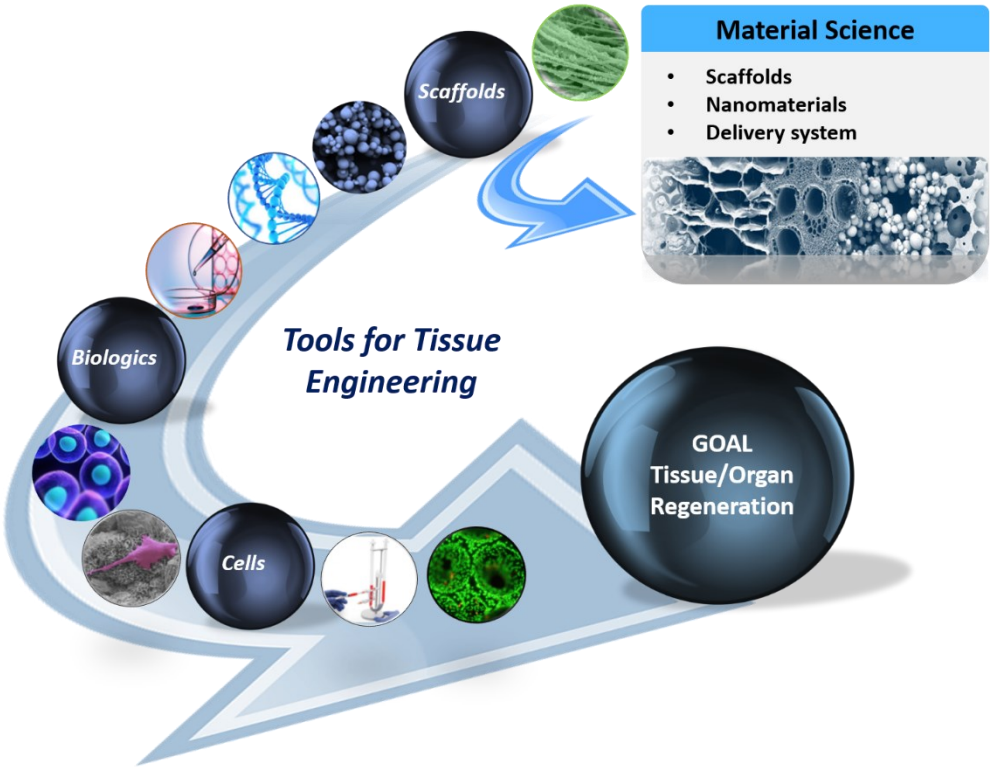

Figure 1.1 *Schematization of the tools involved in tissue engineering: starting from scaffold and through biologicals and cells, to achieve the goal of tissue and organ regeneration.*

Nowadays, tissue engineering advanced in strategies to progress the technology including bio-inspired modeling of human diseases, novel drug screening tools, micro-tissue engineering and biomarker identification with predictive and therapeutic action.

In this research thesis were designed and developed two different devices based on a synthetic hybrid biomimetic scaffold reproducing the whole features of bone tissue.

The first is a medicated osteoinductive and bioresorbable bone scaffold, designed with the aim to perform local and controlled administration of antibiotic drugs to eradicate or prevent infections during surgery or anticancer drugs to treat osteosarcoma. This research was motivated by the challenge of obtaining an effective administrating system that can sustain a local drug release for the reduction of the systemic dosage and thereby the effective decrease of the side effects due to drugs toxicity.

The second is a hybrid bone scaffold functionalized with oxidized alginate to better mimic the chemistry of tumor bone niche and obtain a 3D system enable the design of an in vitro cancer model for the prediction of new and targeted cancer therapy.

1.1 Bone Tissue

Bone is a biological tissue characterized by a remarkable hardness and resistance. The bone tissue forms the vertebrate skeleton and together with muscles, supports the body, protects the vital organs and allows the movement. Bone structure consists in a compact external part and an internal one with the characteristic

trabecular structure, able to endure very high tensions. It is a particular type of supporting connective tissue, consisting of cells dispersed in a hybrid extracellular matrix. Natural bone matrix is a typical example of organic/inorganic hybrid material constituted from the 30 wt% of organic phases, collagen fibers and amorphous substances of glycoproteic origin, and the 70wt% of a mineral apatitic phase. This hybrid material presents at the same time characteristics of strength and toughness, that are not possible to reach with individual components.[11]

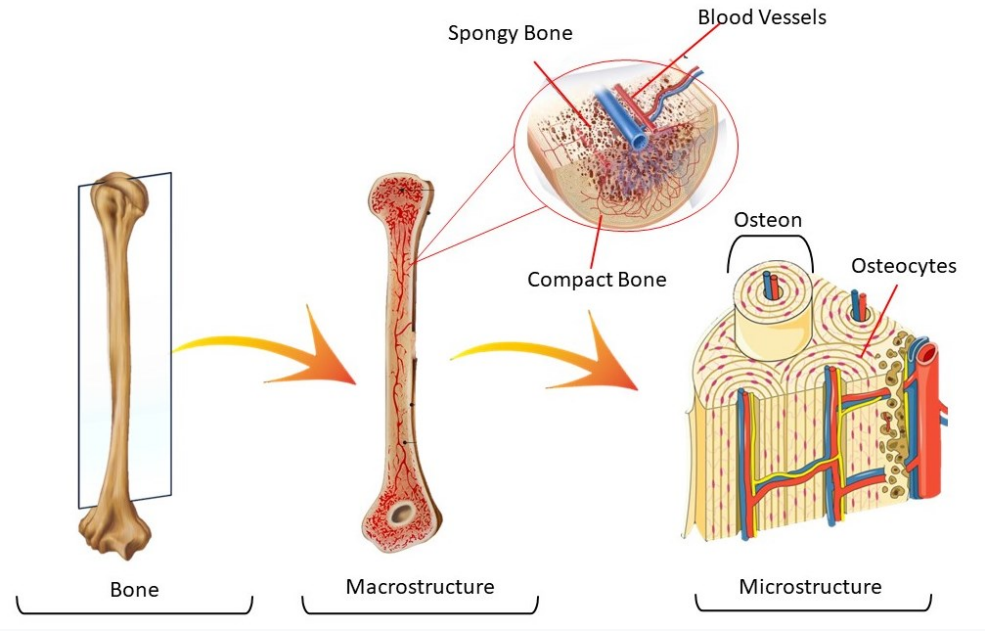

Figure 1.2 *Complex Structure of bone tissue: In macrostructure it's possible to observe the vascularization and the porosity of the spongy bone tissue. In microstructure the populations of bone cells, osteocytes, and osteon, formed by collagen fibers.*

The main extracellular protein is collagen, which have a fibrous structure with diameters on the nanometer or sub-micrometer scales. Collagen, the main structural protein in the extracellular space in the various connective tissues, is a fibrous structural protein with fiber bundle diameter varying from 50 to 500 nm.[12-

13-14-15) It is composed of amino acids wound together to form triple-helices, which form elongated fibrils. There are 10 different types of Collagen in animal body (Table 1.1); all of them own triple-helix, but they have different length of helix and no-helicoid portions; in the human body the 90% of the collagen is type I, present in tendon and bone tissues.(16)

Type	Class	Distribution
I	Fibrillar	Dermis, bone, tendon
II	Fibrillar	Cartilage, vitreous
III	Fibrillar	Blood vessels
IV	Network	Basement membranes
V	Fibrillar	Dermis, bone, tendon
VI	Filaments, 100 nm	Dermis, bone, tendon
VII	Fibers with antiparallel dimers	Dermis, bladder
VIII	Hexagonal matrix	Membrane
IX	Fibrils-associated collagens with interrupted triple helices	Cartilage, vitreous
X	Hexagonal matrix	Cartilage
XI	Fibrillar	Cartilage
XII	Fibril-associated collagens with interrupted triple helices	Tendon

Table 1.1 *List of different Collagen type and their distribution.*

Collagen molecule consists in three polypeptides chains arranged in a helix, where the Gly-X-Y amino acidic unit are repeated and in X and Y often are present proline and hydroxyproline, that confer stiffness at the molecule. Aminoacids are linked through peptide bond, involving the amino and carboxylic functional groups. This

kind of bond constrains the mobility of the chain and thanks to inter-chain hydrogen bonds and other interactions between residues confer stability to the α-helix collagen structure (Fig. 1.3).[17]

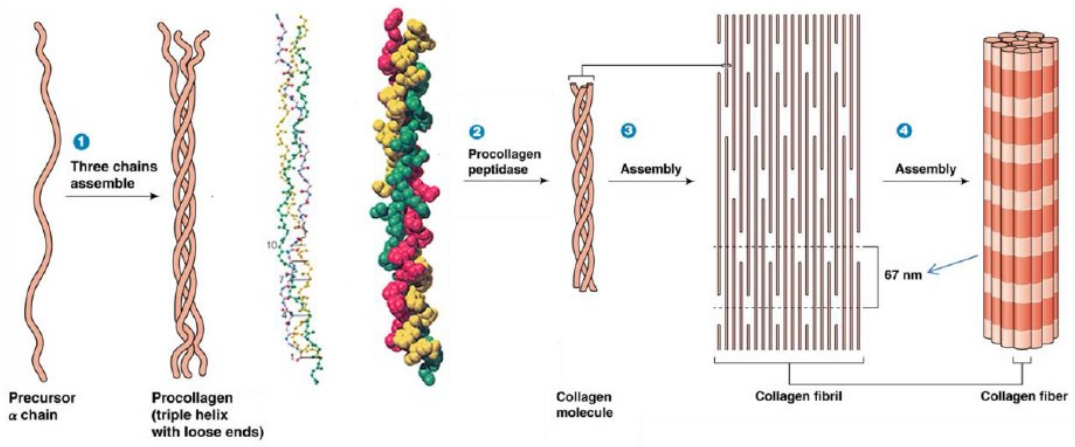

Figure 1.3 *Self-assembly of Collagen: spontaneous and autonomous organization of the single components in orderly and stable structures, thanks to the formation of non-covalent bonds, from the alpha- chain to the collagen fiber.* [18]

A collagen microfibril is composed of the repetition of triple-helix structure and the repetition of microfibrils form the fibrils in which microfibrils are separated by 1.3 nm, that allow to create dense zone detectable at the microscope. Finally, the aggregation of fibrils forms the collagen fibers. The self-assembling of the Collagen featured by the obtainment of the typical 3D architecture provides to the collagen a hydrophobic character. The amino (-NH2), carboxylic (-COOH) and hydroxyl (-OH) functional groups together with peptide bond represent the active site of molecule for chemical interaction. Due to its specific amino acid composition, the isoelectric point (pI) of collagen is 5.5, pH in which the net electrical charge of amino acid is zero and the precipitation of fibers reach the limit.

In bone tissue, collagen fibers are covered from apatite nanoparticles, growing on it during the biomineralization process enable the generation of a hybrid material. Apatites, constitute a large class of mineral phases exploited in several applications in different fields (e.g., biomedical and environmental). The general composition of apatites is M10(XO4)6Z2 where:

- M is a bivalent cation;
- XO4 is a trivalent anion;
- Z is a monovalent anion.

The most common apatite is hydroxyapatite (HA), a basic calcium phosphate characterized by the following composition: Ca10(PO4)6(OH)2, whit a Ca/P ratio of 1.667.

For many years, the stoichiometric HA described above has been considered very close to the apatite present in the human hard tissues, but the biological apatites is very different in term of composition and crystallinity from stoichiometric calcium hydroxyapatite.[18-19-20]

The most important difference between stoichiometric and biological HA is the chemical composition; stoichiometric HA is composed of Ca^{2+}, PO_4^{3-} and OH^- ions while biologic one includes in its structure also several ions through ionic substitution or superficial adsorption (Fig. 1.4).

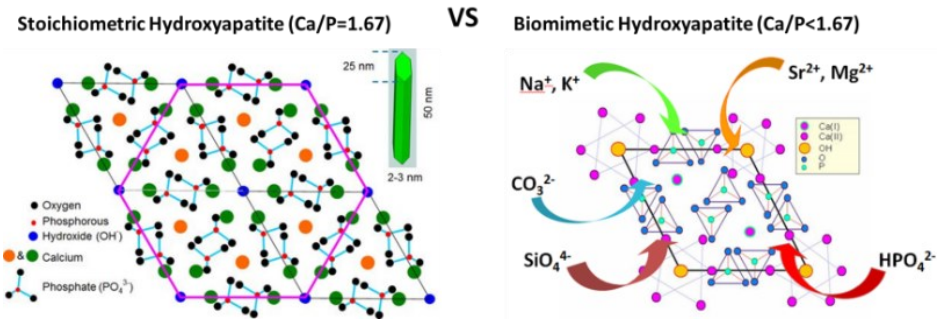

Figure 1.4 *Cristal structure of stoichiometric (on the left) and biomimetic (on the right) hydroxyapatite.*[18]

This incorporation of doping ions modifies several structural and chemical-physical HA parameters, without significantly changing the crystalline structure such as reticular constant, crystal's morphology and size, crystallinity, thermal stability and solubility [18-21]. In particular, magnesium ions, in replace of calcium ions, increase the HA nucleation inhibiting its growth reducing the crystallinity as well as the crystal size and solubility.[19] Furthermore, biologic HA has a low crystallinity and is able to modify its crystalline structure when is undergone to external and internal stimuli. Especially the crystalline degree increases with age and with the presence of carbonate ion promoting the metabolic activity of tissue.[22-23]

Bone should not be considered as a rigid and stable structure with a simple support function, in fact, it's a living tissue highly cellularized and vascularized which is continuously subjected to rearrangement and renewal, to better adapt its properties to the external stresses and respond to fractures and diseases.[24-25-26] Bone cells with the role of synthesizing the components of the matrix, are osteoblasts. Osteoblasts, characterized by endoplasmic reticulum and a Golgi apparatus very extensive, are involved in the synthesis of the collagen fibers and the glycoproteins of the extracellular matrix. When the matrix synthesis and their

mineralization are completed, osteoblasts turn into osteocytes and, while remaining viable cells, they enter in a state of quiescence. Therefore, osteocytes represent a subsequent functional moment of the same cell, characterized by poorly developed Golgi and endoplasmic reticulum.[27] Typical of these cells are the long cytoplasmic extensions in which the cell draws on nutrients and which run within micro galleries.[28-29-30-31] Osteocytes possess membrane receptors for parathyroid hormone (PTH), involved in the reabsorption of calcium and phosphorus, and also control the action of osteoclasts. Osteoclasts, another type of bone tissue cells, are responsible for producing and secreting enzymes suitable for degrading the calcified matrix and allowing bone reabsorption. These enzymes play an important role in bone remodeling, as example in the growth processes, during which it is necessary to replace immature (non-lamellar) bone tissue in adult lamellar bone tissue.[32-33]

1.2 Bone tissue engineering

Bone tissue is able to recover and remodel without scarring, but for several conditions, both congenital and acquired or lesions of critical dimensions, bone replacement is required and 3D bone grafts inducing tissue regeneration, restoring the loss of tissue and their functionality are needed.[24]

Biomaterials play a key role in the stimulation of autologous cells towards damaged tissue regeneration and their function restoration. To do this, scaffolds must be biocompatible and endowed of specific requirements, as example, a well-defined 3D macro- and micro-architecture with an interconnected pore network and a

mimetic chemistry, thus to be able to promote and support bone tissue regeneration.[34-35]

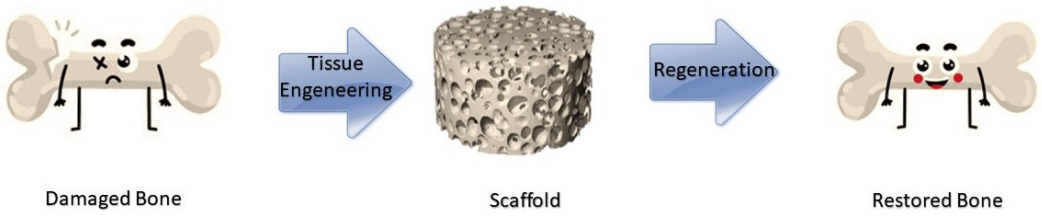

Figure 1.5 *From damaged to recovered tissue thanks to biomaterials*

During the past decade, the progress of new regenerative approaches based on the use of bioactive and biomimetic devices in the orthopedic field avoids the employing of inert substitutes. This stimulates an increasing interest in the design of bioresorbable composite materials, less investigated with respect to ceramics and polymers, and mimetic of the composition and structure of bone tissue.

Tissue engineering has already investigated and exploit materials with high biocompatibility feature. In various medical applications, ceramics materials like calcium phosphates, silica, alumina, zirconia and titanium dioxide were explored and employed thanks to their excellent interaction with tissues, high mechanical strength, and low or none biodegradability. They are involved in orthopedic field [36] and plastic surgery [37] to solve problems with joints, long bones and cranial defects. These types of materials can be defined as bioactive because they react with physiological fluids and create connections with various tissues, promoting cell activity, but due to their poor biodegradability, high density and scarce fluid absorption, ceramic materials are not ideal for tissue engineering purposes, even in the context of bone tissue.

Relatively recent studies have developed techniques for introducing porosity into ceramic scaffold, usually leaching, foaming and sintering, that allow the formation of high porosity and interconnected pores, essential characteristics to enable cell growth and blood flow through the material, providing nutrition to the cells.[38]

To avoid the low biodegradability of ceramics, material scientists designed composite materials with customized physical and mechanical properties, by exploiting the combination of biodegradable polymers with bioactive ceramics. Ceramic phases added to biodegradable polymers favorably alters the degradation behavior of the polymer. Indeed, composite materials can be designed in such a way that their resorption rate can be adapted to the rate of formation of new tissue.[39]

For example, linear aliphatic polyesters such as polycaprolactone (PCL), polylactic acid (PLA), polyglycolic acid (PGA), and their copolymers polylactic acid-co-glycolic acid (PLGA) are frequently employed as polymers for scaffold fabrication thank to the good biocompatibility and mechanical features similar to biological tissues, like cartilage, but without the required biodegradability. To overcome this issue, scaffolds composed of an organic and an inorganic phase were formulated. Furthermore, the ceramic particles added to the polymer lead to increased osteoconductivity and mechanical properties.[40-41]

Recently, by following a biomimetic approach, protein-based biopolymers, such as collagen and gelatin (derivative of collagen), combined with apatitic mineral phase were involved in the design of composite biomaterials.

These polymers are present in natural tissues and allow to develop scaffolds that mimic the mechanical, elastic, chemical-physical and, above all, biological characteristics of the tissues present in the human body.[38]

In a composite scaffold the inorganic component leads to good osteoconductivity while the polymer provides the continuous structure and design flexibility to achieve the high porosity and high surface area, allowing the anchorage of osteoblasts to colonize the scaffold and, then, differentiate and regenerate tissue. The hydroxyapatite (HA), contained in composite scaffolds (such as PLGA/ HA or PLGA/PCL/HA improved the osteoconductivity of PLGA scaffolds) improve osteoblastic cell seeding uniformity and show significantly enhanced expression of mature bone marker genes. Furthermore, HA in the composite scaffolds helps to improve the protein adsorption capacity, suppresses apoptotic cell death and provides a more favorable microenvironment for bone tissue regeneration. The nano-HA/polymer scaffolds not only improved the mechanical properties, but also significantly enhanced protein absorption thanks to the nanosized HA, favoring the cell adhesion and function.[42-43-44] The tissue structural organization, presenting details hierarchically organized on different scale levels, allows them to exist and function with the minimum expenditure of energy and perfect optimization of available resources.[45] The organisms follow a disposition regulate by the genetic heritage, but it's common the evolution and the assembling from a nano structure leading to a macrostructure and microstructure at each position of the part is adapted to the local needs and to ever-changing environmental conditions.[46-47-48] Thanks to its non-specificity, this model is able to adapt to any change, modifying its structure according to the surrounding environment. Spontaneous growth and assembling of building blocks to form natural structures, including bone tissue,

are driven by information exchanged at a molecular scale and combine constructs with features apparently antithetical: mechanical resistance and high flexibility, elective specificity, and high adaptable functionalities.[49-50-51]

In this research thesis we have investigated hybrid biomaterials that respect the principles on which biomimicry of natural bone tissues leads to tissue regeneration, investigating also their behavior as delivery systems for local pharmacological therapies.

1.2.1 The concept of biomimesis

The living organisms around us and their behaviors are the highest models to imitate. This principle about the inspiration from nature is the basis of biomimesis that derives from Greek βίος (life or specifically way of life) and μίμησις (imitation): more precisely ideas from nature or from the life that surrounds us.

The word biomimicry was coined in the late 1950s by the biophysics Otto Schmitt to describe the transfer of ideas and analogues from biology to technology. In particular, he studied and explained how it is possible to synthesize products with artificial mechanisms that mimic nature, thus observing and studying the formation, structure and function of biological substances and materials and biological mechanisms (such as protein synthesis or photosynthesis).[52]

In practice, it is nature that already indicates the protocols and strategies for solving problems, we just have to decipher them. Below you will find some examples of how science has mimicked natural mechanisms.

For a while, man has been studying the adhesive power of the geckos' legs to try to reproduce in the laboratory the strong adhesiveness of their ends, based on a system of bristles, that widen the area of contact with walls, leaves and ceilings, establishing attractive intermolecular forces (Van der Waals Forces).

Researchers from the University of California at Riverside studied this adhesive "power" both before and after 30 minutes after the death of gecko, going to find that the adhesive power remains unchanged even in those minutes after death.(53) This is because the attachment they establish with the surfaces works in total autonomy, without the contribution of muscles or the nervous system.

The adhesiveness of gecko is so impressive that scientists have worked extensively, for over ten years, to replicate it and exploit it in the creation of adhesive tapes and glues for human use. The new research could help to develop new adhesive systems, destined for ambitious targets such as robots that can climb walls or hang on various surfaces; for example, other more futuristic applications could be robots capable of working in extreme environments and areas affected by environmental disasters.(54)

Researchers from Shanghai Jiao Tong University (China) have published a study in Applied Physics Letters in which they demonstrate how the micro-structure of the cicadas' wings can hold the secret to produce anti-reflective surfaces that, applied to solar cells, would make them more and more efficient.(55) The surface of the cicada wings is made up of neat arrays of microscopic cones (of the order of millionths of a millimetre) with the tip facing outwards. Scientists reproduced this structure in the laboratory with titanium dioxide, one of the most promising semiconductor materials. Anti-reflective surfaces have been created that are able to retain visible light that arrives with a wavelength between 450 and 750

nanometers, forming different angles of incidence. These anti-reflective structures manage to maintain their morphology even if exposed to high temperatures, equal to 500 degrees.

For this reason, researchers have seen "enormous potential for photovoltaic devices such as solar cells" here for the future.

Nevertheless, mimicking Nature is not limited to develop biomimetic materials, but also mimic natural process to create new materials.[56] In biomedical field, one of the most interesting natural process is the biomineralization process useful to create highly biocompatible materials with low environmental impact that are recognized by cells as very similar to natural bone.[57-18] *Biomineralization* is a natural process by which organisms form minerals and consists in a complex cascade of phenomena generating hybrid nano-structured materials hierarchically organized from the nano-scale to the macroscopic scale.[7] This process is at the basis of load-bearing structures such as bones, shells, exoskeletons and allows designing biocomposite with unique properties, not obtainable with any conventional approach as with the information exchange with cells and the trigger of the bone regenerative cascade.[7-57]

1.2.2 Design and development of biomimetic hybrid scaffolds for bone regeneration

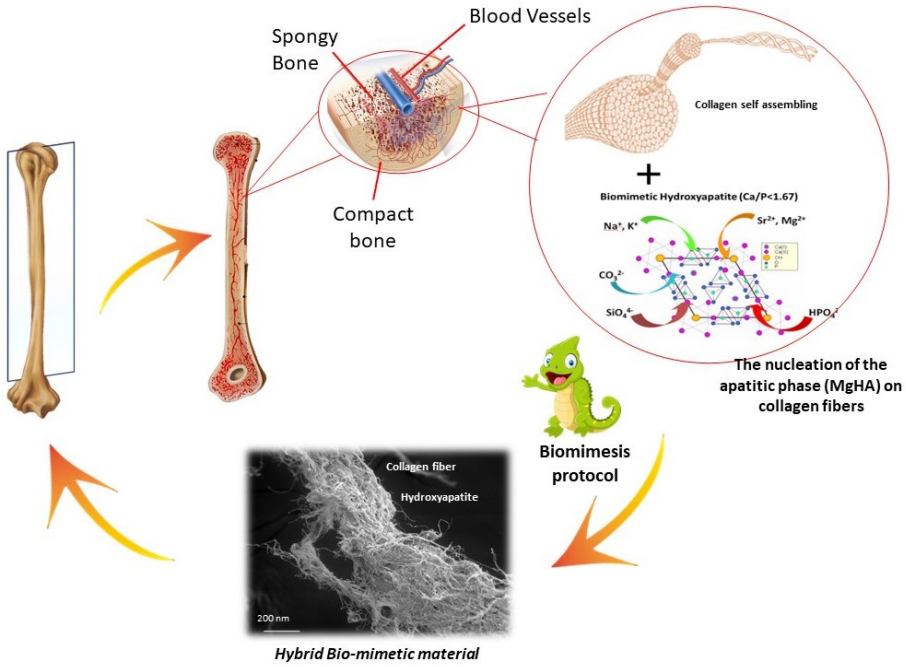

Figure 1.6 *From the concept of biomimesis, the design of innovative scaffold for bone regeneration*

In this research work, taking inspiration from the nature and mimic the biomineralization process, scaffolds, composed of equine collagen I and Mg-Hydroxyapatite (MgHA/coll), are developed as resorbable, biomimetic bone substitutes, with chemical, physical and biological properties close to those of the mineralized matrix of human bone.[26-57-58]

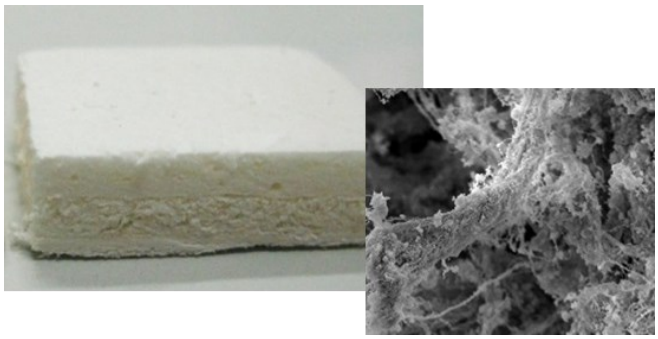

Figure 1.7 *MgHA/coll scaffold: from the macro to the microstructure. ESEM image of the Hydroxyapatite particles covering collagen fibers in the hybrid bone-mimetic material.*

To develop an inorganic/organic hybrid biomaterial, two different processes must occur simultaneously: the nucleation and growth of hydroxyapatite nanoparticles and the self-assembly of macromolecular units. Taking inspiration from the natural biomineralization, both of the processes described above can occur at the same time and place, through a pH-driven process, and guided by chemical, physical, morphological and structural mechanisms capable of generating composites with hierarchical and complex structures.

The nucleation of magnesium-substituted hydroxyapatite nanocrystals into type I collagen fibers resembles the process occurring during biological neo-ossification, favouring cell attachment and proliferation and serving as a scaffold to guide effective bone regeneration, thus providing a reduction of time to osteointegration, with minimal or no local side effects.[59-60-61-62]

The ability of these hybrid scaffolds to interact with cells and the surrounding extracellular matrix (ECM), allows to reconstruct the bone tissue, thanks to the processes implemented by the bone tissue and to the degradation and swelling properties of the material, conducive to colonization and vascularization.

For all these advantageous prerogatives the MgHA/coll scaffold, previously designed and largely investigated [28-58], was selected and involved in this research studies.

1.3 Local therapy: Biomaterials as drug delivery systems

Tissue engineering has solved many pathologies related to traumatic events, thanks to the introduction of bio-materials. However, in these years, the request for more efficient solutions in the field of drug delivery to supplant obsolete and ineffective systemic therapies, has led to the employing of scaffolds as a new solution for the development of local therapies.[29]

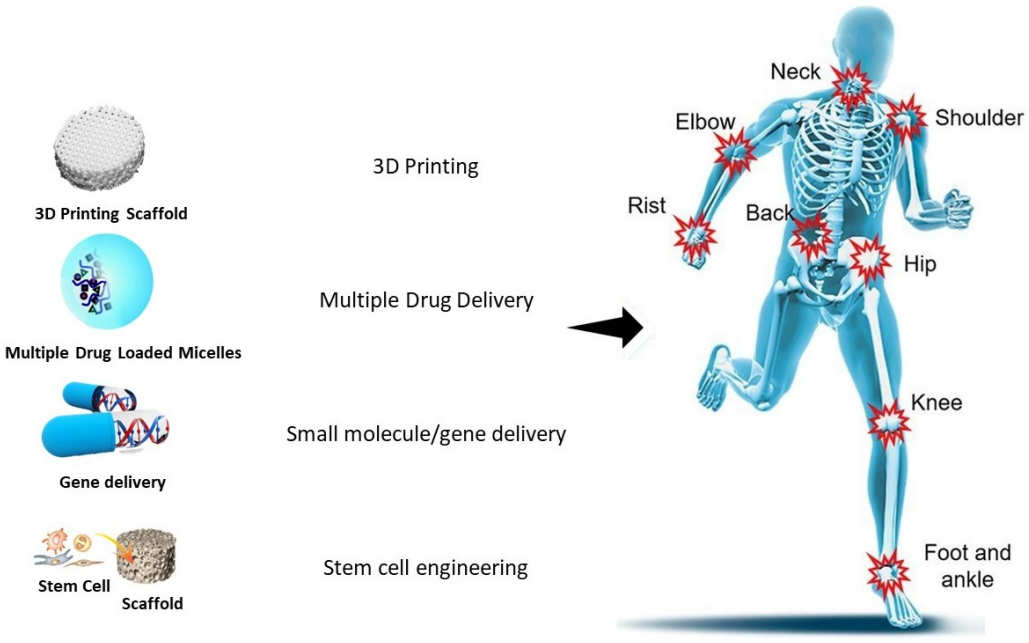

Figure 1.8 *Innovations in tissue engineering: new methods of synthesis of materials and use in drug delivery.*

Even today, systemic therapy is the most employed treatment, especially for the simplicity in the administration, in the range of the common oral administration to the intravenous route. Unfortunately, many times the systemic way is unsuccessful, consequently it is necessary to use high doses of drug, which do not ensure success and with risk of side effects. To solve this problem, the research has investigated local therapies that can act directly in situ, in addition to broadening the prospects of genes and RNA therapy which should decrease side effects.

Our body presents tissues that are poorly vascularized and many drugs show low solubility or are metabolized fast, thereby it is difficult to reach the site of action. Therefore, the local pathway proved to be a solution for reaching the site of action, quickly, without the involvement of metabolisms and vascularization. As example, a gentamicin-loaded collagen sponge was developed lead to reduces sternal wound infections that can occur after heart surgery.(63)

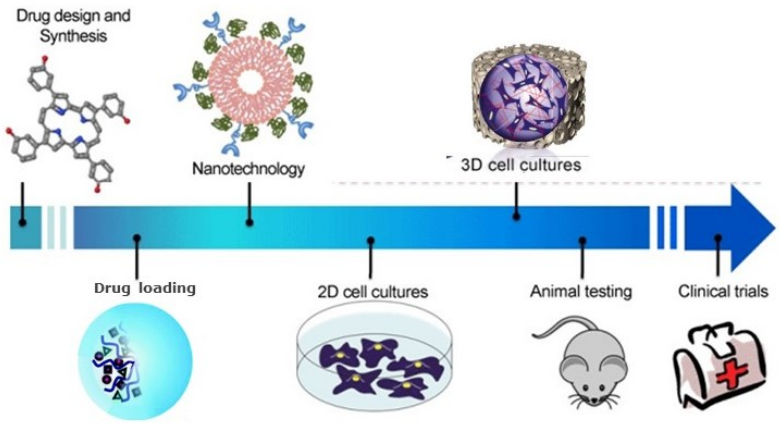

Figure 1.9 *From drug design to pharmaceutical validation.*

Clearly, scaffolds developed for bone tissue engineering can be designed to regenerate tissue and simultaneously to act as drug delivery systems to support a local therapy. It is well-known that the many pathologies that can affect bone tissue, such as infections (osteomyelitis), with a drug-controlled release *in situ* could be resolved or prevented, so as to overcome the major side effects that drugs entail, especially antibiotics.[64-65] Also, about cancer it is important to find new treatments to reduce the amount of chemotherapy and radiotherapy, which today are still the most functional anticancer therapies, but also the most toxic ones. *In situ*, high amount of chemotherapy drugs could be more pharmacologically effective because they act directly on the cancer area, decreasing tissue damage.

To introduce the purpose of this PhD thesis, in the following paragraphs are described the faced bone pathologies, such as osteomyelitis and osteosarcoma, as well as the various innovative therapies, that have been achieved by research in recent years.

1.3.1. Osteomyelitis

Osteomyelitis is an inflammatory process accompanied by bone destruction, caused by bacterial infection (Staphylococcus aureus, Staphylococcus epidermidis, Streptococcus pyogenes, Escherichia coli and Pseudomonas aeruginosa). In children, the long bones of the arms and legs are most commonly involved, while the feet, spine, and hips are most commonly involved in adults.

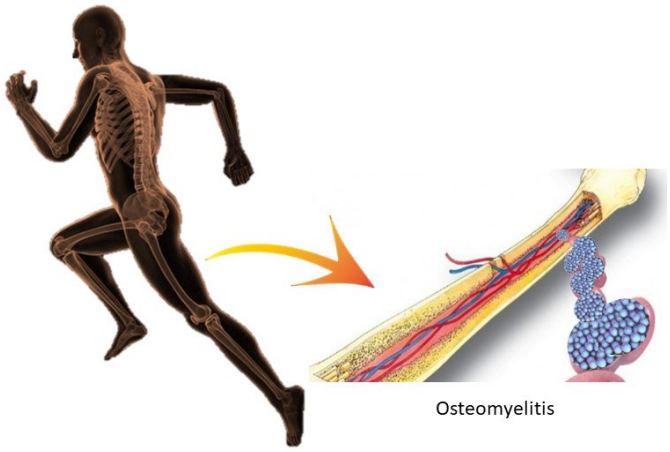

Figure 1.10 *Bone infection causing degenerative osteomyelitis*

Infections can occur also during orthopedic surgery causing implant failure. This happens because biomimetic medical devices are able to recreate *in vivo* a functional microenvironment able to recruit autologous cells and stimulate the whole regenerative process. Besides, as side effects, these well integrated systems can also facilitate the growth of microbes having the potential to adhere to the implanted material and develop biofilms, causing implant failure.

The primary pathogens associated with intervention in orthopedic area are Staphylococcus aureus (SA) and Staphylococcus epidermidis (SE), which are Gram-positive bacteria with high tendency towards forming biofilms and Pseudomonas aeruginosa, Gram-negative bacteria, responsible for over 50% of osteomyelitis cases. [66-67] When bone becomes infected and the antimicrobial therapy is not effective, the bacteria proliferation can lead to tissue damage, involving single portion or several regions of bone, such as marrow and periosteum, until complete bone destruction, causing pain and related major complications. In this scenario, antibiotic administration

is fundamental to reduce infection risks during the implantation procedure and healing process, or to treat pre-existing ones.[68]

It has been established that the systemic administration of therapeutics leads to poor delivery to the site of infection, in particular in or near the bone, and thus its overall performance. Besides, their toxicity excludes the possibility of increase the dosage of antibiotics to avoid the off-target effects and also to reduce the risk of resistance in the target bacteria. It is now clear that to face this challenge new promising approaches must be explored. To mitigate these occurrences, one potential solution is the local administration route, that offers new unprecedented possibilities for an efficacious in situ therapy of preexisting infections and also a reduction of the incidence of implant failure due to contaminations during surgeries, avoiding the adverse effects of conventional systemic treatments.

1.3.2 Osteosarcoma

Many bone diseases are treated with injectable therapies that require very high drug amount to ensure the desired therapeutic features, presenting large side effects.[69] Local therapy can also be effective against cancer, with the possibility of reducing chemotherapy, radiotherapy etc. and therefore the side effects.

The drug-loaded bone graft can be considered as a post-surgical solution. Surgery allows the removal of osteosarcoma, but not the complete safety of removing all cancer cells. Damage to the bone compartment and the need to eliminate the possibility of tumor re-proliferation can be solved through the use of bone substitute devices, loaded with anticancer or innovative molecules.

In fact, medicated scaffolds can respond excellently to the request for post-surgical bone regeneration and aggression of cancer cells, thanks to the release in situ, with the aim of reducing chemotherapy and post-operative radiotherapy.[70-71]

An osteosarcoma is a malignant tumor in bone. Specifically, it is an aggressive malignant neoplasm that arises from primitive transformed cells of mesenchymal origin and that exhibits osteoblastic differentiation producing malignant osteoid.

It is the most common primary bone tumor childhood and adolescence, with a male predominance, and in about 80% of cases it occurs in the long bones of the limbs. In the other 20% of cases, it occurs in the axial skeleton and pelvis.[72]

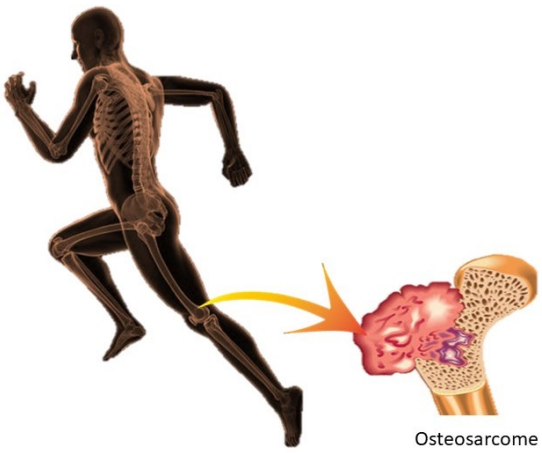

Figure 1.11 *Osteosarcoma is a rare malignant tumor that affects bone cells. It is common among teenagers and young adults*

Osteosarcomas tend to occur at the sites of bone growth, presumably because proliferation makes osteoblastic cells in this region prone to acquire mutations that could lead to transformation of cells (the RB gene and p53 gene are commonly involved). The tumor may be localized at the end of the long bone (commonly in the metaphysis).

Osteosarcoma occurs primarily in the metaphysis of long bones around the knee region of the distal femur or proximal tibia.

The current standard protocol of a three-drug chemotherapy employs cisplatin, doxorubicin and high dose of methotrexate and provides about 70% long-term disease-free survival for osteosarcoma patients without metastasis. Treatment for patients with metastases osteosarcoma, in addition to the based therapy, is high-dose of ifosfamide or radiotherapy.

The most of therapy side effects, overall destroying healthy cells, can be obviated employing locally therapy, that attacks tumor cells directly in the cancer site.

Antitumor drugs are delivered systemically and are absorbed into the blood stream, distributed in all the body and involved in systemic toxicity with associated renal and liver complications, poor penetration into the targeted tissue and sometimes it is necessary the hospitalized monitoring. The local delivery can limit all these disadvantages, employing a higher concentration of medication effectively reaching the targeted site.[73]

1.3.3 Medicated antibiotic scaffold

Local antibiotic therapy has a long tradition and is considered in several sectors of medicine to be a reliable method to prevent and treat unwanted infections. Antibiotics effective against gram-negative organisms dominate in clinical use. [74] The introduction of therapeutics locally has already shown interesting results that have stimulated many different researches focused on the study of different types of active molecules and drug delivery systems, thus to achieve a more effective method of treatment for infections.

Current methods of local antibiotic delivery involve the use of non-biodegradable materials, that require a second surgery for removal, or biodegradable materials. [75] The use of resorbable and biomimetic bone substitutes, loaded with pharmaceutical molecules, would allow, contemporarily to regenerate bone and meanwhile to treat the infection, obviating the removal of the medical device.[76]

For osteomyelitis therapy, the gold standard biomaterial, traditionally used for local antibiotic delivery, is poly-methyl methacrylate (PMMA), in form of medicated beads, however it presents several limitations, is not biodegradable, not able to regenerate bone tissue and often require an additional surgical procedure for its removal and bone grafting, thus exposing the patient to new risks of infection.[77-78-79]

To overcome these issues, novel bioactive and resorbable materials have been recently considered for the local delivery of antibiotics, in the prevention and the treatment of osteomyelitis which are osteoconductive and don't require a second intervention for its removal.[80-81-82] The most largely used are injectable cements loaded with antibiotics [83-84], however, since are only marginally porous, the diffusion of loaded antibiotics into the surrounding bone tissue is limited and are unable to promote an efficient cells penetration and growth of new bone. Between the bioresorbable bone graft the usage of calcium sulfate, as an antibiotic-carrier material, has proven its efficiency as well as its security as a carrier substance.[85-86] Nevertheless, several trials showed a transient cytotoxic effect of calcium sulfate, resulting in inflammatory reactions.[87]

As consequence of these disadvantages, there has been an increasing interest in bioresorbable composite biomaterials, less investigated with respect to ceramics and polymers [88-89-90] and mimicking the composition and structure of bone tissue, thus able to promote bone tissue regeneration.[91-92-93]

Particularly, composites are microporous and easy swellable, and this improve their performance in cells colonization and as drug delivery systems.[94-95-96]

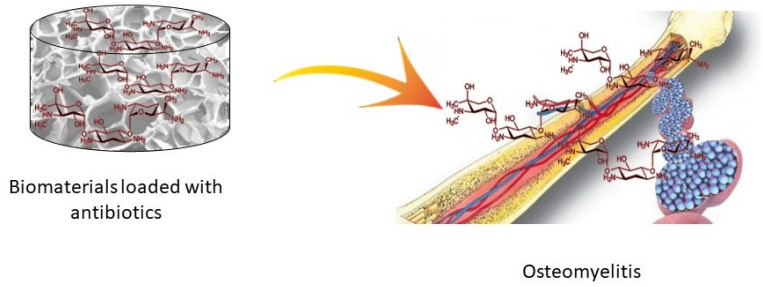

Figure 1.12 *Collagen sponge loaded with antibiotic can locally treat the osteomyelitis*

The purpose of this study is to establish the suitability of previously developed bone hybrid scaffolds MgHA/coll biomimetic and fully bioresorbable in loading aqueous vancomycin hydrochloride (VNC) and gentamicin sulfate (GNT) solutions and preserving their activity, thus to demonstrate their effectiveness as supplier of local therapy for the prevention of bone infection. It represents the first step to understand if these materials are able to retain and preserve these types of therapeutics so as to subsequently study their application in the treatment of pre-existing osteomyelitis which is currently considered an off-label application for these highly bioactive bone grafts.

1.3.4 Medicated hybrid scaffold for antitumor local therapy

Research on cancer treatment was focused, as well as, developing new approaches, to improve the activity of existing drugs by reducing their side effects, such as local delivery. A lot of drug-delivery systems were proposed and tested, by using as carrier

PLGA, chitosan, alginate, hydroxyapatite, or hydroxyapatite combined with collagen loaded with common drug therapy.[97-98]

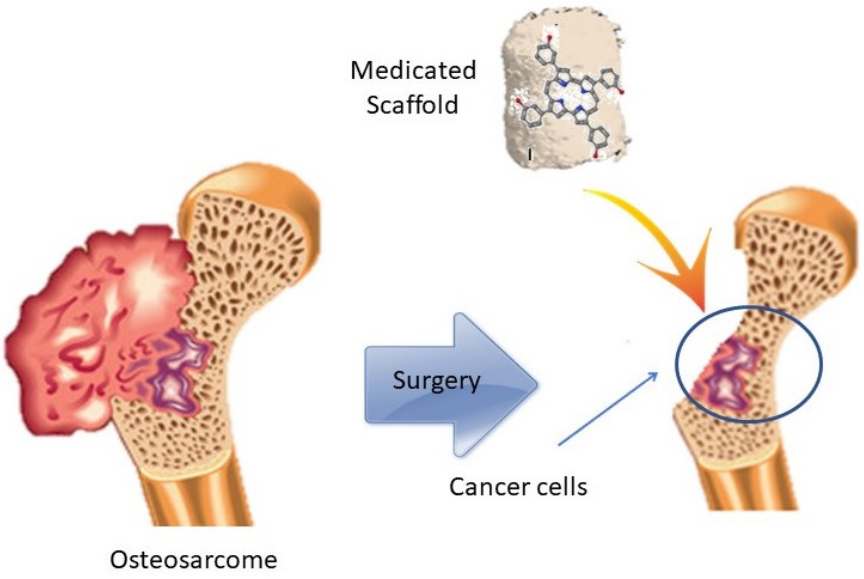

Figure 1.13 *Innovative therapy to treat osteosarcoma: after surgery, a biomaterial loaded with anticancer drugs could restore the bone tissue and eliminate the residual cancer cells, reducing the dosage of chemotherapy drugs.*

The goal of local therapy is to decrease the dosage of chemotherapeutic drugs and thus decrease the side effects of the commonly used drugs, as doxorubicin and methotrexate.[99-100] Exploiting the interaction between drug and biomaterial, the porosity and the swellability of the latter, is here investigated the possibility to perform a local and controlled release of the chemotherapy.[101]

In the article of Andronescu et al., Cisplatin Coll/HA is a material developed for the treatment of bone cancer with immediate release of cisplatin in the first two hours, followed by a slow release in the following 16 hours. This approach has the advantage to reduce the systemic toxicity of cisplatin.[102]

1.4 Hybrid scaffolds as 3D cancer model

Cancer is one of the major causes of death in the world. For the cancers' growth and invasion, favourable chemical interactions should take place between cancer cells and tumour stroma. Tumor is defined as: "an abnormal mass of tissue, the growth of which exceeds and is uncoordinated with that of the normal tissues, and persists in the same excessive manner after cessation of the stimuli which evoked the change".[103]

The majority of cancers (carcinomas) originate from epithelial cancer cells which form cancer foci. The growth is allowed thanks to the interaction with:

- surrounding stroma, which contains non-epithelial cells, mainly fibroblasts and endothelial cells (ECs, lining blood vessels),
- the extracellular matrix (ECM) which is rich in glycosylated proteins,
- vascular endothelial growth factor (VEGF), which are regulated in a temporally distinct manner.

Tumour stroma is also populated by inflammatory cells (macrophages, neutrophils and mast cells). Macrophages and fibroblasts produced proteinases (enzymes) that remodel the ECM helping the tumour. This proteinase is often upregulated in a variety of cancers and degrade collagen IV in the basement membrane, which forms a boundary for the tumour, to allow migration.[103]

From the complexity of the tumor compartment, it can be understood how completely a 2D model is not reproducible of the situation *in vivo*. The cultured cancer cells usually grow as monolayer, therefore their growth does not depend on a surrounding environment, as happen in *in vivo* tumors.

In vivo models have the advantage of providing the native 3D microenvironment in which tumours reside.[104-105]

The first types of 3D tumor models are multicellular tumor spheroids – a small tumor cell aggregates- which consist of tumor cells from tumor cell lines or other tumor fragments. Then they are studied in suspensions, in bioreactors or in 3D matrices at 37°C, to create an environment, that can interact, allowing mimic and approaches the *in vivo* model.[106]

The tissue engineering could be employed to adapt the scaffold as matrices for cell culture and for investigation of proliferation, growth and migration of cancer cells. A 3D scaffold is a temporary structure that supports cells in a given environment, which may eventually be incorporated into the tissue. Scaffold features, including composition, configuration and porosity, allow the cells migration, proliferation and aggregation. As a 3D structure, a scaffold has the potential of well mimic the native geometry, unlike 2D cell monolayer.[107-108]

Tumors grow in a niche that is a complex tumour microenvironment, formed by collagen, hyaluronic acid and other growth factors that interacts with stem cells, promoting their proliferation as cancer cells. Biopolymers, such as collagen and hyaluronic acid, were investigated to reproduce the surrounding extracellular matrix of tumors.[109-110- 111]

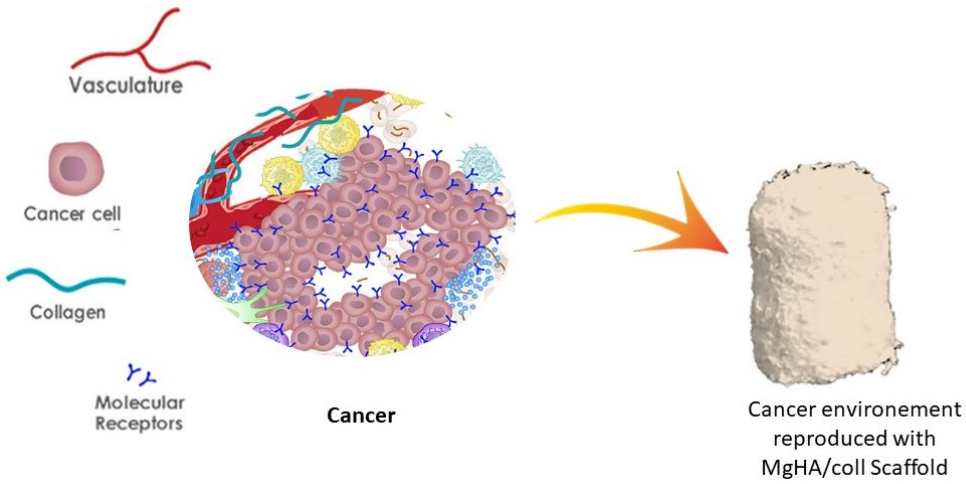

Figure 1.14 *Recreation of the cancer environment with the help of tissue engineering.*

Several studies about 3D models demonstrate better morphology and cell expression in cancer investigations. This further helps to test the efficacy and molecular mechanisms of new and existing drugs. However, in vitro 3D models also have limitations that need to be addressed.[103]

Clearly, although more complex than 2D models, they still cannot fully reproduce the ECM of the tumors and all the various interconnections, as well as only the various blood vessels, it's important in these years to upgrade the complexity in terms of spatial positioning of different cell types, controlling matrix density and with appropriate matrix composition. Such improved biomimetic models present a bridge between 2D systems and *in vivo* models, lead to an alternative, particularly in delineating molecular mechanisms underlying tumour growth and progression and drug action.

[1] Gomes, M. E., Rodrigues, M. T., Domingues, R. M. A. & Reis, R. L. Tissue Engineering and Regenerative Medicine: New Trends and Directions—A Year in Review. Tissue Eng. Part B Rev. 23, 211–224 (2017).

(2) Wegst, U. G. K., Bai, H., Saiz, E., Tomsia, A. P. & Ritchie, R. O. Bioinspired structural materials. Nat. Mater. 14, 23–36 (2015).

(3) Ma, P. X. Biomimetic materials for tissue engineering. Adv. Drug Deliv. Rev. 60, 184–198 (2008).

(4) Loh, Q. L. & Choong, C. Three-Dimensional Scaffolds for Tissue Engineering Applications: Role of Porosity and Pore Size. Tissue Eng. Part B Rev. 19, 485–502 (2013).

(5) Dvir, T., Timko, B. P., Kohane, D. S. & Langer, R. Nanotechnological strategies for engineering complex tissues. Nat. Nanotechnol. 6, 13–22 (2011).

(6) Tampieri, A., Sprio, S., Sandri, M. & Valentini, F. Mimicking natural bio-mineralization processes: A new tool for osteochondral scaffold development. Trends Biotechnol. 29, 526–535 (2011).

(7) Sprio, S. et al. Bio-inspired assembling/mineralization process as a flexible approach to develop new smart scaffolds for the regeneration of complex anatomical regions. J. Eur. Ceram. Soc. 36, 2857–2867 (2016).

(8) Campodoni E, Montanari M, Dozio SM, Heggset EB, Panseri S, Montesi M, Tampieri A, Syverud K, Sandri M. Blending Gelatin and Cellulose Nanofibrils: Biocomposites with Tunable Degradability and Mechanical Behavior. Nanomaterials (Basel). 2020 Jun 22;10(6):1219.

(9) Hench, L. & Wilson, J. W. Surface Active Biomaterials. Science (New York, N.Y.) 226, (1984).

(10) Hench, L. L. & Polak, J. M. Third-Generation Biomedical Materials. Science (80-295), 1014 LP-1017 (2002).

(11) Thomas Pashuck, E. & Stevens, M. M. Designing regenerative biomaterial therapies for the clinic. Sci. Transl. Med. 4, 1–12 (2012).

(12) Baino, F. & Ferraris, M. Learning from Nature: Using bioinspired approaches and natural materials to make porous bioceramics. International Journal of Applied Ceramic Technology 14, 507–520 (2017).

(13) Del Mercato, L. L. et al. Design and characterization of microcapsules-integrated collagen matrixes as multifunctional three-dimensional scaffolds for soft tissue engineering. J. Mech. Behav. Biomed. Mater. 62, 209–221 (2016).

(14) Power, J. & Bernabei, R. in Advances in Manufacturing and Processing of Materials and Structures 51–72 (CRC Press, 2018).

(15) Sun, J. & Bhushan, B. Nanomanufacturing of bioinspired surfaces. Tribol. Int. 129, 67–74 (2019).

(16) M., Grumezescu, A., Holban, A., Mogoşanu, G. & Andronescu, E. Collagen-Nanoparticles Composites for Wound Healing and Infection Control. Metals (Basel). 7, 516 (2017).

[17] Luo, T. & Kiick, K. L. Collagen-like peptides and peptide-polymer conjugates in the design of assembled materials. Eur. Polym. J. 49, 2998–3009 (2013).

[18] Campodoni E. Design and development of bio-hybrid multifunctional materials for regenerative medicine (University of Parma 2018)

[19] Landi E, Logroscino G, Proietti L, Tampieri A, Sandri M, Sprio S. Biomimetic Mg-substituted hydroxyapatite: from synthesis to in vivo behaviour. J Mater Sci Mater Med. 2008 Jan;19(1):239-47. doi: 10.1007/s10856-006-0032-y. Epub 2007 Jun 28. PMID: 17597369.

[20] G. S. Krishnakumar, N. Gostynska, M. Dapporto, E. Campodoni, M. Montesi, S. Panseri, A. Tampieri, E. Kon, M. Marcacci, S. Sprio, M. Sandri. Evaluation of different crosslinking agents on hybrid biomimetic collagen-hydroxyapatite composites for regenerative medicine. International Journal of Biological Macromolecules 106 (2018) 739–748

[21] Krishnakumar GS, Gostynska N, Campodoni E, Dapporto M, Montesi M, Panseri S, Tampieri A, Kon E, Marcacci M, Sprio S, Sandri M. Ribose mediated crosslinking of collagen-hydroxyapatite hybrid scaffolds for bone tissue regeneration using biomimetic strategies. Mater Sci Eng C Mater Biol Appl. 2017

[22] Nabay-Szabo. The structure of Apatite (CaF)Ca4(PO4)3. Zeit. Krist. 75, 387–398 (1930).

[23] Marchegiani, F. et al. Hydroxyapatite synthesis from biogenic calcite single crystals into phosphate solutions at ambient conditions. J. Cryst. Growth 311, 4219–4225 (2009).

[24] Mann, S. in Biomineralization: Principles and Concepts in Bioinorganic Materials Chemistry (2001).

[25] Stegen, S. & Carmeliet, G. The skeletal vascular system–Breathing life into bone tissue. Bone 115, 50–58 (2018).

[26] Bose, S., Tarafder, S. & Bandyopadhyay, A. Effect of chemistry on osteogenesis and angiogenesis towards bone tissue engineering using 3D printed scaffolds. Ann. Biomed. Eng. 45, 261–272 (2017).

[27] Olszta, M. J. et al. Bone structure and formation: A new perspective. Materials Science and Engineering R: Reports 58, 77–116 (2007).

[28] Boskey, A. L. Mineralization of Bones and Teeth. Elements 3, 385 LP-391 (2007).

[29] Gordeladze, J. O., Haugen, H. J., Lyngstadaas, S. P. & Reseland, J. E. Bone tissue engineering: state of the art, challenges, and prospects. Tissue Eng. Artif. Organs Regen. Med. Smart Diagnostics Pers. Med. 2, 525–551 (2017).

[30] Bartl, R. & Bartl, C. in (eds. Bartl, R. & Bartl, C.) 21–30 (Springer International Publishing, 2017).

[31] Katsimbri, P. The biology of normal bone remodelling. Eur. J. Cancer Care (Engl). 26, e12740 (2017).

(32) Beniash, E. Biominerals—hierarchical nanocomposites: the example of bone. Wiley Interdiscip. Rev. Nanomedicine Nanobiotechnology 3, 47–69 (2011).

(33) Wingender, B., Bradley, P., Saxena, N., Ruberti, J. W. & Gower, L. Biomimetic organization of collagen matrices to template bone-like microstructures. Matrix Biol. 52–54, 384–396 (2016).

(34) Iouguina, A., Dawson, J., Hallgrimsson, B. & Smart, G. Biologically informed disciplines: A comparative analysis of bionics, biomimetics, biomimicry, and bio-inspiration among others. International Journal of Design & Nature and Ecodynamics 9, (2014).

(35) Vincent, J. F. V., Bogatyreva, O. A., Bogatyrev, N. R., Bowyer, A. & Pahl, A. K. Biomimetics: Its practice and theory. J. R. Soc. Interface 3, 471–482 (2006).

(36) J.E. Block, M.R. Thorn, Clinical indications of calcium-phosphate biomaterials and related composites for orthopeadic procedures, Calcif. Tissue Int. 66 (2000) 234–238.

(37) H.B. Gladstone, M.W. McDermott, D.D. Cooke, Implants for cranioplasty, Otolaryngol. Clin. North Am. 28 (2) (1995) 381–400.

(38) Habraken, W. J. E. M., Wolke, J. G. C., & Jansen, J. A. (2007). Ceramic composites as matrices and scaffolds for drug delivery in tissue engineering. Advanced drug delivery reviews, 59(4-5), 234-248.

(39) Boccaccini, A. R., Roelher, J. A., Hench, L. L., Maquet, V., & Jérŏme, R. (2002, January). A composites approach to tissue engineering. In 26th Annual Conference on Composites, Advanced Ceramics, Materials, and Structures: B: Ceramic Engineering and Science Proceedings (pp. 805-816). Hoboken, NJ, USA: John Wiley & Sons, Inc.

(40) Raghvendra, K. M. Nanostructured biomimetic, bioresponsive, and bioactive biomaterials. Fundam. Biomater. Met. 35–65 (2018). doi:10.1016/B978-0-08-102205-4.00002-7

(41) Roveri, N., Palazzo, B. & Iafisco, M. The role of biomimetism in developing nanostructured inorganic matrices for drug delivery. Expert Opin. Drug Deliv. 5, 861–877 (2008).

(42) Nair, L. S. & Laurencin, C. T. Biodegradable polymers as biomaterials. Progress in Polymer Science (Oxford) 32, 762–798 (2007).

(43) Daemi, H. & Barikani, M. Synthesis and characterization of calcium alginate nanoparticles, sodium homopolymannuronate salt and its calcium nanoparticles. Sci. Iran. 19, 2023–2028 (2012).

(44) Yan, L. P. et al. Genipin-cross-linked collagen/chitosan biomimetic scaffolds for articular cartilage tissue engineering applications. J. Biomed. Mater. Res. - Part A 95 A, 465–475 (2010).

(45) Mandal, S., Kumar, S. S., Krishnamoorthy, B. & Basu, S. K. Development and evaluation of calcium alginate beads prepared by sequential and simultaneous methods . Brazilian J. Pharm. Sci. (Impresso); Vol 46, No 4 (2010)

(46) Mao, J. S., Zhao, L. G., Yin, Y. J. & Yao, K. De. Structure and properties of bilayer chitosan-gelatin scaffolds. Biomaterials 24, 1067–1074 (2003).

(47) Pulieri, E. et al. Chitosan/gelatin blends for biomedical applications. J. Biomed. Mater. Res. - Part A 86, 311–322 (2008).

(48) Arora, A., Kothari, A. & Katti, D. S. Pore orientation mediated control of mechanical behavior of scaffolds and its application in cartilage-mimetic scaffold design. J. Mech. Behav. Biomed. Mater. 51, 169–183 (2015).

(49) Fratzl, P. & Weinkamer, R. Nature's hierarchical materials. Progress in Materials Science 52, 1263–1334 (2007).

(50) Ramírez-Rodríguez, G. B. et al. Biomimetic mineralization of recombinant collagen type I derived protein to obtain hybrid matrices for bone regeneration. J. Struct. Biol. (2016). doi:10.1016/j.jsb.2016.06.025

(51) Campodoni, E. et al. Polymeric 3D scaffolds for tissue regeneration: Evaluation of biopolymer nanocomposite reinforced with cellulose nanofibrils. Mater. Sci. Eng. C 94, 867–878 (2019).

(52) Monica, S. (2020). Biomimetic Approaches for the Design and Development of Multifunctional Bioresorbable Layered Scaffolds for Dental Regeneration. In Current Advances in Oral and Craniofacial Tissue Engineering (pp. 104-119).

(53) Timothy E. Higham, Anthony P. Russell and Karl J. Niklas 2017Leaping lizards landing on leaves: escape-induced jumps in the rainforest canopy challenge the adhesive limits of geckosJ. R. Soc. Interface.14

(54) Stewart WJ, Higham TE. 2014 Passively stuck: death does not affect gecko adhesion strength. Biol. Lett. 10: 20140701

(55) Zada, Imran & Zhang, Wang & Sun, Peng & Imtiaz, Muhammad & Abbas, Waseem & Zhang, D.. (2017). Multifunctional, angle dependent antireflection, and hydrophilic properties of SiO 2 inspired by nano-scale structures of cicada wings. Applied Physics Letters.

(56) Egan, P., Sinko, R., Leduc, P. R. & Keten, S. The role of mechanics in biological and bio-inspired systems. Nat. Commun. 6, 1–12 (2015).

(57) Tampieri, A. et al. Biologically inspired synthesis of bone-like composite: Self-assembled collagen fibers/hydroxyapatite nanocrystals. J. Biomed. Mater. Res. - Part A 67, 618–625 (2003).

(58) Sprio, S. et al. Biomimesis and biomorphic transformations: New concepts applied to bone regeneration. J. Biotechnol. 156, 347–355 (2010).

(59) Savini Elisa. Design and development of biomineralized nanostructured devices from natural sources for biomedical applications. (University of Bologna, 2016).

(60) Sandri, M. et al. Fabrication and Pilot In Vivo Study of a Collagen-BDDGE-Elastin Core-Shell Scaffold for Tendon Regeneration. Front. Bioeng. Biotechnol. 4, 1–14 (2016).

(61) Tampieri, A. et al. Design of graded biomimetic osteochondral composite scaffolds. Biomaterials 29, 3539–3546 (2008).

(62) Sprio, S., Sandri, M., Panseri, S., Cunha, C. & Tampieri, A. Hybrid scaffolds for tissue regeneration: Chemotaxis and physical confinement as sources of biomimesis. J. Nanomater. 2012, (2012).

(63) Mavros, M. N., Mitsikostas, P. K., Alexiou, V. G., Peppas, G., & Falagas, M. E. (2012). Gentamicin collagen sponges for the prevention of sternal wound infection: a meta-analysis of randomized controlled trials. The Journal of thoracic and cardiovascular surgery, 144(5), 1235-1240.

(64) Biondi, M., Ungaro, F., Quaglia, F., & Netti, P. A. (2008). Controlled drug delivery in tissue engineering. Advanced drug delivery reviews, 60(2), 229-242.

(65) Porter, J. R., Ruckh, T. T., & Popat, K. C. (2009). Bone tissue engineering: a review in bone biomimetics and drug delivery strategies. Biotechnology progress, 25(6), 1539-1560.

(66) Meyers BR, Berson BL, Gilbert M, Hirschman SZ. Clinical Patterns of Osteomyelitis Due to Gram-Negative Bacteria. Arch Intern Med. 1973;131(2):228–233.

(67) Brook I. Microbiology and management of joint and bone infections due to anaerobic bacteria. J Orthop Sci. 2008 Mar;13(2):160-9.

(68) Malizos KN, Gougoulias NE, Dailiana ZH, Varitimidis S, Bargiotas KA, Paridis D. Ankle and foot osteomyelitis: treatment protocol and clinical results. Injury Int. J. Care Injured 41 (2010) 285:293

(69) Malizos K.N., Gougoulias N.E., Dailiana Z.H., Varitimidis S., BargiotasK.A., Paridis D. Ankle and foot osteomyelitis: treatment protocol and clinical results Injury Int. J. Care Injured 41 2010 285-293

(70) Samoto A., Iwamoto Y., Current status and perspectives regarding the treatment of osteosarcoma: Chemoterapy Reviews on recent clinical trials, 2008, 3, 228-231

(71) Janib, S. M., Moses, A. S. & MacKay, J. A. Imaging and drug delivery using theranostic nanoparticles. Adv. Drug Deliv. Rev. 62, 1052–1063 (2010).

(72) Mantyh P., The science behind metastatic bone pain, EJC supplements 4 (2006) 4-8

(73) Palazzo B., Iafisco M., Laforgia M., Margiotta N., Natile G., Bianchi C.L., Walsh D., Mann S., Roveri N., Biomimetic Hydroxyapatite- drug nanocrystals as potential bone substitutes with antitumor drug delivery properties, Adv. Funct. Mater 2007, 17, 2180-2188

(74) Tsourvakas S. Local antibiotic Therapy in the treatment of bone and soft tissue infections Intech

[75] Lew D.P. Waldvogel F.A., Osteomyelitis Lancet vol. 364 July 2004 369-379

[76] Sun, W. et al. Biodegradable Drug-Loaded Hydroxyapatite Nanotherapeutic Agent for Targeted Drug Release in Tumors. ACS Appl. Mater. Interfaces 10, 7832–7840 (2018).

[77] Klemm K. Gentamicin-PMMA-beads in treating bone and soft tissue infections (author's transl) Zentralblatt fur Chirurgie. (1979)

[78] Gogia JS, Meehan JP, Di Cesare PE, Jamali AA. Local antibiotic therapy in osteomyelitis. Semin Plast Surg. 2009 May;23(2):100-7.

[79] McLaren JS, White LJ, Cox HC, Asraf W, Rahman CV, Blunn GW, Goodship AE, Quirk RA, Shakesheff KM, Bayston R and Scammell BE. A biodegradable antibiotic-impregnated scaffold to prevent osteomyelitis in a contaminated in vivo bone defect model. Eur Cell Mater 27 (2017) pp 332:349

[80] Li B, Brown KV, Wenke JC, Guelcher SA. Sustained release of vancomycin from polyurethane scaffolds inhibits infection of bone wounds in a rat femoral segmental defect model J control release 145 (2010) 221:230

[81] Dorati R, De Trizio A, Genta I, Merelli A, Modena T, Conti B. Formulation and in vitro characterizaztion of a composite biodegradable scaffold as antibiotic delivery system and regenerative device for bone J Drug Deliv Sci Technol 35 (2016) 124:133

[82] Inzana JA, Schwarz EA, Kates SL, Awad HA. Biomaterials approaches to treating implant-associated osteomyelitis Biomaterials 81 (2016) 58:71.

[83] Krasko YM, Golenser J, Nyska A, Nyska M, Brin SY, Domb JA. Gentamicin extended release from injectable polymeric implant. J control release 117 (2007) 90:96

[84] Stravinskas M., Horstmann P., Ferguson J., Hettwer W., Nilsson M., Tarasevicius S., Petersen M.M., McNally M.A., Lidgren L. Pharmacokinetics of gentamicin eluted from a regenerating bone graft substitute Bone Joint Res 2016; 5: 427-435

[85] Rauschmann MA, Wichelhaus TA, Stirnal V, Dingeldein E, Zichner L, Schnettler R, Alt V. Nanocrystalline hydroxyapatite and calcium sulphate as biodegradable composite carrier material for local delivery of antibiotics in bone infections. Biomaterials 26 (2005) 2677:2684,

[86] El-Husseiny M., Patel S., MacFarlane R. J., and Haddad F. S. Biodegradable antibiotic delivery systems J Bone Surg. (2011) 151-157

[87] Chang W, Colangeli M, Colangeli S, Di Bella C, Gozzi E, Donati D. Adult osteomyelitis: debridement versus debridement plus Osteoset T pellets. Acta Orthop Belg 73 (2007) 238:43

[88] Joosten U., Joist A., Gosheger G., Liljenqvist U., Brandt B., Eiff C. Effectiveness of hydroxyapaptite-vancomycin bone cement in the treatment Staphylococcus aureus induced chronic osteomyelitis Biomaterials 26 (2005) 5251-5258

[89] Aviv M, Berdicevsky I, Zilberman M Gentamicin-Loaded bioresorbale films for prevention of bacterial infections associated with ortopedic implants. J. Biomed. Mater. Res. Part A (2007) 10:19.

[90] Dorati R, DeTrizio A, Modena T, Conti B, Benazzo F, Gataldi G, Genta I. Biodegradable scaffolds for bone regeneration combined with drug-delivery systems in ostheomyelitis therapy Pharmaceuticals (2017) 10, 96

[91] Stallman H.P., Faber C., Bronckers A. LJJ., Amerongen A.V.N., Wuisma P. I., In vitro gentamicin release from commercially available calcium-phosphate bone substitutes influence of carrier type on duration of the release profile BMC Muscoskeletal disorders 2006, 7:18

[92] Teller M., Gopp u., Neumann H.G., Kuhn K.D. Release of gentamicin from bone regenerative materilas: an in vitro study Journal of biomedical materials research part b: Applied biomaterials 23-29

[93] Gallo J., Bogdanov K., Siller M., Svabova M., Lost ak J., Kolar M., Microbiological and pharmacological properties of bone cement VancogenX Acta Chirurgiae orthopaedicae et traumatologiae cechosl., 80,2013, p69-79

[94] Ruszczak Z., Friess W. Collagen as a carrier for on-site delivery of antibacterial drugs Advanced Drug delivery reviews 55 (2003) 1679-1698

[95] Swieringa A.J., Goosen J.H.M., Jansman F.G.A., Tulp N. J. A. In vivo pharmacokinetics of a gentamicin-loaded collagen sponge in acute periprosthetic infection: serum values in 19 patients Acta Orthopaedica, 79:5, 637-642

[96] Kilian O., Hossain H., Flesch I., Sommer U., Nolting H., Chakraborty T., Schnettler R. Elution kinetics, antimicrobial efficacy and degradation and microvasculature of a new gentamicin-loaded collagen fleece. Journal of biomedical materials research Part B: applied biomaterials (210-222) 2008

[97] Marques C., Ferreira J. MF., Ficai D., Sonmez M., Ficai A., Multifunctional materials for bone cancer treatment International journal of nanomedicine 2014, 9, 2713-2725

[98] Zhang Y., Jin t., Zhuo X. R. Methotrexate-Loaded biodegradable polymeric micelles: preparation, physicochemical properties and in vitro drug release Colloids and surface B: Biointerfaces 44 (2005) 104-109

[99] Barroug, A. and Glimcher, M.J. (2002), Hydroxyapatite crystals as a local delivery system for cisplatin: adsorption and release of cisplatin in vitro. J. Orthop. Res., 20: 274-280. doi:10.1016/S0736-0266(01)00105-X

[100] Yoshioka, T., Ikoma, T., Monkawa, A., Yunoki, S., Abe, T., Sakane, M., & Tanaka, M. (2007). Preparation of Hydroxyapatite-Alginate Gels as a Carrier for Controlled Release of Paclitaxel. Key Engineering Materials, 330–332, 1053–1056.

[101] Hess U., Shahabi S., Treccani L., Streckbein P., Heiss C., Rezwan K., Co-delivery of cisplatin and doxorubicin from calcium phosphate beads/matrix scaffolds for osteosarcoma therapy, Materials Science and Engineering C 77 (2017) 427-435

[102] Andronescu E., Ficai A., Georgiana M., Sonmez M., Ficai D., Ion R., Cimpean A., Collagen-hydroxyapatite drug delivery systems for locoregional treatment of bone cancer Technology in cancer research and treatment Volume 12, Number4, August 2013

[103] Willis, R. A. London: Butterworth & Co. Pathology of tumours. 1948.

[104] Nyga, A., Cheema, U. & Loizidou, M. 3D tumour models: novel in vitro approaches to cancer studies. J. Cell Commun. Signal. 5, 239 (2011).

[105] Fischbach, C., Chen, R., Matsumoto, T. et al. Engineering tumors with 3D scaffolds. Nat Methods 4, 855–860 (2007).

[106] Bassi, G., Panseri, S., Dozio, S. M., Sandri, M., Campodoni, E., Dapporto, M. & Montesi, M. (2020). Scaffold-based 3D cellular models mimicking the heterogeneity of osteosarcoma stem cell niche. Scientific Reports, 10(1), 1-12.

[107] Dietmar W. H. Biomaterials offer cancer research the third dimension Nature Materials vol 9 february 2019

[108] Moreau J.E., Anderson K., Mauney R. J., Trang N., Kaplan D.L. and Rosenblatt M., Tissue-Engineered Bone serves as a Target for Metastasis of human breast cancer in a mouse model. Cancer Res 2007; 67 10304-10308

[109] Cheema U, Alekseeva T, Abou-Neel EA, Brown RA (2010) Switching off angiogenic signalling: creating channelled constructs for adequate oxygen delivery in tissue engineered constructs. Eur Cell Mater 20:274–280

[110] Holliday DL, Brouilette KT, Markert A, Gordon LA, Jones JL (2009) Novel multicellular organotypic models of normal and malignant breast: tools for dissecting the role of the microenvironment in breast cancer progression. Breast Cancer Res 11:R3

[111] David L, Dulong V, Le CD, Chauzy C, Norris V, Delpech B, Lamacz M, Vannier JP (2004) Reticulated hyaluronan hydrogels: a model for examining cancer cell invasion in 3D. Matrix Biol 23:183–193

CHAPTER 2

2. Materials & Methods

2.1. Materials

Several reagents and polymers were used as reported below. Type I collagen (Coll) extracted from equine tendon, purified and telopeptide-free, and supplied as acetic gel (an aqueous acetic buffer solution with pH = 3.5 containing 1 wt% of pure collagen) was purchased from Opocrin S.p.A., Italy. Calcium hydroxide (Ca(OH)2; ≥95.0% pure), sodium hydroxide (NaOH; ≥98% pure), chloridric acid (HCl; 37% pure), nitric acid (HNO3; 65% pure), magnesium chloride hexahydrate (MgCl2·6H2O; ≥99% pure), calcium chloride (CaCl2; ≥97% pure), phosphate buffered saline (PBS; pH 7.4), 4-butanediol diglycidyl ether (BDDGE; 95 wt.% pure), Sodium periodate ($NaIO_4$), Sodium boroHydryde ($NABH_4$), Methanol (CH_3OH), Isopropanol (C_3H_8O), phtalaldialdehyde ($C_6H_4(CHO)_2$), Mercaptoethanol (C_2H_6OS) were all provided by Sigma. Sodium alginate, Vancomicyn Chloride and Gentamicin Sulfate were purchased from Sigma-Aldrich.

2.2. Materials processing

Freeze-drying techniques. All synthetized materials were manufactured by unidirectional freeze-drying technology (see chapter 1.4). If do no differently mentioned, the freezing ramp was 50 °C/min until -40 °C and heating ramps were performed from -40 °C to -10°C at 5 °C/h and from -10 °C to 15 °C at 2 °C/h under

vacuum conditions (at least P = 0.1 mbar). The equipment employed in the present work was a 5Pascal LIO-1000P.

2.3. Analytical techniques

All analytical techniques exploited in this Ph.D. research are the same of a thesis previously published. The principles of techniques and the sample preparation are reported below according to previous thesis.[1-2]

2.3.1. X-Ray Diffraction (XRD)

X-ray diffraction (XRD) is a non-destructive analytical technique primarily used for phase identification of a crystalline material. The material is finely ground, homogenized and the average bulk phase composition is analysed.

An X-ray beam hit a sample and the scattered intensity was evaluated as a function of incident and scattered angle, polarization and wavelength or energy. X-ray wavelength is comparable with inter-atomic distances (~150 pm) and thus is an excellent probe for this length scale. This technique is commonly used to evaluate heterogeneous solid mixed substance to determine their relative amount or to recognize unknown substances, by comparing diffraction data against a database of International Center for Diffraction Data (ICDD). Powder diffraction is also a common method for determining strains in crystalline materials. A simple preparation, a fast analysis on single or mixed phase are the advantages of this technique.

The X-ray wavelength (λ between 10 nm and 1 pm) is generated by a cathode ray tube, filtered to produce monochromatic radiation, collimated to concentrate that hits the sample. When it hits an atom, the electrons around the atom start to oscillate with the same frequency as the incoming beam. As consequence of the oscillation the electrons will diffuse the incidence radiation in all the directions; this phenomenon is known as the Rayleigh scattering (or elastic scattering). These kinds of radiations interfere with each other destructively in the most of the directions, but also in a constructive way if some atoms are arranged in a regular pattern (crystalline cell) and a diffracted ray is produced because the Bragg's law is satisfied (Fig. 2.1). Miller indices (hkl) were usually used to indicate which of the various intersection planes of the mineral's crystal cell refers the constructive interference (dhkl: interplanar distance).

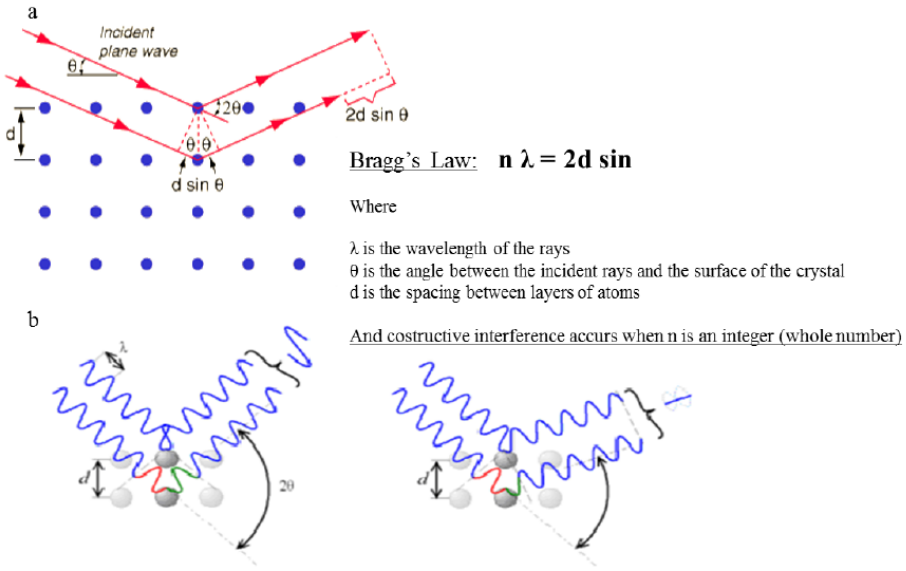

Figure 2.1. *a) Bragg's law and constructive interference; b) difference between constructive (on the left) and destructive interference in Rayleigh scattering of X-rays.*

The overlapping waves will give rise a well-defined scattered X-ray beams leaving the sample at various directions. In the diffraction analysis, the wave interference pattern was shown as diffracted intensity in function of diffraction angle (2θ), each single phase or materials show a typical pattern with specific positions and relative intensity of the lines. In contrast to a crystalline pattern consisting of a series of sharp peaks, amorphous materials produce a broad background signal. Many polymers, organic molecules or inorganic glasses usually exhibit this kind of pattern, but often also inorganic nanostructured crystalline phases can contain also an amorphous fraction. X-ray diffractometers is composed by three basic elements:

- X-ray tube: a cathod tube generates X-ray by heating a filament and producing electrons. A voltage applied accelerates electron toward a target that reach and hit material (Figure 2.2);

- a sample holder;

- X-ray detector. The most focusing geometry used in powder diffractometers is the Bragg-Brentano were the incident beam produced and the detector move on a circle where sample in the center.

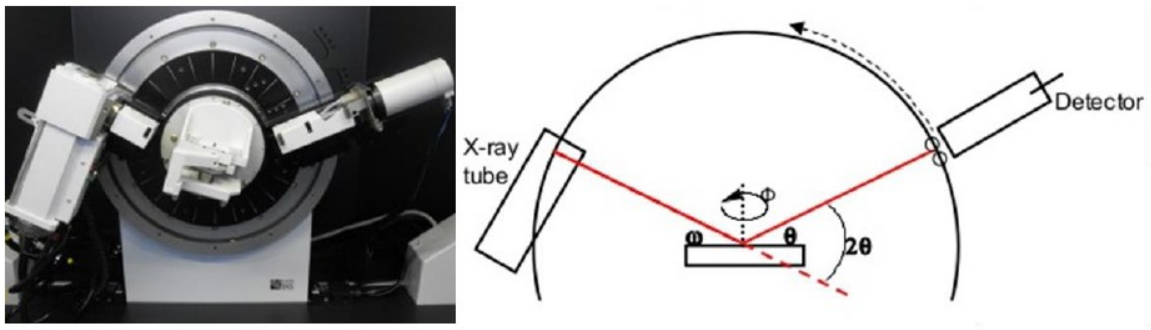

Figure 2.2. *D8 Advance diffractometer (on the left) and a typical scheme of a Bragg-Brentano type diffractometer (on the right).*

The model of diffractometer employed in this activity is a D8 Advance diffractometer (CuKα radiation) working with Bragg-Brentano configuration, equipped with a LINXEYE detector (Bruker, Karlsruhe, Germany). The XRD patterns were recorded in the 2θ range 10°-80°, scan step 0.02° and step time 0.5 seconds.[1-2]

2.3.2. Fourier-Transform Infrared Spectroscopy (FTIR)

Among spectroscopy techniques, Infrared spectroscopy deals with the region of the electromagnetic spectrum ranging from 14000 to 10 cm-1 (from near to far-IR). The signal is acquired in the time domain, and through the Fourier transform it's possible to obtain the spectrum in function of frequencies.

Infrared spectroscopy exploits the fact that at specific frequencies the interaction with the radiation causes vibrational transitions (Fig. 2.3). The strength of the bond, the mass of the atoms and also its around determine different absorption frequencies. Thus, each particular bond type shows a specific frequency and

intensity of absorption and can be used for the characterization of very complex mixtures.

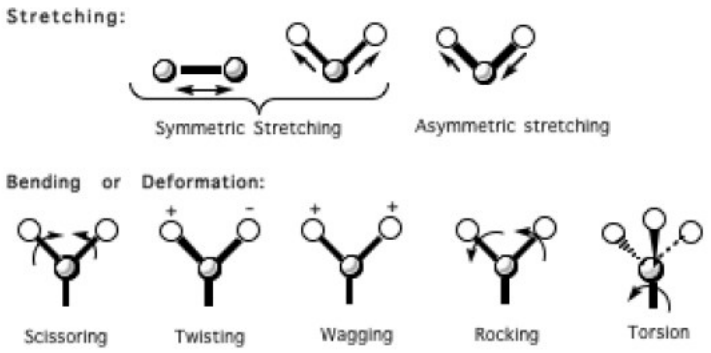

Figure 2.3. *Possible vibrations detected by infrared spectroscopy.*

In the FTIR instrument a beam of infrared light goes through an interferometer and onto the sample absorbing all the different wavelengths characteristic of its spectrum at once. Instead, in standard IR spectrometer with a monochromator the source radiation is separated into its different wavelengths limiting the amount of signal which can be obtained at a particular resolution. In FTIR instrument, all wavelengths are simultaneously reported thank to the beam splitter which send the light through moving and stationary mirrors the beam passing through the sample (Figure 2.4).

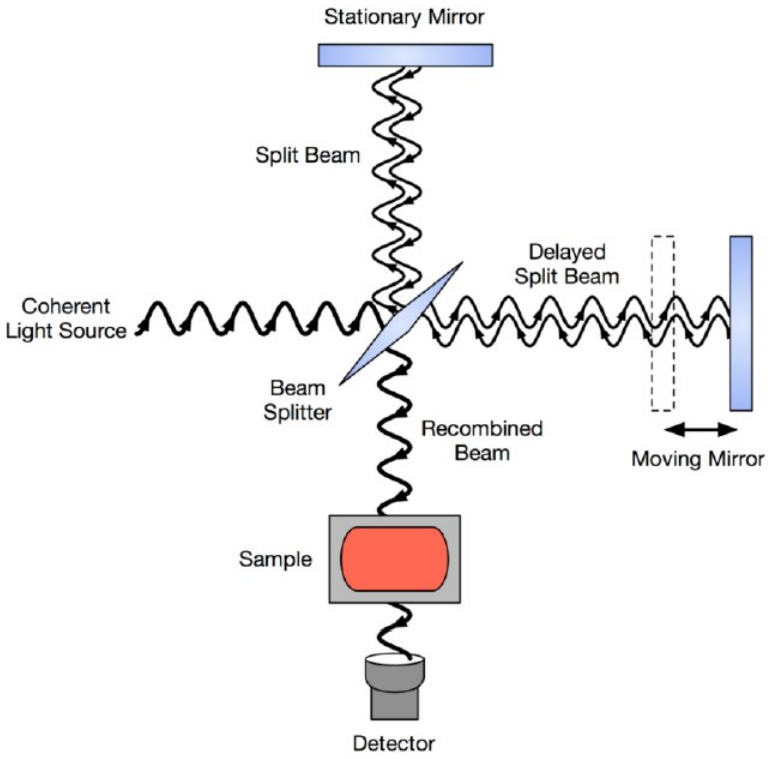

Figure 2.4. *Scheme of FTIR spectrometer.*

During preparation about 2 mg of the sample is ground finely with 100 mg of anhydrous potassium bromide (KBr) to remove scattering effects from large crystals. This powder mixture is then pressed at 8000 psi into 7 mm diameter disc to form a translucent pellet through which the beam of the spectrometer can pass through. All the spectra are the average of 64 spectra, acquired at room temperature in the range of 400-4000 cm-1 at a resolution of 4 cm-1; potassium bromide is used as control.

The equipment employed in the present work was a Thermo Nicolet-Avatar 320 FT-IR (Thermo Fisher Scientific Inc., Waltham, MA, USA).[1-2]

2.3.3. Inductively Coupled Plasma Optical Emission Spectroscopy (ICP-OES)

The Inductively Coupled Plasma Optical Emission Spectroscopy (ICP-OES) is one of the most powerful and popular analytical tools for the determination of trace elements. A spontaneous emission of photons from atoms and ions that have been excited in a radiofrequency (RF) discharge is the source of this technique where the sample can be directly injected in liquid or gas form. Instead, solid samples require extraction or acid digestion so that the analytes will be present in a solution. Standard solutions allow to create a calibration curve in order to evaluate the concentration of the elements that are proportional to the intensity of the radiation. A torch that is composed of three concentric tubes, usually made of quartz, keeps the plasma. The end of this torch is placed inside an induction coil supplied with a radio-frequency electric current. A flow of argon gas is introduced between the two outermost tubes of the torch and an electrical spark is applied for a short time and free electrons are introduced into the gas stream (Figure 2.5).

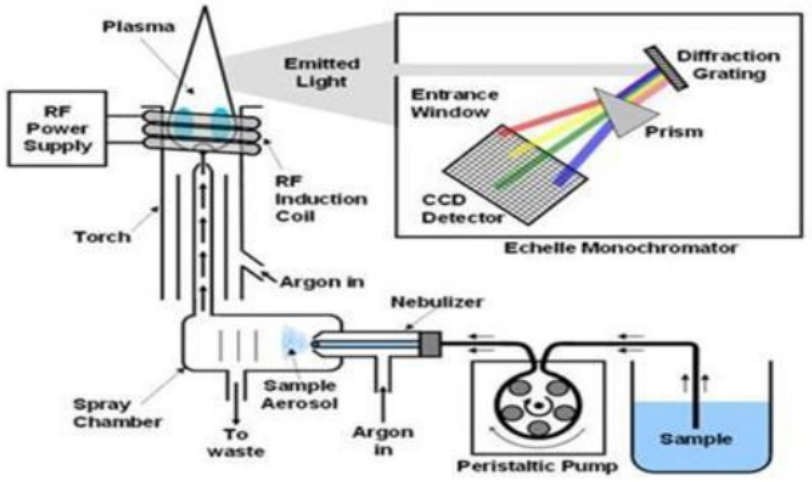

Figure 2.5. *Schematic view of ICP-OES spectrometer.*

Before entering in middle channel of plasma, the sample solution is converted into an aerosol and after is quickly vaporized due to the inductively coupled plasma (ICP) kept a temperature of approximately 10000K. In this way, sample is converted in free atoms in the gaseous state. Further collisional excitation within the plasma imparts additional energy to the atoms, promoting them to excited states. Sufficient energy is often available to convert the atoms to ions and subsequently promote the ions to excited states. Both the atomic and ionic excited species may then relax to the ground state via the emission of photons. These photons have characteristic energies that are determined by the quantized energy level structure for the atoms or ions. Elaborating the wavelength of the photons, the starting elements can be recognized and their concentrations is directly proportional to the amount of photon.

The equipment employed in the present work was a Liberty 200, Varian (Clayton South, Australia); 20 mg of sample was dissolved in 2 mL of nitric acid (HNO3) and deionized water was added up to 100 mL. Standard solutions of investigated atoms were used as reference solutions and an equally diluted solution of nitric acid was also analysed and the corresponding spectrum subtracted by the experimental one.[1-2]

2.3.4. Thermogravimetric analysis (TGA)

Thermogravimetric analysis is a useful test to determine changes in weight in relation to change in temperature. Such analysis relies on a high degree of precision in three measurements: weight, temperature, and temperature change. As many weight loss curves look similar, the weight loss curve may require transformation

before results may be interpreted. A derivative weight loss curve can be used to tell the point at which weight loss is most apparent. The instrument is composed of a high-precision balance with a pan loaded with the sample. The sample is placed in a small electrically heated oven with a thermocouple to accurately measure the temperature. Different gas can be used such as air, argon, nitrogen to prevent oxidation or other undesired reactions. During analysis, temperature is gradually increased and weight is measured and plotted against temperature. After the data is obtained, some tools can be used to elaborated curves. The equipment employed in the present work was the Simultaneous Thermal Analyser (STA 409C, Netsch, Germany).[1-2]

2.3.5. Scanning Electron Microscopy (SEM)

The scanning electron microscope is a device able to provide high magnification images of a sample (up to 200000X) with both resolution and field depth higher than the conventional optical microscope. The characteristic of the instrument is to explore the surface of the sample with a beam of high-energy electron, while a real-time monitoring of the intensity of the emitted secondary electrons is performed. Afterward, several signals are detected from the interaction of the incident electrons with the sample's surface (Figure 2.6).

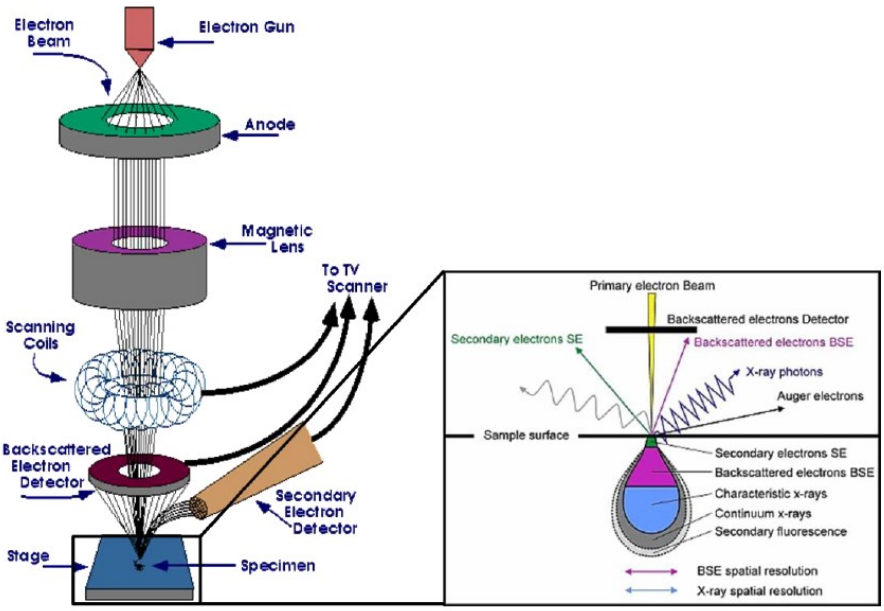

Figure 2.6. *Schematic view of a SEM; in the inset, the electron-matter interaction was shown.*

Part of the incident electron beam (primary electrons) is reflected without decreasing the initial energy, giving rise to backscattered electrons. Secondary electrons are specific electron which escape outside of the sample because they are able to diffuse toward the surface thank to the energy received by primary electrons. In particular, only primary electrons that are not reflected; and the secondary electron escape with a low energy (energy < 50 eV). Furthermore, characteristic x-ray photons are emitted when the primary beam causes the expulsion of inner shell electrons from the sample and are used to investigate the elemental composition of the sample. Finally, back-scattered electrons emitted from the sample may be used alone to form an image or in conjunction with the characteristic x-rays as atomic number contrast clues to the elemental composition of the sample.

In a typical SEM, the source is a tungsten cathode (electron gun), used because has high melting point and low vapour pression, that generates electrons and it is accelerated towards an anode. Before hitting the sample, the electron beam is focused by condenser lenses and passes through pairs of scanning coils or pairs of deflector plates in the electron optical column and it is endowed by a fine focal spot sized 0.4 nm to 5 nm and an energy of few hundred eV up to 100 KeV. Electron beam, the atomic number of the specimen and its density determines the interaction volume. The secondary electrons, due to their low energy, are detected by a scintillator photomultiplier device and the resulting signal is rendered into a two-dimensional intensity distribution that can be viewed and saved as a digital image. The number of electrons secondary in the detector and the size of the electron spot determine the brightness and the spatial resolution respectively. Furthermore, the size of the electron spot depends on both the wavelength of the electrons and the magnetic electron optical system which produces the scanning beam.

Equipments employed in the present work were two a FEG-SEM (Field Emission Gun Scanning Electron Microscope) for high resolution images at high magnification (FEI, Quanta 200, USA) and ESEM (Environmental Scanning Electron Microscope) for high resolution imagines at low magnification (Quanta 600 FEG, FEI Company, Hillsboro, OR). For SEM analyses the specimens were previously mounted on aluminum stubs with carbon tape and coated with Au using a coating units Polaron Sputter Coater E5100 (Polaron Equipment, Watford, Hertfordshire, UK). [1-2]

The equipment employed in the present work was a Tecnai F20 (FEI, 124 Hillsboro, USA) equipped with a Schottky emitter and operating at 120 and 200 keV.

2.3.6 Ultraviolet Visible Spectroscopy

UV / Visible spectrophotometry is based on the selective absorption by radiation molecules with a wavelength between 10 nm and 780 nm, that can be divided into three regions:

- UV far (10-200 nm)
- near UV (200 - 380 nm)
- Visible (380 - 780 nm)

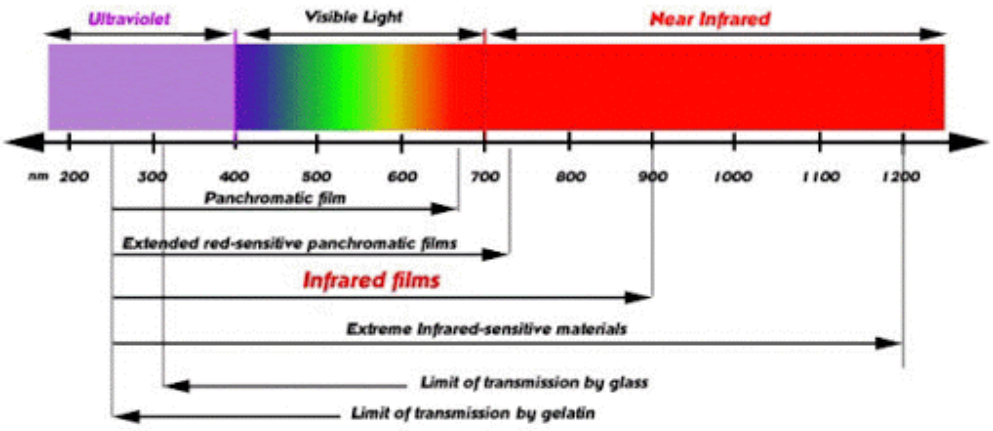

Figure 2.7. *Spectral range: UV far, Near UV, Visible and infrared*

This type of absorption involves the excitation of valence electrons, which requires energies the higher the greater the distance from the electronic level of departure and arrival of the transitions. This phenomenon can exploit a length of current, of fictitious intensity (I); detecting then the intensity of the emerging radiation (I-x) the magnitude is defined as transmittance:

T= (I-x) / I

Each individual substance absorbs at a specific wavelength and the law that describes this type of absorption is the Lambert-Beer law, which is applicable only in the case of monochromatic radiation.

The equation is:

$$\mathbf{A = a \cdot b \cdot C}$$

A = absorbance (log1/T)

a = Extinction Coefficient (molar if the concentration is expressed in mol/l)

b = Cell Thickness

C = Sample Concentration

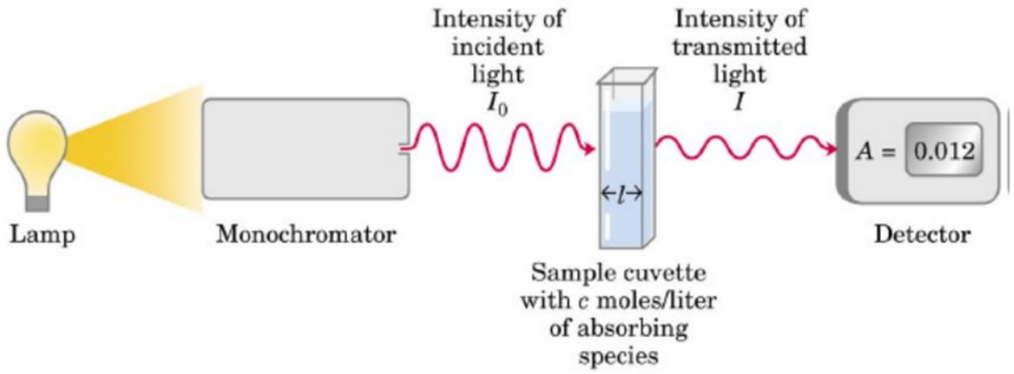

Figure 2.8. *Schematic view of a UV-visible instrument.*

The Uv-Visible instruments consists in a source (a lamp) which must emit as constant and reproducible radiation as possible. This light beam is then directed towards a moving mirror which reflects it towards the monochromator.

The monochromator consists of two parts: a dispersing element and an optical filter. This instrument manages to break down the polychromatic radiation emitted into monochromatic bands. The quality of this tool depends on two parameters: the

width of the passband (responsible for choosing a particular radiation) and the resolving power (the ability to separate multiple wavelengths from each other).

The cell compartment is the section where the incident beam is doubled in two radiations of equal intensity and directed towards the sample and towards the blank. This dual beam mode allows to eliminate problems due to the variable emission of the lamp; in fact, it is possible with this device to detect an absorption by making a blank / sample ratio.

The solutions to be analyzed are placed in cells (about 1 cm wide) of different material depending on whether you are working with radiation of wavelength included in the UV or visible region, rectangular quartz or glass cuvettes are used respectively. The absorption is analyzed by a detector that will be photovoltaic cells, photodiodes, phototubes, photomultipliers.

In particular, in this thesis the Uv analysis employs Thermo Scientific™ NanoDrop™ One Microvolume UV-Vis Spectrophotometers. With this instrument it's possible to quantify and qualify DNA, RNA, protein and chemical samples with only a drop (1-2 μL) and obtain full-spectral data.

2.3.7 High performance Size-Exclusion Chromatography-Evaporative Light Scattering Detector (HPSEC-ELSD)

The methods for mass estimation of polymers, Size-Exclusion Chromatography (SEC) coupled with Evaporative Light Scattering Detector (ELSD). It's a qualitative and quantitative method, useful to detect molecular weight and amount of polymer present in the polymer.

Each sample is dialyzed before the analysis.

Separation was achieved by HPSEC with two TSK-Gel columns G5000 PWXL (7.8mm×300 mm, 10μm) and G2500 PWXL (7.8mm×300 mm, 6 μm) connected in series with a TSK-Gel guard column (6.0mm×400 mm) (Tosoh Bioscience, Stuttgart, Germany). These columns were connected at two different chromatographic systems. The HPSEC-ELSD analysis was carried out on a LC chromatograph Agilent Technologies 1220 Infinity and a detector ELSD 1260 Infinit (Agilent Technologies, Boeblingen, Germany). Samples (50μL) were eluted with mobile phase 0.1M NaCl and 0.01M NH4Ac, at flow rate 0.5 mL/min for 50 min at 30 °C. Before analysis, all samples and standards were filtered through 0.45 μL Millipore membrane. [3]

2.3.8 Atomic Force Microscopy (AFM)

The atomic force microscope consists of a microscope (cantilever) at the end of which a sharp tip is mounted, typically composed of silicon or silicon nitride (silicon nitride have good durability and suffer less wear than silicon tips), which has a radius of curvature of the order of nanometers. The tip is placed in proximity to the surface of the sample to be scanned. The van der Waals force acting between the tip and the sample causes a deflection of the microlift (whose elastic constant is known), in accordance with Hooke's law.

The deflection of the lever is measured using piezoresistive AFM probes. Generally, the sample is placed on a piezoelectric tube, which can move it in the perpendicular direction (z direction), to maintain a constant force, and in the plane (x and y

directions), to analyse its surface. The resulting map (x, y) represents the topography of the sample surface. The motion of the cantilever can also be used to interrogate the mechanical properties of the sample.

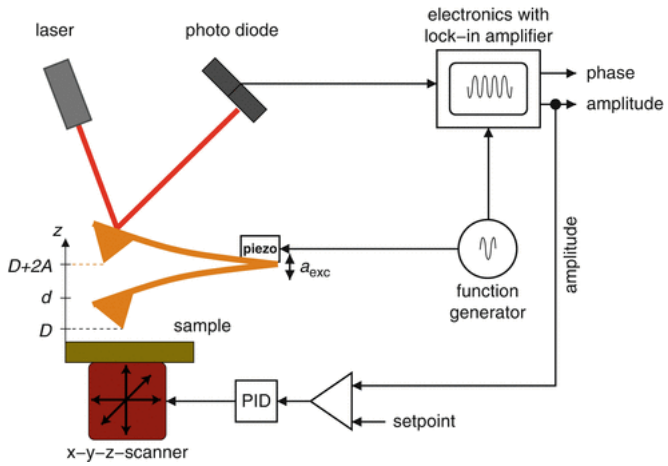

Figure 2.9. *Schematic view of AFM; the operating principle*

Tapping mode AFM images were acquired with an Atomic Force Microscope from Agilent Technologies 5500 with the substrate immersed in 0.1 M HEPES buffer solution at pH 7.6. All images were recorded at room temperature employing rectangular silicon nitride cantilevers with a nominal spring constant of 0.72 Nm-1 and nominal resonant frequency of 70 kHz (Olympus OMCL-RC). Data acquisition and analysis were performed using PicoView 1.3 (Agilent Technologies) and WSxM 5.0 Develop 8.0 (NanoTech), respectively.[4-5]

2.4. Characterization methods of scaffolds

2.4.1. Pore size and porosity

Scanning electron microscopy (SEM) was exploited to evaluate the morphology of the scaffolds which are mounted onto aluminium stubs using black carbon tapes and sputter coated with gold (Sputter Coater Q150TES, Quorum, Italy). The specimen surface was examined using high resolution SEM (FEI, Quanta 200, UK) at a pressure of 0.1 m Torr at an accelerating voltage of 10 kV.

The scaffold porosity was evaluated by two different methods: the density method and the water squeezing method.

The density method measures the scaffold density with weight and volume of dried scaffold; and from the scaffold density, the porosity is calculated.2 Firstly, the density of the scaffold (ρ) was determined with the following equation:

$$\rho = W/V$$

where

W is the weight of the scaffold,

V is the volume of the scaffold (depending on its shape).

The density was divided by theoretical density of the material determined from the different weight fraction (Xi) and the different theoretical density of the reagents:

$$\rho_{theoretical} = (\rho_{theoretical(A)} \times X_A) + (\rho_{theoretical(B)} \times X_B)$$

Finally, the total porosity of the scaffolds was calculated as described in the equation below.

The values were expressed as the mean ± standard error and the number of replicates (n) was three (n=3). total porosity (%) =100−(ρtheoretical×100)

The water squeezing method measures the amount of water inside a scaffold before and after scaffold squeezing.3 The method is based on the principle that the water is present in small and big pores inside the polymer network. The water in its latter form is relatively free and represents the porosity requirement for the cell penetration and proliferation. The method measures the macropores volume percentage with the following procedure: the scaffold was equilibrated in deionized water for one hour and weighed (Mswollen), subsequently; it was squeezed to remove the water filling the pores and weighed again (Msqueezed).

Macropores volume was calculated using the following equation:

$$\text{Macropores volume percentage} = \frac{(\text{Mswollen} - \text{Msqueezed})}{\text{Mswollen}} \times 100$$

The values were expressed as the mean ± standard error (n=3).[1-2]

2.4.2. Swelling and degradation test

For the evaluation of the swelling degree cylindrical samples (Ø = 9 mm, h = 4mm) were weight and put in phosphate buffered saline solution (pH 7.4) at 37° in a shaking incubator. [2] At various times, samples were drained superficially by gentle contact with a filter paper and weighed again. The swelling percentage was calculated as:

$$Swelling = \frac{Ws - Wi}{Wi}$$

where

Wi is the initial weight of dry sample

Ws is the sample weight after swelling.

For the degradation degree, at the same way, the samples were weighed and put in phosphate buffered saline solution (pH 7.4) at 37° in a shaking incubator. [6] At various times they were removed, freeze-dried and weighed again. The degradation degree, as percentage of weight remaining, was calculated as:

$$Degradation(\%) = \frac{Wo - Wd}{Wi} X100$$

where

Wo is weight of dried sample before degradation test

Wd is weight of dried sample at the end of the degradation test.

The values were expressed as the mean ± standard error (n= 5).[1-2]

2.4.3. In vitro biological evaluation

Some of cell culture experiments illustrated in this Ph.D. thesis were carried out in collaboration with the biological group of Institute of Science and Technology for Ceramics, ISTEC-CNR, Faenza, Italy (Dr. Silvia Panseri and Dr. Monica Montesi).

2.4.3.1 Biological tests

An *in vitro* preliminary study was carried out investigating the effect of the two drugs-medicated MgHA/Coll 70/30 scaffolds on cell viability and proliferation. For the *in vitro* experiment, two different procedures were carried out, in order to evaluate the effect of the released drugs on cell viability. 2D and 3D *in vitro* culture were analysed at different time setting points.

2.4.3.2 Cell Culture

MG63 Human Osteoblast-like Cell Line purchased from American Type Culture Collection (ATCC® CRL-1427™) were cultured within standard medium composed by Dulbecco's Modified Eagle Medium/F-12 Nutrient Mixture (DMEM/F-12) with Glutamine (GlutaMAX) (Gibco), supplemented with 10% Foetal Bovine Serum (FBS) and 1% Penicillin-Streptomycin (Pen/Strep) (100 U/mL-100 µg/mL). The cultures were kept in an incubator at 37 °C, 5% CO_2 atmosphere and controlled humidity conditions. The cells were detached from culture flasks by trypsinization and centrifuged. The cell number and viability were defined with Trypan Blue Dye Exclusion Test.

2.4.3.3 Scaffold treatment and cell seeding

For the *in vitro* preliminary study, the cells were cultured in standard 2D conditions. In brief, cells were seeded with $2.5 \cdot 10^4$ cells/well and treated with free GNT (25 mg/mL) and VNC (50 mg/mL). In order to maintain the ratio of volume used for the study of kinetic release, 2 mL/well and 5 mL/well of culture medium

were added to cell culture with GNT and VNC medication, respectively, and the analysis was carried out at 24 and 72 hours by using not treated cells (cells only) as negative control.

For the 3D *in vitro* experiment, MgHA/Coll 70/30 scaffolds were washed and sterilized by performing > 25 kGy γ-ray irradiation. The dry scaffolds were loaded with Gentamicin (50 mg/mL) and Vancomycin (25 mg/mL) by carefully dropping 100 µL of drug solution on material upper surface, followed by 10 minutes incubation at 37 °C, 5% CO_2 and controlled humidity conditions, then a density of $5.0 \cdot 10^4$ cells/scaffold were seeded by dropping 20µl of cell suspension on the scaffold surface. From now, the scaffolds with this treatment were named loaded scaffolds. In order to access the cytocompatibility of the scaffolds after the releasing of the drugs, a group of scaffolds were also evaluated after GNT and VNC release. Briefly, the dry scaffolds were loaded with the same amount of the drugs before mentioned and then incubated for 7 days with 2 mL/well and 5 mL/well PBS 1X for GNT-loaded scaffold and VNC-loaded scaffold, respectively. The PBS 1X was changed every day. After 7 days, $5.0 \cdot 10^4$ cells/scaffold were seeded by dropping 20µl of cell suspension on the scaffold surface. From now these scaffolds were named unloaded scaffolds.

For both the loaded and unloaded scaffolds after the cell seeding the samples were incubated for 30 minutes at 37°C and controlled humidity allowing cell pre-adhesion before standard culture medium addition. The scaffolds analysis was carried out at day 1 after cell seeding, by using the no-medicated scaffolds as control. The scaffolds were kept in an incubator at 37 °C, 5% CO_2 atmosphere and controlled humidity conditions. All cell handling procedures were performed under laminar flow hood and in sterility conditions.

2.4.3.4 MTT Assay

A preliminary quantitative analysis of the *in vitro* 2D cell culture systems was carried out by performing the cell viability and proliferation MTT Assay by using no-treated cells as negative control, according to manufacturer's instructions. In brief, MTT reagent [3-(4,5-dimethylthiazol-2-yl)-2,5-diphenyltetrazolium bromide] (5 mg/mL) was firstly dissolved in Phosphate Saline Buffer 1X (PBS 1X). At each time point (24 and 72h of culture), the cells were incubated with 10% well-volume MTT solution for 2 hours at 37 °C, 5% CO_2 and controlled humidity conditions. Then the media were gently removed and substituted with Dimethyl Sulfoxide (DMSO) dissolving insoluble formazan crystals derived from MTT conversion. After 15 minutes incubation under constant slight stirring conditions, the absorbance was read at 570 nm by using a Multiskan FC Microplate Photometer (Thermo Scientific). The values of absorbances proved the concentration of formazan, which is directly proportional to the number of live cells in each well. N. 2 samples for each group were analysed in technical triplicate.

2.4.3.5 PrestoBlue Assay

Quantitative cell viability and proliferation analysis of the two groups of the scaffolds (loaded and unloaded) was carried out by performing PrestoBlue™ Cell Viability Reagent (Invitrogen) according to manufacturer's instructions as follows. In brief, after 1 day of culture the scaffolds were incubated with 10% PrestoBlue Reagent for two hours at 37 °C, 5% CO_2 atmosphere and controlled humidity conditions. After incubation the media were transferred in 96 well-plate (200 μL/well) for the detection of the fluorescence at excitation and emission wavelength

of 544 and 590 nm, respectively, by using the Fluoroskan™ Microplate Fluorometer (Thermo Scientific). The values of RFU (Relative Fluorescence Units) proved the concentration of reduced resazurin-based PrestoBlue reagent from live cells, which is proportional to the fluorescent red colour-change in each well. For the test n. 3 samples for each group were analysed in technical triplicate.

2.4.3.6 Live/Dead Assay

Qualitative cell viability and cytotoxicity analysis of the two groups of medicated scaffolds was performed via Live/Dead Assay, allowing to discriminate live from dead cells by simultaneously staining the esterase activity and the loss of plasma membrane integrity, respectively. In brief, at day 1 of culture, the Live/Dead Assay Kit (Invitrogen) was performed, according to manufacturer's instructions. The scaffolds were washed in PBS 1X for 5 minutes before incubation with Live/Dead solution composed by PBS 1X supplemented with acetoxymethyl calcein (AM-calcein) 2 μM and Ethidium homodimer-1 (EthD-1) 4 μM for 15 minutes at 37 °C in dark conditions. The samples were washed and rinsed in PBS 1X before the image acquisition at the inverted Ti-E fluorescent microscope (Nikon). For each group of treatment, one scaffold was analysed for Gentamicin and Vancomycin, respectively.

2.4.3.7 Statistical analysis

The results of MTT and PrestoBlue Assays were elaborated by performing the two-way analysis of variance (ANOVA) test and w\ere expressed as mean ± standard error of the mean (SEM) plotted on graph. The results were analysed by using the

Tukey and Sidak's multiple comparisons test as *post-hoc* test for MTT and Presto Blue Assay, respectively. Statistical analyses were performed by the GraphPad Prism software (version 6.0).

2.5 Microbiological tests

To assess the antibacterial activity of the eluted drugs, each scaffold formulation was placed in 2 ml of PBS solution and the liquid sample recovered after 24h of incubation at 37°C was tested by means of standardized sensitivity tests based on Kirby-Bauer (KB) diffusion method.[7-8]

2.5.1 Bacterial strains

The *in vitro* antibacterial property of the released drugs was evaluated against a panel of Gram positive and Gram negative reference bacterial strains obtained from the American Type Culture Collection and including *Staphylococcus aureus* (ATCC 25923), *Staphylococcus epidermidis* (ATCC 12228) and *Pseudomonas aeruginosa* (ATCC 27853).

2.5.1.1 Evaluation of drug functionality after loading and release from the hybrid scaffold

The inhibitory activity of the samples, containing the released drugs from the hybrid scaffold, was evaluated by measuring the diameters of the bacterial-free zone obtained in KB disk diffusion assay. For the analysis, each bacterial suspension was prepared in PBS solution and adjusted to an approximate optical

density (at 630 nm) of 0.08−0.1. The working solution was inoculated on the surface of the Mueller-Hinton agar plate (MHA) (Sigma-Aldrich), then sterile paper disks (Ø= 6 mm) were loaded with 10 µL of the eluted drugs, and lean on the agar surface. As controls, paper disks containing 10 µg of vancomycin hydrochloride and 10 µg of gentamicin sulphate (Sigma Aldrich-Merck, Germany) were included in all experiments. After 24 h of incubation at 37°C the agar plate was observed and the diameter of the inhibition zone was measured to the nearest whole millimeter with a ruler. All experiments were performed on duplicate in different days.

---

(1) Campodoni E. Design and development of bio-hybrid multifunctional materials for regenerative medicine (University of Parma 2018)

(2) Savini Elisa. *Design and development of biomineralized nanostructured devices from natural sources for biomedical applications*. (University of Bologna, 2016).

(3) Muñoz-Almagro, N., Rico-Rodriguez, F., Villamiel, M., & Montilla, A. (2018). Pectin characterisation using size exclusion chromatography: A comparison of ELS and RI detection. *Food chemistry*, *252*, 271-276.

(4) Partouche D. et al. (2018) Techniques to Analyze sRNA Protein Cofactor Self-Assembly In Vitro. In: Arluison V., Valverde C. (eds) Bacterial Regulatory RNA. Methods in Molecular Biology, vol 1737. Humana Press, New York, NY.

(5) Durante-Rodríguez G, Gutiérrez-del-Arroyo P, Vélez M, Díaz E, Carmona M. Further Insights into the Architecture of the P_N Promoter That Controls the Expression of the *bzd* Genes in *Azoarcus*. *Genes*. 2019; 10(7):489.

(6) Gostynska, N. *et al. 3D porous collagen scaffolds reinforced by glycation with ribose for tissue engineering application.* Biomed. Mater. **12**, (2017).

(7) EUCAST: The European Committee on Antimicrobial Susceptibility Testing, Breakpoint Tables for Interpretation of MICs and Zone Diameters, Version 6.0, 2016. http://www.eucast.org

(8) Clinical and Laboratory Standards Institute, Performance Standards for Antimicrobial Susceptibility Testing; Twenty-fifth Informational Supplement, CLSI document M100-S25 (2015).

CHAPTER 3

Medicated hydroxyapatite/collagen hybrid bone graft for local antimicrobial therapy preventing bone infection.

3.1 INTRODUCTION

The common thread of this research is based on a hybrid biomaterial fully bioresorbable previously designed as a graft for bone defects and developed by following a biomimetic approach, allowing to achieve a composition perfectly matching with that of the damaged tissue and that demonstrated its potential in bone tissue regeneration.[1-2-3] This family of biomimetic medical devices recreate in vivo a functional microenvironment able to recruit autologous cells and stimulate the whole regenerative process. Besides, as side effects, these well integrated systems can also facilitate the growth of microbes having the potential to adhere to the implanted material and develop biofilms, causing implant failure. In particular this chapter was focused on two pathologies that can afflict bone tissue and which still today present treatments that often fail:

(1) bone infections, resulting in osteomyelitis. The primary pathogens associated with orthopedic surgery are both Gram positive, such as Staphylococcus aureus (SA) and Staphylococcus epidermidis (SE), and gram negative such as Pseudomonas aeruginosa.[4-5]

(2) osteosarcoma the most common type of primary bone cancer which interests children and adolescents [6] as well as the old people [7], especially affecting the long bones, dangerous because of the fast metastasis. [8] The treatment against infection or to reduce the risk of ones include systemic drug administration leads to poor delivery to the site

of infection, particularly in or near the bone, and thus to its overall performance. Furthermore, their toxicity excludes the possibility of increasing the dosage of antibiotics to avoid off-target effects and also to reduce the risk of resistance in the target bacteria. The osteosarcoma treatment procedure includes surgery matching with different chemotherapeutic agents and radiotherapy, implying toxicity and the well-known side effects of anticancer therapy.[9-10]

It is now clear that promising new approaches need to be explored to address this challenge. To mitigate these events, a potential solution is the local route of administration, which offers unprecedented new possibilities for effective in situ therapy (1) for pre-existing infections and for a reduction in the incidence of implant failure due to contamination during surgery, and (2) as a support to anticancer therapies, to try to reduce them. In particular for this second point the local therapy should assist the surgery and reduce the chemotherapy and radio therapy, when the sarcoma is removed, the bone tissue is damaged and could present some tumor cells survive.[11-12] In this case the application of a medicated biomaterials loaded with anticancer drugs, could avoid the survival of the residual cancer cells and regenerate the damaged tissue.[13-14] The study about infections was conducted by involving vancomycin hydrochloride (VNC) a broad-spectrum antibiotic, typically administered intravenously, which is able to penetrate most body tissues and one of the few antibiotics that is effective against SA. Due to increasing resistance, vancomycin is frequently used in combination with gentamicin sulfate GNT, an aminoglycoside antibiotic, which has a broad bacterial spectrum (Gram positive and negative) and for these reasons selected as second antibiotic to be involved in this study.

About osteosarcoma, it is decided to employ folic acid (FA), molecule like of methotrexate, due to cancerogenic characteristics of the methotrexate. Methotrexate is an anticancer

drug and an antimetabolite of the antifolate type. It competitively inhibits dihydrofolate reductase (DHFR), an enzyme that participates in the tetrahydrofolate synthesis and block the uncontrolled growth of cancer cells. The affinity of methotrexate for DHFR is about 1000-fold that of folate.[15]

In particular this chapter is divided in three main goals:

(1) medication of hybrid MgHA/coll scaffolds with GNT and VCN end evaluation of their release kinetics in PBS and 37°C.

Here we have explored the combination of highly biomimetic materials, made of type I collagen biomineralized with bioresorbable Mg-doped hydroxyapatite (MgHA) conceived for bone regeneration, with the selected antimicrobial agents, studied their release kinetics and the preservation of the antimicrobial activity of therapeutics after loading. Samples with different amount of MgHA (0, 50, 60 and 7 0wt%) have been prepared and tested to investigate its influence in linking drugs and in release timing. The preparation and the uptake of the antibiotic formulations under clinical conditions were simulated by dripping the drug solutions onto the biomaterials exploiting its well asses swelling capacity. For the drug release evaluation, the loaded biomaterial was dipped in PBS solution at 37°C and the concentration of the antibiotic was measured at specific time-points in the eluted medium. This method allows to measure the release behavior of different drugs and assess their interaction whit the considered hybrid biomaterial.

The antibacterial activity and function preservation of the antibiotics, after loading on the biomaterial and releasing in the aqueous solution, is monitored. For this, antimicrobial evaluations were performed by following the procedures established by a number of committees, [16-17] testing different microbes potentially hazardous during orthopedic procedures. The cytotoxicity of medicated scaffold was assessed by in vitro

tests performed with human osteoblast-like cells and they acquire the known characteristics of cytocompatibility, after unloading show no cytotoxic effect.

(2) medication of hybrid MgHA/coll scaffolds with folic acid end evaluation of its release kinetics in PBS and 37°C.

The biomimetic hybrid material MgHA/coll, mentioned above, was synthesized with different percentages of MgHA (0, 30, 50, 60 and 70 wt%) and stabilized with different crosslinking treatments (thermal treatment and chemical crosslinking with BDDGE) to investigate not only the involvement of hydroxyapatite in the control of release profile, but also the effect of the crosslinking process. The medication of the scaffolds by absorption of folic acid was achieved by dripping the drug solutions onto the biomaterials, exploiting their high swelling capacity. Also, in this case, for the evaluation of drug release, the loaded biomaterial was immersed in a PBS solution at 37 ° C and the antibiotic concentration was measured at specific time points in the eluted medium, using UV spectroscopy.

(3) Development of drug loaded polymeric microbeads as a tool to increment the amount of loaded drug into the hybrid scaffolds.

Preliminary studies were carried out on alginate (Alg) microbeads loaded with gentamicin (GNT). The Alg particles were synthesized by dripping an alginate solution in an aqueous calcium chloride solution. Calcium ions react immediately with Alg generating an insoluble salt (Ca-Alg) and performing a sort of crosslinking of the alginate. To evaluate the influence of hydroxyapatite on drug release, also composite particles made of alginate added with hydroxyapatite (Alg:HA wt ratio 80:20) were synthetized. For the evaluation of drug release, the loaded particles were immersed in a PBS solution at 37°C

and the antibiotic concentration was measured at different time points in the eluted medium, using UV spectroscopy.

These drug-loaded microbeads are conceived as a tool to be incorporate into the hybrid scaffold to allow a more controlled and sustained release, thus to make it suitable for preventing infections in the following weeks after surgery and also for treating pre-existing infections.

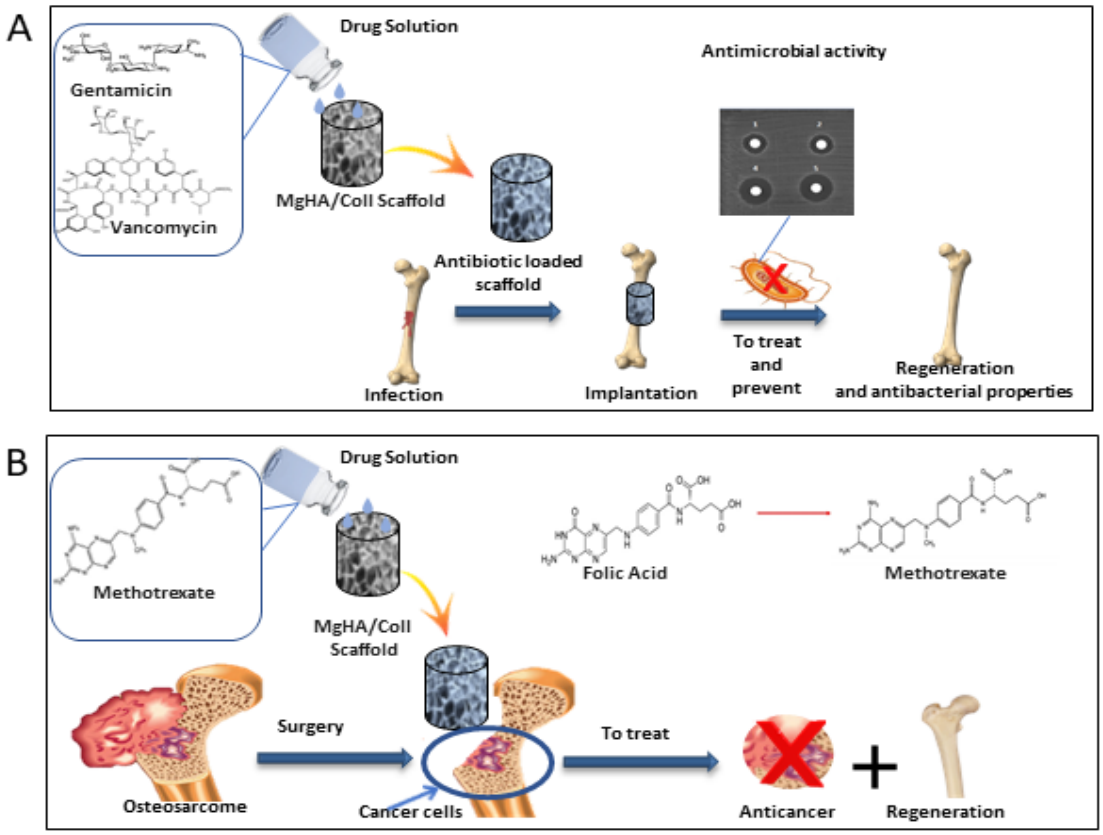

Figure 3.1 *Schematic representation of the goals of this research. A) Medicated bone hybrid scaffold for local antibiotic delivery, to prevent infections during surgeries. B) Medicated bone hybrid scaffold for local chemotherapy delivery. The tumor is removed with surgery and the damaged tissue is treated with a medicated bone scaffold to remove residual cancer cells and guide bone tissue healing and regeneration.*

3.2. MATERIALS AND METHODS

Development of hybrid scaffolds with different MgHA/Coll ratio

Different hybrid materials were prepared varying the collagen and magnesium-doped hydroxyapatite (MgHA) ratio from 0% to 70 wt %.

Synthesis of MgHA/Coll scaffold (70/30 wt.%)

150 g of equine tendon derived Type I collagen 1 wt.% in acetic buffered solution (pH 3.5) (Opocrin SpA, Modena, Italy) were added to a 300 ml of phosphoric acid aqueous solution (2,40 g of H_3PO_4 85 wt.% pure Sigma Aldrich- Merck, Germany) to obtain a homogenous acid collagen suspension. A basic suspension was prepared with 2,71 g of calcium hydroxide ($Ca(OH)_2$, 95% pure, Sigma Aldrich-Merck, Germany) in 300ml of water under constant and vigorous stirring. Once formed homogeneous suspension, 0,35 g of Magnesium Chloride ($MgCl_2 \cdot 6H_2O$, Sigma Aldrich-Merck, Germany) were added and stirred. The acid dispersion was slowly poured in the basic suspension, shaking manually to guarantee a better fibres desegregation. After 2 hours at room temperature, the obtained hybrid hydrogel was filtered and washed for three times with MilliQ water to eliminate the residues of reaction. The MgHA/Coll slurry was filled into a polystyrene well-plate and lyophilized by consecutive freezing (at -40°C) and drying at (20°C) for 48 h under constant vacuum of 0,086 mbar (5Pascal, LIO 3000 PLT, Italy).

Synthesis of MgHA/Coll scaffold (60/40 wt.%)

150 g of equine tendon derived Type I Collagen 1 wt.% in acetic buffered solution (pH 3.5) (Opocrin SpA, Modena, Italy) were added to a 300 ml of phosphoric acid aqueous solution (1,55 g of H_3PO_4 85 wt.% pure Sigma Aldrich-Merck, Germany) to obtain a homogenous acid collagen suspension.

A basic suspension was prepared with 1,74 g of calcium hydroxide ($Ca(OH)_2$, 95% pure, Sigma Aldrich-Merck, Germany) in 300 ml of water under constant and vigorous stirring. Once formed homogeneous suspension, 0,22 g of Magnesium Chloride ($MgCl_2 \cdot 6H_2O$, Sigma Aldrich-Merck, Germany) were added and stirred. The acid dispersion was slowly poured in the basic suspension, shaking manually to guarantee a better fibres desegregation. After 2 hours at room temperature, the obtained hybrid hydrogel was filtered and washed for three times with MilliQ water to eliminate the residues of reaction. The MgHA/Coll slurry was filled into a polystyrene well-plate and lyophilized by consecutive freezing (at -40°C) and drying at (20°C) for 48 h under constant vacuum of 0,086 mbar (5Pascal, LIO 3000 PLT, Italy).

Synthesis of MgHA/Coll scaffold (50/50 wt.%)

150 g of equine tendon derived Type I Collagen 1 wt.% in acetic buffered solution (pH 3.5) (Opocrin SpA, Modena, Italy) were added to a 300 ml of phosphoric acid aqueous solution (1,03 g of H_3PO_4 85 wt.% pure Sigma Aldrich-Merck, Germany) to obtain a homogenous acid collagen suspension. A basic suspension was prepared with 1,16 g of calcium hydroxide ($Ca(OH)_2$, 95% pure, Sigma Aldrich-Merck, Germany) in 300 ml of water under constant and vigorous stirring. Once formed homogeneous suspension, 0,15 g of Magnesium Chloride ($MgCl_2 \cdot 6H_2O$, Sigma Aldrich-Merck, Germany) were added and stirred. The acid dispersion was slowly poured in the basic suspension, shaking manually to guarantee a better fibres desegregation. After 2 hours at room temperature, the obtained hybrid hydrogel was filtered and washed for three times with MilliQ water to eliminate the residues of reaction. The MgHA/Coll slurry was filled into a polystyrene well-plate and lyophilized by consecutive freezing (at -40°C) and drying at (20°C) for 48 h under constant vacuum of 0,086 mbar (5Pascal, LIO 3000 PLT, Italy).

Synthesis of MgHA/Coll scaffold (30/70 wt.%)

150 g of equine tendon derived Type I collagen 1 wt.% in acetic buffered solution (pH 3.5) was purchased from Opocrin SpA, (Modena, Italy) is weighted and is added to thread of phosphoric acid (H_3PO_4) diluted in water 0,04 M, manually (0,44g in 300ml) shaking to obtain an acid collagen suspension. 0,5 g of calcium hydroxide ($Ca(OH)_2$) is dispersed in water under constant and vigorous stirring. Once formed homogeneous suspension, 0,064 g of Magnesium Chloride is added ($MgCl_2$). The acid dispersion has slowly poured in the basic suspension, shaking manually. After 2 hours at room temperature, the hydrogel is filtered and washed for three times with water to eliminate the residues of the reaction. The MgHA/Coll slurry is filled into a polystyrene well-plate and lyophilized by consecutive freezing (at -40°C) and drying at (20°C) for 48 h under constant vacuum of 0,086 mbar (5Pascal, LIO 3000 PLT, Italy).

Synthesis of pure collagen scaffold (Coll)

150 g of equine tendon derived 1 wt.% in acetic buffered solution (pH 3.5) (Opocrin SpA, Modena, Italy) were treated with a basic aqueous solution of NaOH (0,1 M, Sigma Aldrich-Merck, Germany), added until the achievement of the isoelectric point of collagen (pI 5.5) to induce the precipitation of collagen due to fibers assembling. The mixture was kept for fibers maturation at room temperature for 2 hours. The precipitated collagen was filtered with a metallic sieve (150 µm) and washed three times with MilliQ water. The washed hydrogel was poured in polystyrene 96-multiwell and lyophilized by consecutive freezing at (-40°C) and drying at (20°C) for 48 h under constant vacuum of 0,086 mbar (5Pascal, LIO 3000 PLT, Italy).

Cross-linking treatments of hybrid scaffolds with different MgHA/Coll ratio (0-70 wt.%)

Two different cross-linking are chosen, a dehydrothermal cross-linking (DHT) and a chemical crosslinking with 1,4-Butanediol diglycidyl ether (BDDGE) to improve and modulate the scaffold preservation during the interaction and the release between scaffolds and active molecules.

Crosslinking with BDDGE - Hybrid scaffolds were crosslinked with 1wt.% and 2 wt.% of BDDGE respect to Collagen. BDDGE solution was added to the hybrid wet slurry before freeze-drying and the slurry with crosslinking solution was maintained at 25 ± 2◦C for 24 h and at 4 °C for 24h. Later the slurry solution was rinsed twice in milli-Q water to remove any residues and later freeze-dried using the same above-mentioned conditions. The MgHA/Coll and Coll slurry are filled into a polystyrene well-plate and lyophilized by consecutive freezing (at -40°C) and drying at (20 °C) for 48 h under constant vacuum of 0,086 mbar (5Pascal, LIO 3000 PLT, Italy).

DHT crosslinking: after freeze-drying, hybrid scaffolds were cross-linked through a heat treatment performed at 160 °C under vacuum (0.01 mbar) for 48h.

Scaffolds loading

For the preparation of medicated samples, the same procedure was followed for each scaffold composition:

1. (MgHA/Coll 70/30, 60/40, 50/50 wt% and Coll) and for both antibiotics, Vancomycin hydrochloride (Sigma Aldrich-Merck, Germany) (VNC) and Gentamicin sulphate (Sigma Aldrich-Merck, Germany) (GNT)

2. (MgHA/Coll 70/30, 60/40, 50/50, 30/70 wt% and Coll) and for Folic Acid (Sigma Aldrich-Merck, Germany).

To load a specific amount of drug, samples of the same weight (40 mg for each) and shape (cylinder 4x4 mm) were prepared and their maximum medium uptake capacity, was evaluated as about 100 µl. (8) The antibiotics were solubilized in Phosphate Buffer Saline (PBS, pH 7.4, Sigma Aldrich-Merck, Germany) to obtain drug solutions with a concentration of 25mg/ml for GNT, 50mg/ml for VNC and 1,3 mg/ml for Fol Ac. 100 µl of the prepared solutions were soaked in each scaffold so as to have 2,5 mg of GNT, 5 mg of VNC and 0,13 mg for Fol Ac in each scaffold.

Release tests started after 10 minutes from soaking, so as to have a homogeneous distribution of the drug in the whole scaffold. Each drug is tested independently. Details about the prepared and tested samples (scaffolds composition, type and amount of drug loaded) are reported in Table 1.

Samples composition (wt%)	Scaffold weight	Gentamicin loaded solution (mg/ml)	Vancomicyn loaded solution (mg/ml)	Folic Acid loaded solution (mg/ml)
MgHA/Coll 70/30	40 mg	25 mg/ml	50 mg/ml	1,3 mg/ml
MgHA/Coll 60/40	40 mg	25 mg/ml	50 mg/ml	1,3 mg/ml
MgHA/Coll 50/50	40 mg	25 mg/ml	50 mg/ml	1,3 mg/ml
MgHA/Coll 30/70	40 mg	-	-	1,3 mg/ml
Coll (100% collagen)	40 mg	25 mg/ml	50 mg/ml	1,3 mg/ml

***Table 1**. Description of developed and tested samples.*

Drug release from each scaffold formulation

To register the drug release kinetics, the loaded scaffold was placed in a test tubes with 2 ml of PBS solution (pH 7.4, Sigma Aldrich-Merck, Germany) and incubated at 37°C in dynamic conditions (oscillating and thermostatic plate) to better simulate the *in vivo* conditions. Measures of the released drug were done at predetermined time points (1 hour, 3 hours, 6 hours, 24 hours, 48 hours, 72 hours, 168 hours, 336 hours, 480 hours). A portion of the volume was collected (10 vol.%) and replaced with the same amount of fresh PBS solution every time. Quantitative analysis of the released drug was carried out with UV-Vis Spectrophotometer (NanoDrop™ One/One^{c} Microvolume) at 280 nm for VNC, 332 nm for GNT and 280 and 350 nm for Fol Ac. Measurements were repeated on 5 samples and performed in triplicate for each type of scaffolds. Not medicated scaffolds were used as reference.

For these experiments the quantification limit for VNC and GNT was determined and calibrations curve with standard solutions of drug were recorded.[18]

GNT functionalization for UV detection

GNT is not UV-visible thus, for its detection, was previously functionalized with a chromophore group.

Preparation of UV Reagent: 50 ml of acid solution of KCl (0,75 g) and boric acid (0,62 g) was prepared. At the same time, NaOH (0,48 g) was dissolved in 50 ml of water and poured in the acid solution to achieve a final pH of 8. Then were added 11,16 ml of methanol, 0,54 ml of mercaptoethanol and phtaldialdehyde (0,45g) and stirred overnight. The reactive was prepared in a dark bottle and freshly prepared each time before the analyses because it is photo sensible.[19-20-21-22] The GNT eluted

solution, after collection, was mixed with methanol and UV reagent in a volume ratio of 1:1:1 just before measurement with UV-Vis Spectrophotometer (NanoDrop™ One/One^{c} Microvolume).

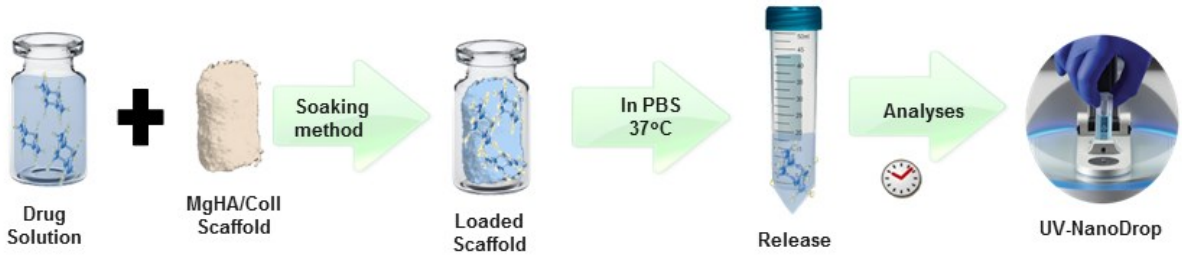

Figure 3.2 *Schematic representation of drug loading into the scaffold and setting of the release test. The concentration of drug release at various time points was evaluated by UV-Vis spectrophotometer.*

Release from alginate beads

A solution of 50 mg of gentamicin in 20 ml of water is prepared, then 1 g of sodium alginate (Sigma Aldrich) is added. The solution is stirred until completely dissolution. After that the solution is dropped in a solution of $CaCl_2$, 8 g dissolved in 100 ml of water. The alginate reacts very fast with Ca^{2+} ions forming a not soluble Alg-Ca salt and allowing the formation of beads. At predetermined time (5 minutes, 10 minutes and 30 minutes) the beads are collected and dried with two different procedures, some beads in the stove and some in the freeze drier. After beads preparation the residual $CaCl_2$ solution is analyzed to evaluate the concentration of the drug eventually released in the solution during the beads synthesis.

After drying, the beads are divided in tubes to have for each, 2,5 mg of GNT, PBS is added and is incubated at 37°C in a dynamic condition, to reproduce vivo

conditions. To analyse the antibiotic release, at a predetermined time, 1h, 3h, 6h, 24h, 48h for 21 days, a portion of the volume are collected (10%) and then are analysed with UV-Vis Spectrophotometer (NanoDrop™ One/One^{c} Microvolume). The gentamicin is not UV-visible, so was previously combined with UV chromophore reagent.

Release from HA/alginate beads

A solution of 50 mg of gentamicin in 20 ml of water is prepared, then 800 mg of sodium alginate and 200 mg of HA is added. The suspension is stirred until complete homogenization. The suspension is dropped in a solution of $CaCl_2$, 8 g dissolved in 100 ml of water. The alginate reacts very fast with Ca^{2+} ions forming a not soluble Alg-Ca salt and allowing the formation of composite beads (HA/Alg). At predetermined time (10 minutes and 30 minutes), the beads are collected and then dried in the stove. After beads preparation the residual $CaCl_2$ solution is analyzed to evaluate the concentration of the drug eventually released in the solution during the beads synthesis. After drying, the beads are divided in tubes to have for each, 2,5 mg of GNT, PBS is added and is incubated at 37°C in a dynamic condition, to reproduce vivo conditions. To analyse the antibiotic release, at a predetermined time, 1h, 3h, 6h, 24h, 48h for 21 days, a portion of the volume is collected (10%) and then analysed with UV-Vis Spectrophotometer (NanoDrop™ One/One^{c} Microvolume). The gentamicin is not UV-visible, so was previously combined with UV chromophore reagent.

3.3 RESULTS AND DISCUSSION

Evaluation of GNT and VNC release from hybrid scaffolds

Scaffold chemical-physical characterization

In this work, 3D hybrid biomaterials (MgHA/Coll) were synthetized through a biomineralization process allowing the nucleation of biomimetic MgHA nanoparticles on type I collagen fibers during their self-assembly.

Four different samples differing for MgHA content (from 0 to 70 wt.%) were prepared and their performance as drug delivery systems to prevent infection during surgery and avoid the onset of osteomyelitis was evaluated. The chemical and morphological characterization of the four prepared biomaterials was performed by FTIR spectroscopy, XRD, TGA and ESEM. In addition, vancomycin and gentamicin release kinetics were assessed and the antibacterial activity of eluted drugs was tested by inhibition zone assay performed on a panel of Gram positive and negative reference bacterial strains, that includes the primary pathogens associated with osteomyelitis. Finally, their effect on human osteoblast-like cell viability was studied.

In detail, these materials were developed by means of a neutralization reaction involving a basic suspension of calcium hydroxide, added with magnesium chloride, and an acid suspension of phosphoric acid, enriched with type I collagen. During the synthesis, the pH variation of reaction medium, from 10 to 6, drives the precipitation of the mineral phase nanoparticles and the self-assembling of collagen fibers.

These simultaneous processes enable to obtain a hybrid material where MgHA nanoparticles and collagen fibers are joined in a hybrid material that reproduces the same chemical feature of natural bone matrix. With the same reaction, performed by changing the relative ratio between collagen and reactants for MgHA synthesis, were developed scaffolds with different percentage of mineral phase from 70 wt% (MgHA/Coll: 70/30, 60/40, 50/50 wt.%) to 0 wt% (Coll). Before testing their loading and releasing abilities, all the specimens were chemical-physically and morphologically analysed.

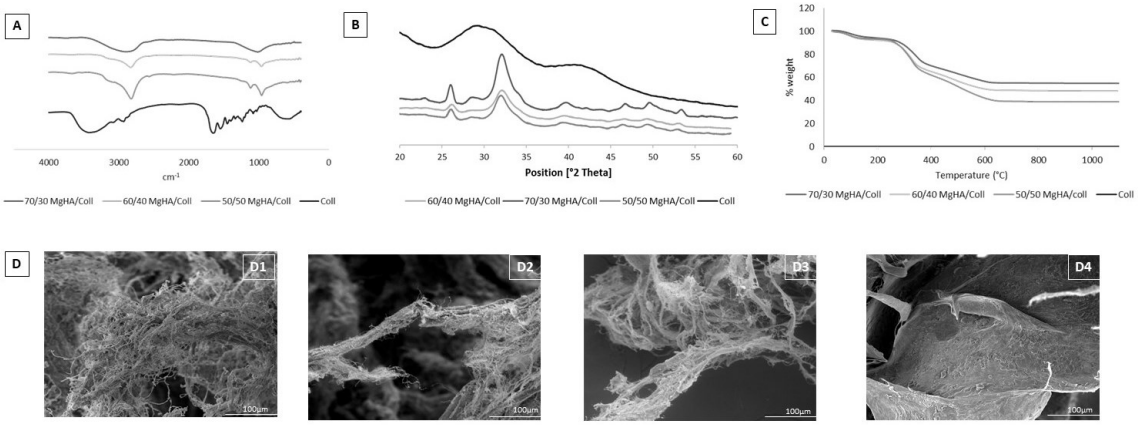

Figure 3.3. *Chemical-physical characterizations of the four different scaffold formulations (MgHA/Coll 70/30, 60/40, 50/50 and Coll). (A) FTIR analyses, (B) XRD diffractograms, (C) TGA analyses, (D) ESEM analyses: (D1) MgHA/Coll 70/30, (D2) MgHA/Coll 60/40, (D3) MgHA/Coll 50/50, (D4) Coll, show scaffolds porosity and a fibrous morphology typical of the collagen component, while (D1-D3) highlight the uniformly distribution of mineral MgHA nanoparticles.*

Examining FTIR spectra (Fig 3.3A), Coll sample is characterized by the typical peaks of amides (I, II, III) stretching and bending vibrations at 1640, 1545 and 1236 cm^{-1}, corresponding to the alpha-helical structure. It is important to note the

presence of a shoulder at 1713 cm^{-1}, which is representative of the ester bonds induced by dehydrotermal treatment.[23-24] The chemical interaction of mineral phase MgHA with collagen fibres are evidenced by the shift from 1340 cm^{-1} to 1337 cm^{-1} due to the chemical bond between carboxylic groups of collagen and Ca^{2+} ions of the apatite. The spectra revealed the characteristic peaks of phosphate ion PO_4^{3-} (474, 569, 602, 962, 1045 and 1091 cm^{-1}) and OH^- (633 and 3572 cm^{-1}) groups, corresponding to the typical hydroxyapatite peaks. While the bands at approximately 3497 and 1638 cm^{-1} indicate the presence of lattice water in the material. Both spectra of the hybrids MgHA/Coll samples exhibits similar peaks and bands, confirming the presence of the same interaction even by changing the ratio of MgHA.

For all MgHA/Coll samples, XRD analyses revealed the purity of the hydroxyapatite phase without detection of further secondary phases. The XRD spectra (Fig. 3.3B) exhibit broad reflections ascribed to hydroxyapatite with low crystallinity and nanosized dimensions. The low crystallinity of apatite, due to the biomineralization process, in particular to the low temperature during synthesis and the chemical interaction between the mineral MgHA particles and collagen molecules, indicates the achievement of a high biomimetic mineral phase.

The chemical composition of mineral components was quantitatively evaluated by ICP-OES indicating that all MgHA/Coll samples (70/30, 60/40 and 50/50 wt%) are characterized from a (Mg+Ca)/P molar ratio between 1.45 and 1.51, low respect to the typical Ca/P = 1.67 of stoichiometric apatites, and distinctive of substituted and low crystalline phase.

The effective mineral content in MgHA/Coll samples was assessed by thermogravimetric analysis (Fig. 3.3C). TGA curves exhibit three main weight loss steps: the first from 25°C to 170°C due to the release of adsorbed and bound water (7-8 wt.%), the second loss from 170 °C to 360 °C due to degradation of Type I collagen and the last, from 360 °C to 660 °C, due to the complete combustion of organic residues. The residual weights correspond to the mineral phase content, which were 55 wt.% for MgHA/Coll (70/30), 48 wt.% for MgHA/Coll (60/40) and 40 wt.% for MgHA/Coll (50/50). The tridimensional structure of samples was investigated with the ESEM (Fig. 3.3D), highlighting an isotropic structure with the presence of randomly distributed and interconnected macro- and micro-porosity. This property has an important role in stimulating bone regeneration since it facilitates cell adhesion, permeation and proliferation, as well as vascularization and extracellular matrix deposition in the whole scaffold. Allowing to oxygen, nutrients and metabolites to permeate in the structure is essential for a proper bone tissue growth and regeneration. At high magnification, on the wall of pores are clearly distinguishable the MgHA nanoparticles that are completely embedded and homogeneously distributed on the collagen fibers matrix. ESEM micrographies show that for all scaffolds compositions the porosity and the homogeneity were maintained, despite the different MgHA/Coll ratio.

Moreover, the interaction of the scaffolds was investigated with water medium, by study their degradation and swelling in the same conditions used for the drug release tests (37°C and PBS medium). From the charts in Fig. 3.4A and 3.4B is possible to observe the hydrophilic behaviour and the characteristic low degradability of these materials, lower than 7 wt% in 21 days, demonstrating the

suitability of the DHT cross-linking process in improving the stability of the 3D hybrid structures.

Both these properties, controlled to guaranty the right persistency of the scaffold in vivo and fundamental to assist the completion of the regenerative process, have an important role also in the drug loading capacity and release behaviour: hydrophilicity allows to have great water up-take and the low degradation determines good drug retention.

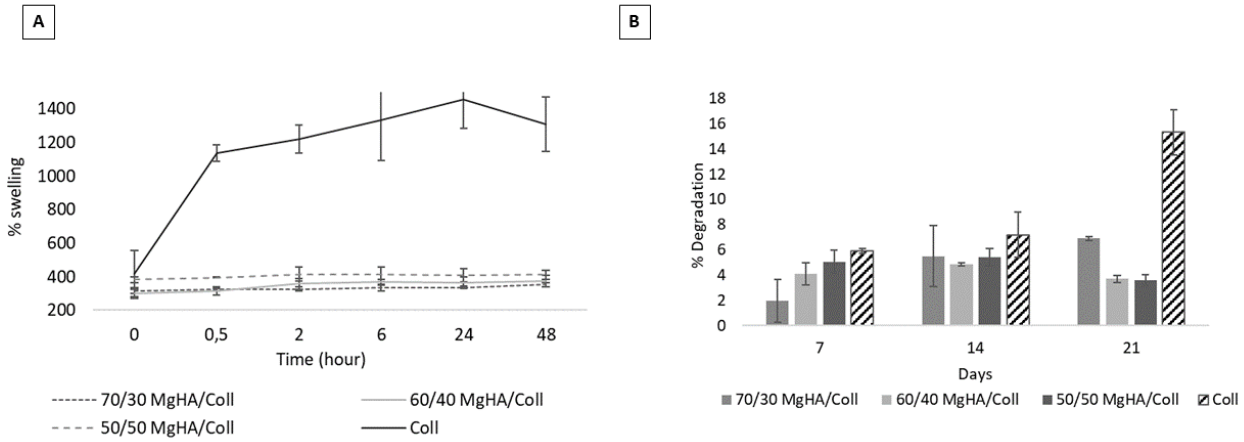

Figure 3.4 *(A) Evaluation of swelling capability, in PBS and 37°C, of all the developed dried materials (MgHA/Coll 70/30, 60/40, 50/50 e Coll). (B) Evaluation of percentage of scaffold degradation in PBS and 37°C.*

Scaffold loading and release test

Taking advantage from swelling properties and the highly porous structure of these hybrid materials, the antibiotic loading process is performed by soaking, thus to be easy and reproducible in the operating room: the medium volume, that each scaffold is able to absorb, is measured, then employed to dissolve the drug, and finally the solution is soaked on the material.

Because VNC and GNT are water soluble, this procedure is applied for both and is able to guarantee the total absorption of the solution and the loading of exactly known amount of drug. This simple and fast procedure, results in an adequate time for the implant preparation, in terms of antibiotic loading, prior to surgery.

Different amounts of GNT and VNC were selected to be loaded on the scaffold, decided considering different important aspects. The most important is that relative to the minimum inhibitory concentration (MIC), that is typical for each drug and about 4 ml/L for GNT and ≤2 ml/L for VNC, variable depending from the site of infection and of the nature of bacteria that must be treated. It is important that the initial release is significantly above the MIC level locally to prevent bacterial adhesion leading to the establishment of infection. Furthermore, considering the experimental setup and the used diagnostic technique was decided to load 2.5 mg of GNT and 5 mg of VNC on each scaffold thus to obtain concentrations of the drugs, in the elution medium, over the limit of detection of UV-Vis Spectrophotometer (NanoDrop™ One/One^{c} Microvolume).

Release tests were performed with an experimental setup reproducing the physiological conditions, PBS medium at 37°C and under constant and slow oscillation. At specific time-points (from 0 to 480 hours) the 10 vol.% of the total PBS was collected and replaced with the same amount of fresh PBS solution every time. This procedure was selected to guarantee a dynamism in the elution environment mimicking the exchange of physiological fluid during and after surgery. The experiment was monitored until 480 h (20 days) and the collected measurements enabled the registration of an elution chart reported in Fig.3.5.

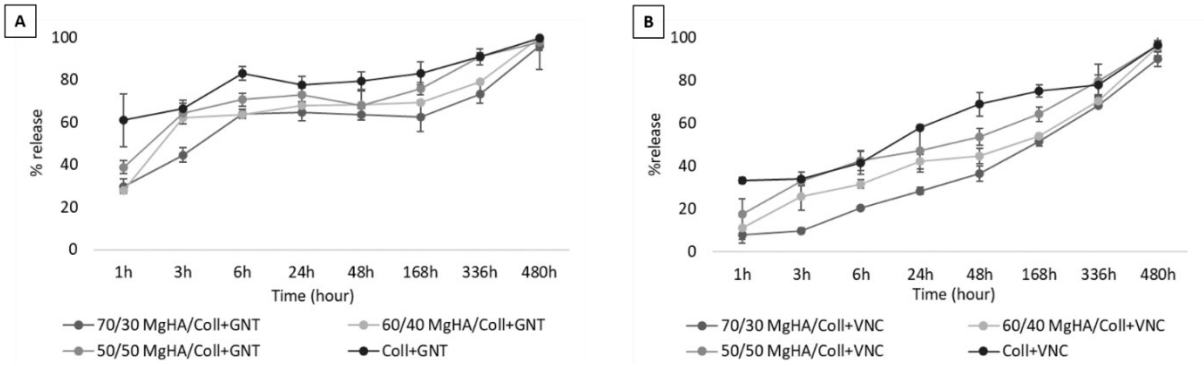

Figure 3.5. *Gentamicin and Vancomycin release kinetics at 37 °C and PBS, from the different compositions of MgHA/Coll hybrid scaffolds loaded with (A) 2.5 mg of Gentamicin and (B) 5.0 mg of Vancomycin, recorded from time zero to 20 days.*

Graphs in Fig. 3.5 (A) highlighted a quite fast elution of GNT from the three hybrid scaffolds compositions (MgHA/Coll: 70/30, 60/40, 50/50 wt.%) constantly increasing up to 6hs, delivering about the 67 wt.% of the total drug and showing a typical burst release trend. Then, the residual 33 wt.% of GNT, was slowly and gradually released until 20 days. While, Coll scaffold, released the 60 wt.% of GNT in only 1h and above 80 wt.% in 6hs, highlighting a poorly retention property. Since the drug is not encapsulated in the scaffold, but loaded by absorption, weak bonds with the device are formed and delivery follows a burst release in the first few hours, resulting in an adequate concentration for an effective antibacterial activity during the early postoperative period.

Instead, elution graphs of VNC show a slower and gradual release of drug until 20 days, thus it can't be classified as burst release. Both these results clearly demonstrate that MgHA, due to its well know affinity for organic molecules, provides binding capability respect to the tested drugs and the percentage of apatitic phase exposed at the surface of the collagen matrix, influenced the drug

release kinetics from the hybrids, prolonging the release timing. In fact, Fig. 3.5 (A) and (B), clearly shows that the scaffold with the major ratio of MgHA (MgHA/Coll 70/30) having many binding sites respect to the others, elute both the drugs more slowly respect the two other hybrid scaffold compositions (60/40 and 50/50). This also explains why Coll in both cases showed a faster antibiotic release as compared to the hybrid MgHA/Coll materials.

Anyway, some clear differences can be perceived which confirm a stronger interaction between MgHA and VNC instead of GNT. This behavior is more clearly evident in Fig. 3.6 and could be explained considering their different chemical formula, 3D structure and size of molecules, responsible for different steric hindrance and therefore of different chemical interaction with the material surface.

All these achievements confirmed the good properties of degradation and swelling of the developed hybrid scaffolds, and that these materials expose at the surface the mineral phase particles representing an effective active binding sites important for the adsorption and further release of drug molecules, ensuring suitable for a local pharmaceutical delivery.

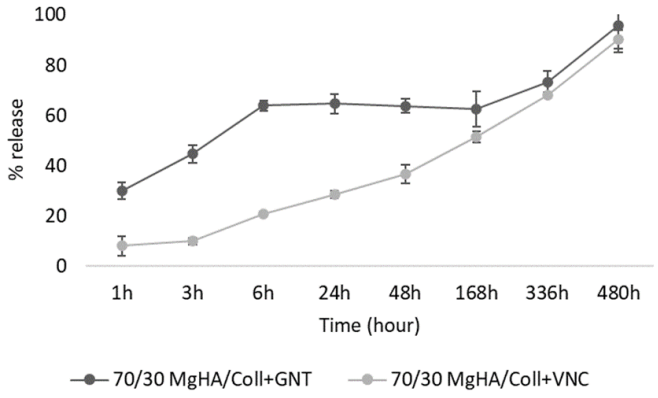

Figure 3.6: *Comparison of the release profile for GNT and VNC from MgHA/Coll 70/30 wt% scaffolds*

These considerations highlighted that the release didn't depend only from the scaffold composition but for sure also from the organic chemistry of the various drugs loaded over the material, resulting in different interactions and therefore different delivery profiles. This means that the loading and delivery procedure must be re-validated for each type of selected drug molecule.

Moreover, the amount of drug loaded on the device must be optimized depending from the medical situation, if low amounts of drug (however above the MIC) could be enough when the objective is to prevent the enlargement of infection during the first period after the surgery, they are not sufficient for an eradication of preexisting bone infections or biofilms caused by resistant bacteria. In all those cases, specific and higher therapeutic concentrations may be required, typically in the order of a 1000-fold higher than conventional. [25-26]

Microbiological study by disk diffusion method

The antibacterial properties of the GNT and VNC released from the hybrid scaffold were evaluated *in vitro* by measuring the clear bacterial-free zone around the paper disks filled with 10 μl of the eluted drugs. Results are reported in Table 2.

Reference strains	VNC	VNC 10 μg[b]	GNT	GNT 10 μg[b]
S. aureus ATCC 25923	14 ± 1	14 ± 1	18 ± 1	18 ± 1
S. epidermidis ATCC 12228	15 ± 1	15 ± 1	23 ± 1	22 ± 1
P. aeruginosa ATCC 27853	NA	NA	17 ± 1	18 ± 1

[a]NA, not appeared as expected because VNC is generally ineffective against Gram negative bacteria; [b]Disks containing vancomycin hydrochloride or gentamicin sulfate used as positive controls.
All experiments were performed on duplicate, on different days.

Table 2. *Antibacterial activity: diameter of the inhibition zone (in millimeter) against ATCC reference strains*

Considering the amounts of drug loaded on the hybrid scaffold and the drug concentrations released in the PBS solution, results demonstrate the effectiveness of the samples to inhibit the bacterial growth of all susceptible strains. No differences were observed in terms of inhibition zone diameters between samples containing the drugs loaded/released from the materials and samples containing the corresponding amount of pure drugs. As expected, (Fig. 3.7), VNC and GNT diffuse through the agar maintaining their potencies towards the selected bacteria, indicating that the scaffolds made of MgHA/Coll 70/30 are suitable to preserve the antibiotic drug activity.

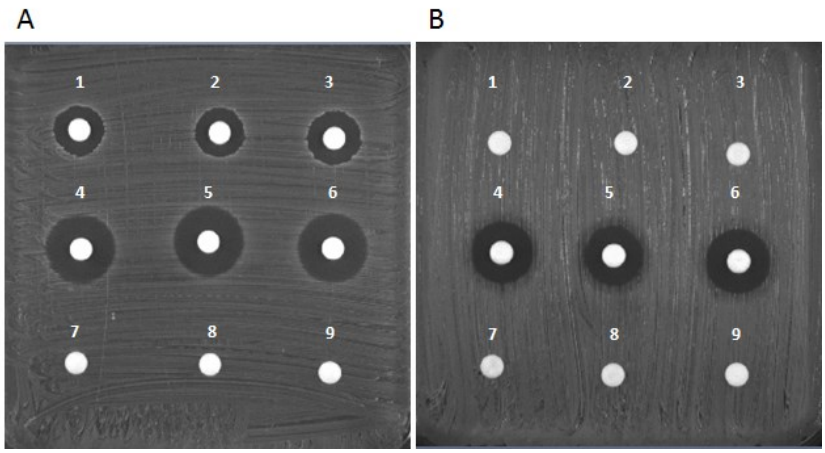

Figure 3.7: *Disk diffusion test results for S. aureus ATCC 25923 (A) and P. aeruginosa ATCC27853 (B). Samples 1-2: MgHA/Coll 70/30 + VNC; sample 3: VNC 10 µg; samples 4-5: MgHA/Coll 70/30 + GNC; sample 6: GNC 10 µg; sample 7-8: MgHA/Coll 70/30; sample 9: sterile paper disk.*

Those set of analyses demonstrated the preservation of antibacterial activity of both drugs also after loading and delivery procedure on the hybrid MgHA/Coll materials, proving their safety as a drug delivery system, and their suitability in preserving and fully releasing the drug into the defective site.

Biological evaluations

In order to confirm the cytotoxicity of the high concentration of Vancomycin (50 mg/mL) and Gentamicin (25 mg/mL) used to obtain the medicated scaffolds, a preliminary 2D *in vitro* study was carried out. The quantitative MTT Assay was performed in order to evaluate the cell viability and proliferation in the presence of the two free antibiotics.

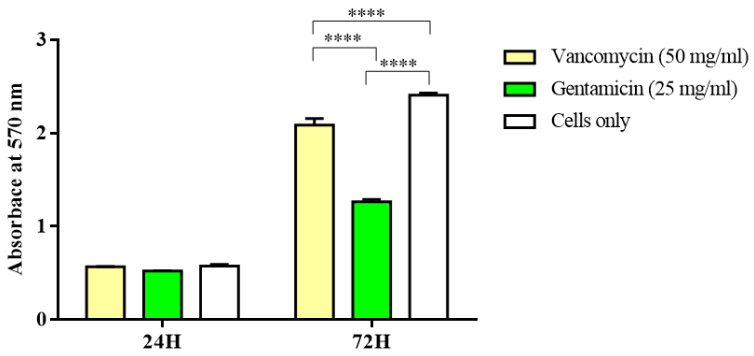

Figure 3.8. MTT Assay. *Quantitative analysis of cell viability on 2D in vitro MG63 cell culture in the presence of free Vancomycin and Gentamicin after 24 and 72 hours of culture. (****p-value ≤ 0.0001).*

The results demonstrated that Vancomycin and Gentamicin do not compromised MG63 viability after 24H (Fig. 3.8). However, after 72 hours of culture, the graph shows the high cytotoxicity of Vancomycin (p-value ≤ 0.0001) and Gentamicin (p-value ≤ 0.0001), as demonstrated by the decreasing of viable cells compared to cells only. In detail, the results demonstrated the major cytotoxicity of Gentamicin, compared to Vancomycin, confirming the well-known effect already reported in literature.[24]

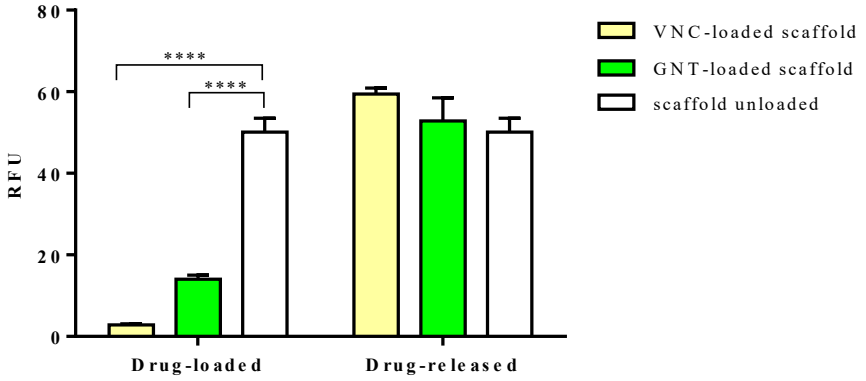

Figure 3.9. PrestoBlue™ Cell Viability Reagent. Quantitative analysis of MG63 viability cultured on the 3D medicated-MgHA/Coll scaffolds. (****p-value ≤ 0.0001).

In order to study the effect of the medicated 70/30 MgHA/Coll scaffolds on cell behaviour, the evaluation of MG63 viability grown onto the scaffold were performed. For this test the MgHA/Coll scaffolds were medicated with the same concentration of antibiotics above mentioned and then treated in two different ways. A first group of scaffolds, named unloaded, after medication was incubated for 7 days in 2 mL and 5 mL of PBS 1X for each scaffold with Gentamicin and Vancomycin medication, respectively, changing it every day in order to induce the released of the drugs. A second group, named loaded, has been seeded with cells directly after the loading of the antibodies.

The analysis of cell viability in the 3D medicated-MgHA/Coll scaffolds was evaluated by performing the colorimetric PrestoBlue Reagent after 1 day of culture. The reagent is a ready-to-use resazurin-based solution that acts cell viability indicator through the exploitation of live cell reducing power, measuring cell presence by performing a colorimetric change. The results show that in both the

loaded scaffolds, Vancomycin and Gentamicin maintained their high cytotoxicity (p-value ≤ 0.0001 for both antibiotics), demonstrating the same effect exert by the free antibiotics (Fig. 3.9). However, the unloaded scaffolds showed absence of cells cytotoxicity. These results demonstrate that after the release of the drugs, the scaffold is able to exert again its well-known bioactivity [1-23] on the cells. The graph showed that after 7 days of release in PBS 1X, the antibiotics' concentration remained into the scaffolds (47.9% Vancomycin and 33.02% Gentamicin) allow cell viability. Those results demonstrate that the drugs incorporated in the scaffold, not alter the physico-chemical structure of the biomaterial and do not affect also its biocompatibility.

The qualitative analysis with Live & Dead shows on day 1 a greater number of dead cells (in red) compared to the live ones (in green) in the non-downloaded scaffolds compared to the loaded ones, confirming the quantitative results at the same experimental time. In detail, in the unloaded scaffolds a greater vitality is observed in the treatment with Vancomycin, where an optimal cell morphology is highlighted in the enlargement at the bottom right, indicating a good state of cellular health, further confirming the PrestoBlue quantitative analysis on day 1 The images of the unloaded scaffolds apparently do not show significant differences between the two antibiotics, contrary to what was reported in the quantitative analysis; however, it is a less reliable qualitative analysis.

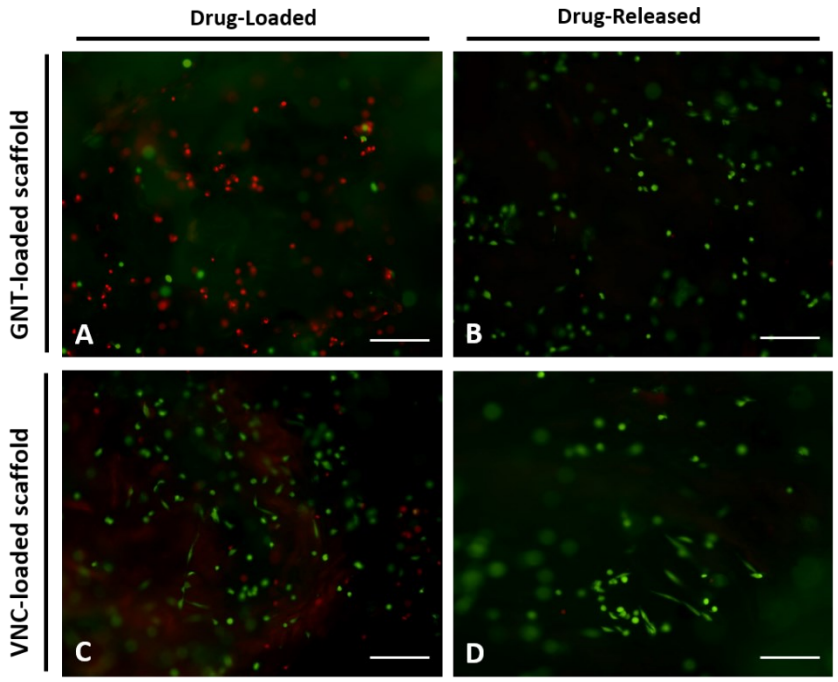

Figure 3.10. *Qualitative cell viability analysis performed with the Live/Dead kit 1 day after seeding. Calcein AM label living cells in green, Ethidium homodimer-1 label dead cells in red. Scale bar: 200 µm*

The observed behaviours of the antibiotics loaded MgHA/Coll ascertains that the medicated biomaterials can be proposed as new strategy to treat infection in orthopaedic application. In fact, the medicated device can act as a dual-functional biomaterial; immediately after the implant the local release of the antibiotics can eradicate the infection and then the bioactivity of the scaffold can recruit and sustain the proliferation of endogenous cells.

Evaluation of Folic acid release from hybrid scaffolds

Different parameters were changed in the synthesis of the hybrid scaffold in order to evaluate the different interaction between folic acid and hybrid scaffolds such as MgHA/Coll ratio, crosslinking treatment and different soaking method.

Firstly, different MgHA/Coll ratio was evaluated in order to appreciate if an increase of mineral phase (MgHA) could modulate the folic acid kinetics. Secondly, two different amounts of cross-linking agent (1wt% and 2 wt%) was used to cross-linking hybrid scaffolds in order to evaluate if it could result in a different drug release because cross-linking changes morphological structure and the amount of free functional groups present on the collagen fibers that are suitable for the interaction between drug and hybrid material. Finally, another parameter taken into consideration in this work is the soaking method, in particular in both cases scaffolds were soaked with the right volume of folic acid in order to obtain a complete loading of the drug. After that, scaffolds were: i) used immediately, in wet form, putting them in the release solution; ii) used after freeze-drying, in dry form, putting them in the release solution. Changing this last parameter (wet or dry form), it is possible to evaluate if different state can influence the drug release.

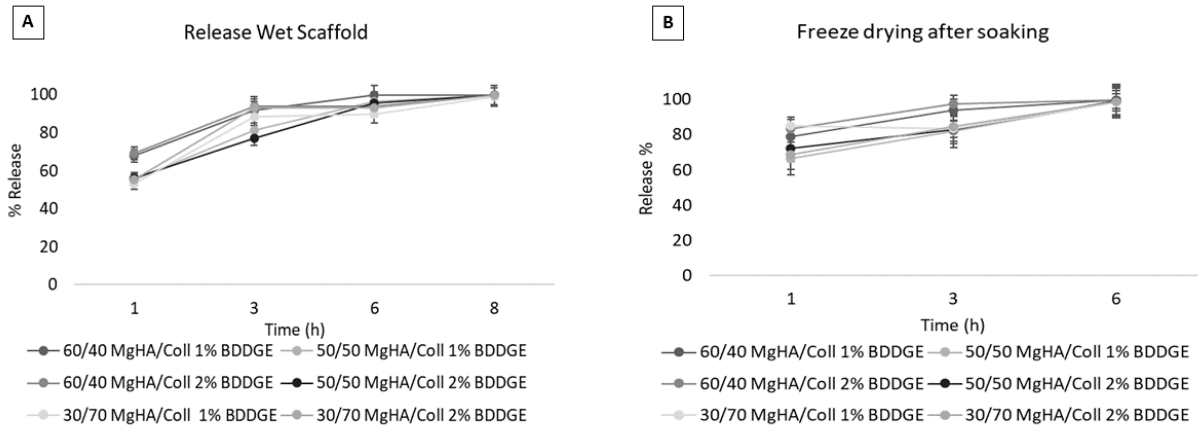

Figure 3.11: *Release profile of folic acid from hybrid scaffolds changing: i) MgHA/Coll ratio; ii) amount of BDDGE; iii) the final form (wet or dry) of the loaded scaffolds). A) Release profile of Wet Scaffold and B) Release profile of Freeze-drying scaffold*

As can be seen, the different MgHA/Coll compositions and also the different ratio of BDDGE (1% and 2%) didn't influence the release; each scaffold releases with the same timeline: at 1h was all scaffolds released about 60 wt.% and the total release happened in 8 h.

After the results obtained, we tried to modulate and improve the release of folic acid, freeze-drying scaffolds after loading in order to slow down the release profile. As can be possible to observe from the fig. 3.11, the elution is faster than wet scaffolds: all the amount is released in 6 h respect to 8h of the wet loaded scaffold. Probably, the dry form favoured the access of PBS in the pores of the scaffold, releasing the pharmaceutical molecule more easily. Instead by directly immersing the wet scaffold in the release solution, balance is more established and allows a slower release.

As said before, different cross-linking treatment were taken into account to evaluate a different drug release depending on the cross-linking. DHT treatment (160 °C, 48h, 0.01 mbar) was chosen to compare with BDDGE cross-linking.

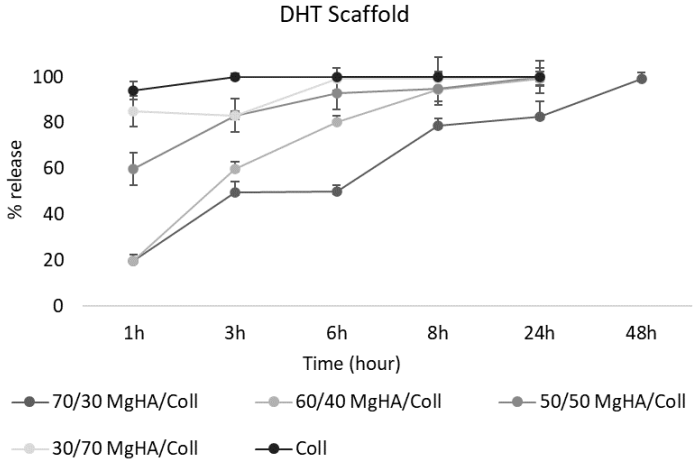

Figure 3.12: *Release profile of folic acid from hybrid scaffolds with different ratio of Hydroxyapatite and crosslinking with DHT method.*

The highlighted interaction properties of MgHA nanoparticles, resulted in the antibiotics release profile, are confirmed in MgHA/coll crosslinked with DHT (Fig. 3.12). In fact, the scaffolds 70/30 MgHA/coll, with the major ratio of HA, presents higher retention properties.

Future perspectives

To improve and extend pharmaceutical release from the scaffolds, a preliminary study is developed about the design of drug loaded alginate (Alg) beads and composites Alg/HA beads (20 wt.% of hydroxyapatite and 80 wt.% of alginate) with the aim to internalize them in MgHA/Coll scaffolds. The beads are loaded during

the synthesis with gentamicin, the antibiotic with large spectrum of activity against bacteria.

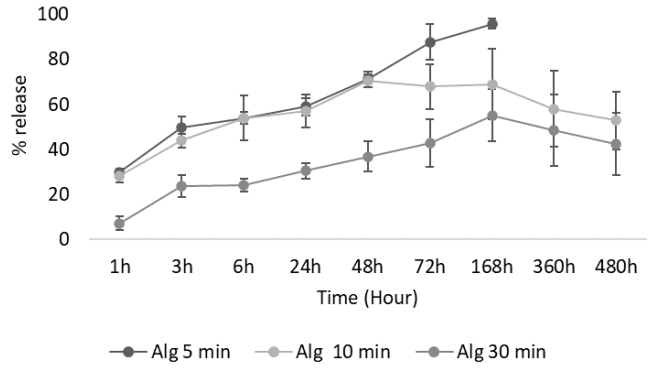

***Figure 3.13**: Gentamicin Release profile: release kinetics at 37 °C and PBS, from alginate beads crosslinked at different time: 5 minutes, 10 minutes and 30 minutes.*

The alginate (Alg) beads are synthetized dropping the solution of Alg in a solution of Calcium chloride. Sodium alginate is a soluble salt and alginate is a hydrophilic polymer, but it forms hydrogels when it exposed on Ca^{2+} ions and others divalent cations. The guluronic residues of alginate structure chelate Ca^{2+} forming an insoluble salt characterised from the typical "egg-box" structure.[27-28]

The beads are leave in contact with calcium chloride for several minutes to have an exchange between calcium and sodium ions of the alginate. Three times were considered: 5 minutes, (Alg. 5min), 10 minutes (Alg. 10 min), 30 minutes (Alg. 30 min).

From fig.3.13, the beads left 5 minutes in the calcium chloride solution have a controlled release profile for one week. About the other beads, it's possible to

observe a decrease of drug elution profile with the increase of the Calcium-Alginate salt amount, as expected. However, after one week the addition of UV reagent, necessary for the analysis of GNT, involves the formation of a precipitate, due to alginate solubilized interference, resulting in a lower signal for the evaluation of the concentration of gentamicin. Probably the alginate that degrades reacts with the chromophore through the hydroxyl group of alginates in solution.[29-30]

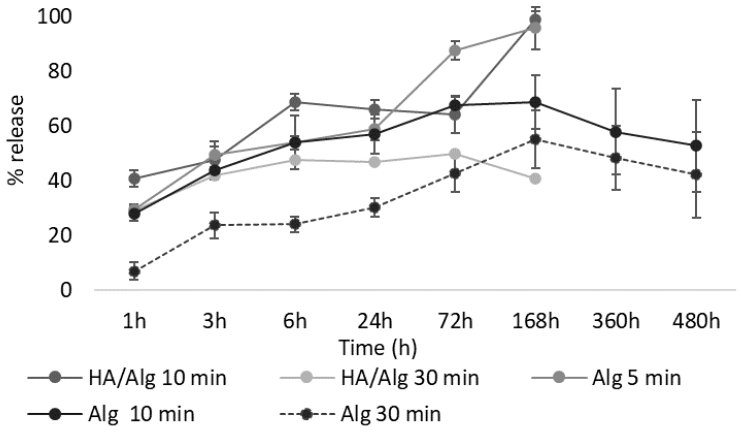

***Figure 3.14**: Release of GNT from HA/alginate beads*

Alginate and hydroxyapatite (80/20) beads containing gentamicin were synthesized. Also, in this case, the drained alginate was left in contact with the calcium chloride solution for various predetermined times (10 minutes and 30 minutes). As can be seen from the release study, the addition of hydroxyapatite in such a small amount did not particularly affect the elution profile. Also, in this case, it's present the interference produced by the alginate with the chromophore used for the Visible UV analysis.

3.4 CONCLUSION

Increased use of implantable biomedical devices demonstrates their potential in treating a wide variety of diseases and disorders in bone trauma and orthopedic applications. However, the number of cases involving implant failure or malfunction due to bacterial infection are also increased in recent years. In an effort to mitigate these events, biomaterials containing antimicrobial agents that can be released or presented within the local microenvironment have become an important area of research.

The present work showed that the MgHA/Coll hybrid scaffolds for bone replacement and regeneration here considered, can be easily combined with antibiotics whose release is partially controlled from the interaction with the functional groups over the MgHA particle' surface. In this study was also investigated the effect of the presence of different amount of MgHA nucleated on collagen fibers (from 70 to 0 wt.%) and confirmed the important role of the mineral phase in binging drug molecules, in fact, the achieved results, demonstrate that higher amount of MgHA induce a greater drug retaining, slowing down its release. In all the cases, the eluted solutions of VNC and GNT, the antibiotic drug involved in the study, when tested with different microbes, exhibited a totally preserved antibacterial activity demonstrating the safety of the material in terms of conservancy of the loaded drug. Considering these results Mg-hydroxyapatite/collagen hybrid biocomposite medicated with vancomycin and gentamicin represents a promising solution for the inhibition towards the proliferation of Gram-positive and Gram-negative microbes during surgery, without compromising their well assessed biocompatibility and regenerative potential after the releasing of the drugs.

This protocol takes advantage from the possibility of an easy medication of the scaffold with a proper amount of drug that can be easily replicate in surgery room just before the device implantation. This partially avoids the assumption of big amounts of drug by systemic route. A huge benefit offered from these biomaterials is also their complete bioresorbability that enable a one-step solution for those challenging situations which usually require a double intervention, the first one for the local treatment of infection and the second one to remove the medicated material and implant the definitive prosthesis. Normally, infected bone defects (due to osteomyelitis and biofilm) are intractable and regarded as contraindications for bone grafting, so larger prospective studies involving these Mg-hydroxyapatite/collagen hybrid resorbable biocomposite in facing these challenging situations will be further designed, as example, by incorporating drugs loaded particles or beads encapsulating the medication in the scaffold matrix and thereby assisting a prolonged drug supply in situ.

Larger prospective studies will be investigated to confirm the promising results obtained in these trials. Furthermore, a preliminary study has been started on probable particles / nanoparticles that can be inserted into biohybrid scaffolds, trying to create a device that can have a fast release with large quantities in the first hours (thus introducing the drug through absorption) and a release prolonged given by the nanoparticles that produce a gradual elution, useful in the following weeks, both for infections and tumors.

---

(1) Tampieri A, Celotti G, Landi E, Sandri M, Roveri N, Fallini G. Biologically inspired synthesis of bone-like composite: Self-assembled collagen fibers/hydroxyapatite nanocrystals. J. Biomed. Mater. Res. part A. (2003) 619:625

[2] Tampieri A, Sandri M, Landi E, Pressato D, Francioni S, Quarto R, Martin I. Design Of graded biomimetic ostheocondral composite scaffolds. Biomaterials 29 (2008) 3539:3546

[3] Tampieri A, Landi E, Valentini F, Sandri M, D'Alessandro T, Dediu V, Marcacci M. A conceptually new type of bio-hybrid scaffold for bone regeneration Nanotechnology 22 (2011) 015104

[4] Hall, B B; Fitzgerald, R H Jr; Rosenblatt, J E Anaerobic osteomyelitis., The Journal of Bone & Joint Surgery: Jan 1983 - Volume 65 - Issue 1 - p 30-35

[5] Meyers BR, Berson BL, Gilbert M, Hirschman SZ. Clinical Patterns of Osteomyelitis Due to Gram-Negative Bacteria. Arch Intern Med. 1973;131(2):228–233.

[6] Mantyh P., The science behind metastatic bone pain, EJC supplements 4 (2006) 4-8

[7] Samoto A., Iwamoto Y., Current status and perspectives regarding the treatment of osteosarcoma: Chemoterapy Reviews on recent clinical trials, 2008, 3, 228-231

[8] Marques C., Ferreira J. MF., Ficai D., Sonmez M., Ficai A., Multifunctional materials for bone cancer treatment International journal of nanomedicine 2014, 9, 2713-2725

[9] Zhang Y., Jin t., Zhuo X. R. Methotrexate-Loaded biodegradable polymeric micelles: preparation, physicochemical properties and in vitro drug release Colloids and surface B: Biointerfaces 44 (2005) 104-109

[10] Andronescu E., Ficai A., Georgiana M., Sonmez M., Ficai D., Ion R., Cimpean A., Collagen-hydroxyapatite drug delivery systems for locoregional treatment of bone cancer Technology in cancer research and treatment Volume 12, Number 4, August 2013

[11] A.C. Jayasuriya, A.J. Darr, Controlled release of cisplatin and cancer cell apoptosis with cisplatin encapsulated poly(lactic-co-glycolic acid) nanoparticles, J. Biomed. Sci. Eng. 6 (2013) 586–592.

[12] D.W. Shen, L.M. Pouliot, M.D. Hall, M.M. Gottesman, Cisplatin resistance: a cellular self-defense mechanism resulting from multiple epigenetic and genetic changes, Pharmacol. Rev. 64 (2012) 706–721.

[13] J. Lehàr, A.S. Krueger, W. Avery, A.M. Heilbut, L.M. Johansen, E.R. Price, R.J. Rickles, G.F. Short III, J.E. Staunton, X. Jin, M.S. Lee, G.R. Zimmermann, A.A. Borisy, Synergistic drug combinations improve therapeutic selectivity, Nat. Biotechnol. 27 (2009) 659–666.

[14] J.T. Thigpen, M.F. Brady, H.D. Homesley, J. Malfetano, B. DuBeshter, R.A. Burger, S. Liao, Phase III trial of doxorubicinwith orwithout cisplatin in advanced endometrial carcinoma: a gynecologic oncology group study, J. Clin. Oncol. 22 (2004) 3902–3908

[15] Hess U., Shahabi S., Treccani L., Streckbein P., Heiss C., Rezwan K., Co-delivery of cisplatin and doxorubicin from calcium phosphate beads/matrix scaffolds for osteosarcoma therapy, Materials Science and Engineering C 77 (2017) 427-435

[16] Clinical and Laboratory Standards Institute, Performance Standards for Antimicrobial Susceptibility Testing; Twenty-fifth Informational Supplement, CLSI document M100-S25 2015

[17] (Clinical and Laboratory Standards Institute, Performance Standards for Antimicrobial Susceptibility Testing; Twenty-fifth Informational Supplement, CLSI document M100-S25, 2015; EUCAST: The European Committee on Antimicrobial Susceptibility Testing, Breakpoint Tables for Interpretation of MICs and Zone Diameters, Version 6.0, 2016

[18] Minardi S., Sandri M., Martinez J.O., Yazdi I.K., Liu X., Ferrari M., Weiner B.K., Tampieri A. Tasciotti E., Multiscale patterning of a biomimetic scaffold integrated with composite microspheres Small Wiley 2014

[19] Wu T., Zhang Q., Ren W., Yi X., Zhou Z., Peng X., Yu X., lang M. Controlled release of gentamicin from gelatin/genipin reinforced beta-tricalcium phosphate scaffold for the treatment of osteomyelitis J. Mater. Chem. B, 2013, 1, 3304-3313

[20] Cabanillas F.P., Pena D.E., Barrales-Rienda J.M., Frutos G. Validation and in vitro characterization of antibiotic-loaded bone cement release International Journal of Pharmaceutics 209 (2000) 15-26.

[21] Simons S.S., Johnson D.F: Reaction of o-phtalaldehyde and thiols with primary amines formation of 1-Alkyl(and aryl)thio-2-alkylisondoles J.Org.Chem.,Vol.43, No.14 1978

[22] Lewis G., Janna Si The in vitro Elution of gentamicin sulfate from a commercially available gentamicin-loaded acrylòic bone cement Wiley Interscience (2004) 77-84

[23] G. S. Krishnakumar, N. Gostynska, M. Dapporto, E. Campodoni, M. Montesi, S. Panseri, A. Tampieri, E. Kon, M. Marcacci, S. Sprio, M. Sandri. Evaluation of different crosslinking agents on hybrid biomimetic collagen-hydroxyapatite composites for regenerative medicine. International Journal of Biological Macromolecules 106 (2018) 739–748

[24] E. Campodoni, E. B.Heggset, A. Rashad, G. B.Ramírez-Rodríguez,K. Mustafa,K. Syverud,A. Tampieri, M. Sandri Polymeric 3D scaffolds for tissue regeneration: Evaluation of biopolymer nanocomposite reinforced with cellulose nanofibrils Materials Science and Engineering: C Volume 94, (2019), 867-878

[25] Dorati R, De Trizio A, Genta I, Merelli A, Modena T, Conti B. Formulation and in vitro characterizaztion of a composite biodegradable scaffold as antibiotic delivery system and regenerative device for bone J Drug Deliv Sci Technol 35 (2016) 124:133

[26] Inzana JA, Schwarz EA, Kates SL, Awad HA. Biomaterials approaches to treating implant-associated osteomyelitis Biomaterials 81 (2016) 58:71

[27] G. T. Grant, E. R. Morris, D. A. Rees, P. J. C. Smith, and D.Thom, “Biological interactions between polysaccharides and divalent cations: the egg-box model,” FEBS Letters, vol. 32, no. 1, pp. 195– 198, 1973

[28] Lorena Segale, Lorella Giovannelli, Paolo Mannina, Franco Pattarino, "Calcium Alginate and Calcium Alginate-Chitosan Beads Containing Celecoxib Solubilized in a Self-Emulsifying Phase", Scientifica, vol. 2016,

[29] Hanne Hjorth Tønnesen & Jan Karlsen (2002) Alginate in Drug Delivery Systems, Drug Development and Industrial Pharmacy, 28:6, 621-630,

[30] Lannuccelli, V., Coppi, G., & Cameroni, R. (1996). Biodegradable intraoperative system for bone infection treatment. I. The drug/polymer interaction. International Journal of Pharmaceutics, 143(2), 195–201

CHAPTER 4

Covalent functionalization of biomineralized collagen scaffold with alginate for tissue regeneration

4.1 INTRODUCTION

Innovation in biomimetic prostheses has found good solutions for treating bone trauma, defects and fractures, but treating other bone pathologies, such as osteosarcomas, a malignant tumor, remain a challenge. Further studies are needed to induce bone regeneration but also treating abnormal cell growth. Treating a tumor does not only involve in innovative therapies research, but also possessing the appropriate techniques that can reproduce the tumor environment complexity. Research studies conducted on 2D models only partially reflect the morpho-molecular pattern of human cancer cells, as they grow as a monolayer, not depending on the surrounding extracellular matrix like that observed in vivo.[1-2]

Nowadays 3D cell culture models are becoming increasingly important for the study of cancer biology because they recapitulate developmental dynamics and tumor progression observed in vivo.[3-4]

Tumors grow in a niche, formed by collagen, hyaluronic acid and other growth factors that interacts with stem cells, promoting their proliferation as cancer cells.[5-6] This study focuses on the development of new bone-like scaffolds formed by collagen, hydroxyapatite and a carbohydrate polymer. We used a material previously described a magnesium doped hydroxyapatite nucleated on type I collagen matrix (MgHA/Coll) obtained through pH-guided bio-inspired

mineralization process; in particular in this work the way to attach carbohydrate polymers through covalent bonds to the collagen matrix was investigated.[7-8-9]

Carbohydrate polymers are very common in tissue engineering because they have excellent characteristics of biocompatibility due to the chemical-physical behaviors, similar to the tissues present in the human body. [10- 11] Alginate, in particular, shows features similar to hyaluronic acid, component of connective tissue. Hyaluronic acid is a glycosaminoglycan copolymer composed by D-glucuronic acid and N-acetyl-D-glucosamine and a major intracellular component of connective tissues such as cartilage. [12-13] Hyaluronic acid is involved in lubrication, cell differentiation, cell growth and other processes, such as morphogenesis, wound repair, inflammation, and metastasis.[14-15-16]

The study was carried out with alginate because it is more accessible, commercially more available, and shares biocompatibility and hydrophilicity characteristics with hyaluronic acid present in bone tissue.

Alginate-based hydrogels are employed in tissue engineering because they also share other features with the extracellular matrix of human tissues. Alginate, anionic linear polysaccharide, derived from algae and bacteria, is composed by 1,4 β-D-mannuronic acid and α-L-glucuronic acid. Alginate shows low in vivo degradability, an important feature for the biomedical applications, so that it can supports the regenerative process, always maintaining the bioresorbable properties. In recent years, the oxidized form of alginate has been investigated, because leads to increasing the biodegradability characteristics. [17-18]

In particular the oxidation is induced by periodate, which cleaves the carbon–carbon bond of the cis-diol group in the uronate residue, promoting the hydrolysis of alginate in aqueous solutions. The product of periodate oxidation – alginate dialdehyde – crosslinks with free amino groups of lysine or hydroxylysine amino acid residues of the polypeptide chains.[19]

The goals of this chapter are:

1. Functionalizing collagen covalently with oxidized alginate to lay the foundations for creating 3D tumor models
2. Creating new binding sites to be able to bind other bio-molecules
3. Creating a functionalization protocol that can be common for all sugar polymers

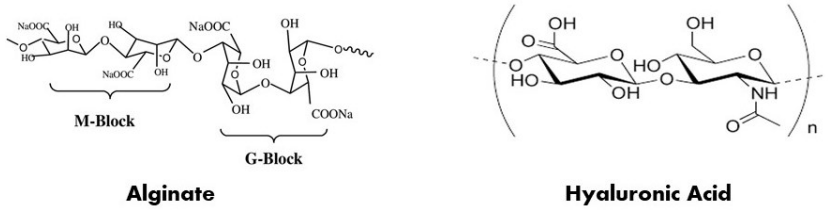

Figure 4.1: *Alginate and hyaluronic acid: similarity in chemical elements, molecules and structure; similar compounds have similar properties*

4.2 MATERIALS AND METHODS

Development of hybrid scaffolds with different MgHA/Coll ratio

Different hybrid materials were prepared varying the collagen and magnesium-doped hydroxyapatite (MgHA) ratio from 0% to 70 wt %.

Synthesis of MgHA/Coll scaffold (70/30 wt.%)

150 g of equine tendon derived Type I collagen 1 wt.% in acetic buffered solution (pH 3.5) (Opocrin SpA, Modena, Italy) were added to a 300 ml of phosphoric acid aqueous solution (2,40 g of H_3PO_4 85 wt.% pure Sigma Aldrich- Merck, Germany) to obtain a homogenous acid collagen suspension. A basic suspension was prepared with 2,71 g of calcium hydroxide ($Ca(OH)_2$, 95% pure, Sigma Aldrich-Merck, Germany) in 300ml of water under constant and vigorous stirring. Once formed homogeneous suspension, 0,35 g of Magnesium Chloride ($MgCl_2 \cdot 6H_2O$, Sigma Aldrich-Merck, Germany) were added and stirred. The acid dispersion was slowly poured in the basic suspension, shaking manually to guarantee a better fibres desegregation. After 2 hours at room temperature, the obtained hybrid hydrogel was filtered and washed for three times with MilliQ water to eliminate the residues of reaction. The MgHA/Coll slurry was filled into a polystyrene well-plate and lyophilized by consecutive freezing (at -40°C) and drying at (20°C) for 48 h under constant vacuum of 0,086 mbar (5Pascal, LIO 3000 PLT, Italy).

Synthesis of MgHA/Coll scaffold (60/40 wt.%)

150 g of equine tendon derived Type I Collagen 1 wt.% in acetic buffered solution (pH 3.5) (Opocrin SpA, Modena, Italy) were added to a 300 ml of phosphoric acid aqueous solution (1,55 g of H_3PO_4 85 wt.% pure Sigma Aldrich-Merck, Germany) to obtain a homogenous acid collagen suspension. A basic suspension was prepared with 1,74 g of calcium hydroxide ($Ca(OH)_2$, 95% pure, Sigma Aldrich-Merck, Germany) in 300 ml of water under constant and vigorous stirring. Once formed homogeneous suspension, 0,22 g of Magnesium Chloride ($MgCl_2 \cdot 6H_2O$, Sigma Aldrich-Merck, Germany) were added and stirred.

The acid dispersion was slowly poured in the basic suspension, shaking manually to guarantee a better fibres desegregation. After 2 hours at room temperature, the obtained hybrid hydrogel was filtered and washed for three times with MilliQ water to eliminate the residues of reaction. The MgHA/Coll slurry was filled into a polystyrene well-plate and lyophilized by consecutive freezing (at -40°C) and drying at (20°C) for 48 h under constant vacuum of 0,086 mbar (5Pascal, LIO 3000 PLT, Italy).

Synthesis of MgHA/Coll scaffold (40/60 wt.%)

150 g of equine tendon derived Type I Collagen 1 wt.% in acetic buffered solution (pH 3.5) (Opocrin SpA, Modena, Italy) were added to a 300 ml of phosphoric acid aqueous solution (0,63 g of H_3PO_4 85 wt.% pure Sigma Aldrich-Merck, Germany) to obtain a homogenous acid collagen suspension. A basic suspension was prepared with 0,75 g of calcium hydroxide ($Ca(OH)_2$, 95% pure, Sigma Aldrich-Merck, Germany) in 300 ml of water under constant and vigorous stirring. Once formed homogeneous suspension, 0,09 g of Magnesium Chloride ($MgCl_2 \cdot 6H_2O$, Sigma Aldrich-Merck, Germany) were added and stirred. The acid dispersion was slowly poured in the basic suspension, shaking manually to guarantee a better fibres desegregation. After 2 hours at room temperature, the obtained hybrid hydrogel was filtered and washed for three times with MilliQ water to eliminate the residues of reaction. The MgHA/Coll slurry was filled into a polystyrene well-plate and lyophilized by consecutive freezing (at -40°C) and drying at (20°C) for 48 h under constant vacuum of 0,086 mbar (5Pascal, LIO 3000 PLT, Italy).

Synthesis of MgHA/Coll scaffold (30/70 wt.%)

150 g of equine tendon derived Type I Collagen 1 wt.% in acetic buffered solution (pH 3.5) (Opocrin SpA, Modena, Italy) were added to a 300 ml of phosphoric acid aqueous solution (0,44 g of H_3PO_4 85 wt.% pure Sigma Aldrich-Merck, Germany) to obtain a homogenous acid collagen suspension. A basic suspension was prepared with 0,5 g of calcium hydroxide ($Ca(OH)_2$, 95% pure, Sigma Aldrich-Merck, Germany) in 300 ml of water under constant and vigorous stirring. Once formed homogeneous suspension, 0,064 g of Magnesium Chloride ($MgCl_2 \cdot 6H_2O$, Sigma Aldrich-Merck, Germany) were added and stirred. The acid dispersion was slowly poured in the basic suspension, shaking manually to guarantee a better fibres desegregation. After 2 hours at room temperature, the obtained hybrid hydrogel was filtered and washed for three times with MilliQ water to eliminate the residues of reaction. The MgHA/Coll slurry was filled into a polystyrene well-plate and lyophilized by consecutive freezing (at -40°C) and drying at (20°C) for 48 h under constant vacuum of 0,086 mbar (5Pascal, LIO 3000 PLT, Italy).

Synthesis of pure collagen scaffold (Coll)

150 g of equine tendon derived 1 wt.% in acetic buffered solution (pH 3.5) (Opocrin SpA, Modena, Italy) were treated with a basic aqueous solution of NaOH (0,1 M, Sigma Aldrich-Merck, Germany), added until the achievement of the isoelectric point of collagen (pI 5.5) to induce the precipitation of collagen due to fibers assembling. The mixture was kept for fibers maturation at room temperature for 2 hours. The precipitated collagen was filtered with a metallic sieve (150 μm) and washed three times with MilliQ water. The washed hydrogel was poured in polystyrene 96-multiwell and lyophilized by consecutive freezing at (-40°C) and

drying at (20°C) for 48 h under constant vacuum of 0,086 mbar (5Pascal, LIO 3000 PLT, Italy).

Alginate oxidation

A ratio of alginate:collagen of 1:1 (by weight) was used for each sample. 1,5 g of Alginate is solubilized in water for 1h, through stirring. Then sodium periodate is added (2,2 eq.) and the solution is stirred for two hours. The consumption of periodate (directly related to the aldehyde residue generated in the support) was checked after oxidation process, adding 0.1 mL of the supernatant of the oxidizing suspension to a mixture of 0.45 mL of 10% (w/v) KI and 0.45 mL of saturated sodium bicarbonate. The absorbance was read at 419 nm, considering the initial sodium periodate solution as 100% (0% aldehyde production). If all the periodate is consumed, another equivalent has to add, until 10% is left. After two hours, the product is dialysed for 24 h to remove the excess periodate. The aldehyde presence is detected by Schiff reagent.[20]

Functionalization of MgHA/coll Scaffold with oxidized alginate

MgHA/Coll hydrogel is mixed with oxidized alginate and stirred for 24 h. For the reduction, after 24h, a solution of 1 mg/ml of $NaBH_4$ dissolved in bicarbonate pH 10, is added for 30 minutes. To destroy $NaBH_4$, the hydrogel is washed in phosphate buffer pH 7. The hydrogel is freeze-dried for 24h.

4.3 RESULTS AND DISCUSSION

4.3.1 Synthesis

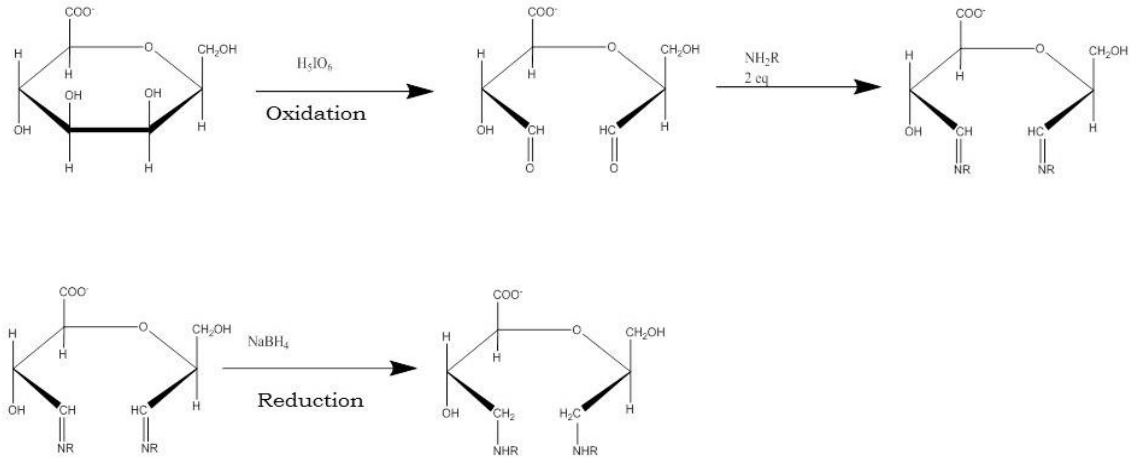

Figure 4.2 *Reaction scheme of collagen functionalization with alginate, based on oxidation and reduction reactions in water environment at room temperature*

The functionalization has been optimized through periodate oxidation, that is a typical reaction of carbohydrates.[21-22] Periodate can oxidize both M and G subunits in the alginate structure, but Gomez at al., reported that sodium periodate reacts preferentially with G units than with M units.[23-24] Oxidation reactions on –OH groups at C-2 and C-3 positions of the G units of sodium alginate are performed with sodium periodate which leads, by cleavage of carbon–carbon bond, to the formation of two aldehyde groups in each oxidized monomeric unit(fig.4.2).[25-26]

The oxidized alginate (Ox.Alg.) reacts with amino group of collagen and a reduction of the imino group is performed by treatment with sodium borohydride, to generate a more stable bond, then the hydrogel is freeze-dried to obtain a porous scaffold.

We have not characterized alginate oxidation using H^1NMR because Gomez at al., have reported that in H^1 NMR spectra, the characteristic aldehyde peak at 11 ppm is not observed because the resulting aldehyde groups react simultaneously with hydroxyl groups of adjacent non-oxidized uronic residues in the polymer chain and form cyclic hemiacetals. [27]

Furthermore, the oxidation process induces alginate degradation leading to secondary product. The alginate degradation occurs via two mechanisms. The first mechanism is not mediated by hydroxyl free radical. This leads to the fast infrequent and unusual monomers in the alginate. The second one is free radical-dependent. Free radicals generated from phenolic impurities contained in alginate during oxidation cause a slow polymer cleavage. [28]

The oxidized alginate was characterized by High Performance Size Exclusion-Evaporative Scattering Detector (HPSEC- ELSD), qualitative and quantitative technique based on chromatography and size-exclusion allowing to measure Molecular weight, the average of impurities and then sample percentage.

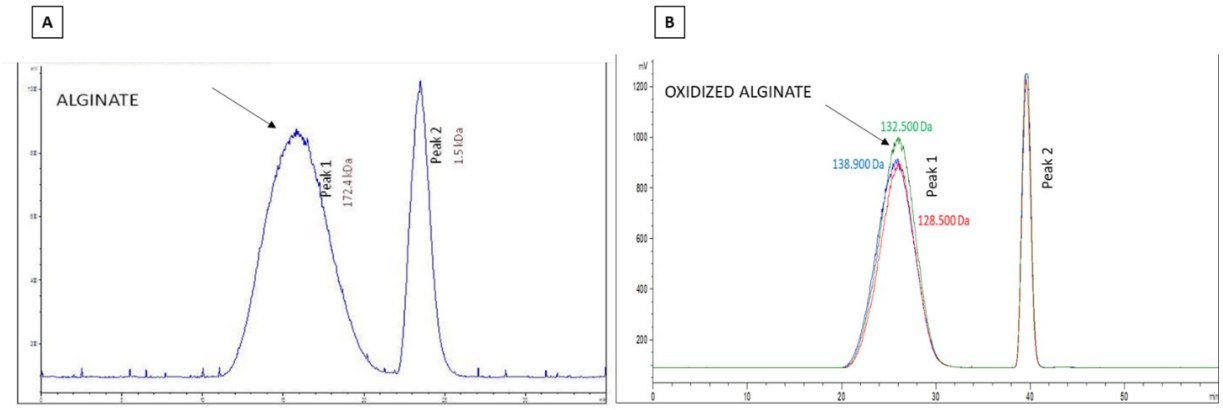

Figure 4.3: *HPSEC-ELSD spectra of Alginate (A) and Oxidized alginate (B), representative of decrease of Molecular weight in oxidized alginate samples, due to cleavage of carbon bonds*

	Media MW kDa		% of product
	Mean	SD	Mean
Oxidized Alginate 1	128,5	6,4	73,3
Oxidized Alginate 2	132,5	2,5	74,0
Oxidized Alginate 3	138,9	0,4	75,2
Alginate	172,3	3,7	71%

Table 1: *Molecular weight and ratio of oxidized Alginate present in the samples analysed by HPSEC-ELSD*

The chromatogram (fig.4.3A) quantifies the molecular weight of alginate, 172400 Da, (peak 1) and the percentage of pure alginate present in the sample, 71% (29% are considered impurities- peak 2). The formation of aldehyde group on oxidized alginate is confirmed by HPSEC-ELSD, (fig. 4.3B). The analysis (peak1) highlights the decrease of molecular weight about 39.100 Da (133.300 Da of Ox.Alg. vs 172.400 Da of Alginate), due to the oxidation process leading to the cleavage of carbon-carbon bonds.

4.3.2 30/70 MgHA/Coll functionalized with oxidized alginate

MgHA / Coll hybrid scaffolds feature collagen fibers covered entirely by hydroxyapatite nanoparticles, leaving the collagen amino groups less available for interaction with molecules. Therefore, the first test was carried out with a low percentage of hydroxyapatite, 30%, in order to evaluate the formation of covalent bonds between collagen and the aldehyde group of the oxidized alginate in a sample with many collagen amino groups available. The ratio of alginate/collagen (5:1) presents an excess of alginate that will be scale (1:1 Coll:Alg) in subsequent syntheses in order to optimize the method. At the same time, only the mixture of the hydrogel with alginate was evaluated. In the fig. 4.4, it's highlighted the loss of stiffness in the 3D scaffold mixed with alginate, probably due to a supersaturation of the alginate on the collagen fibers.[29-30]

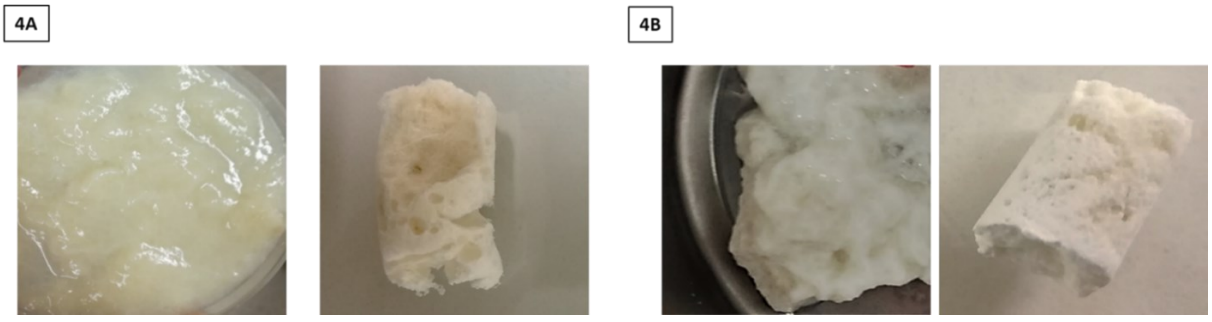

Figure 4.4: *4A) MgHA/Coll mixed with alginate (hydrogel and 3D scaffold); 4B) MgHA/Coll link with oxidized alginate (hydrogel and 3D scaffold)*

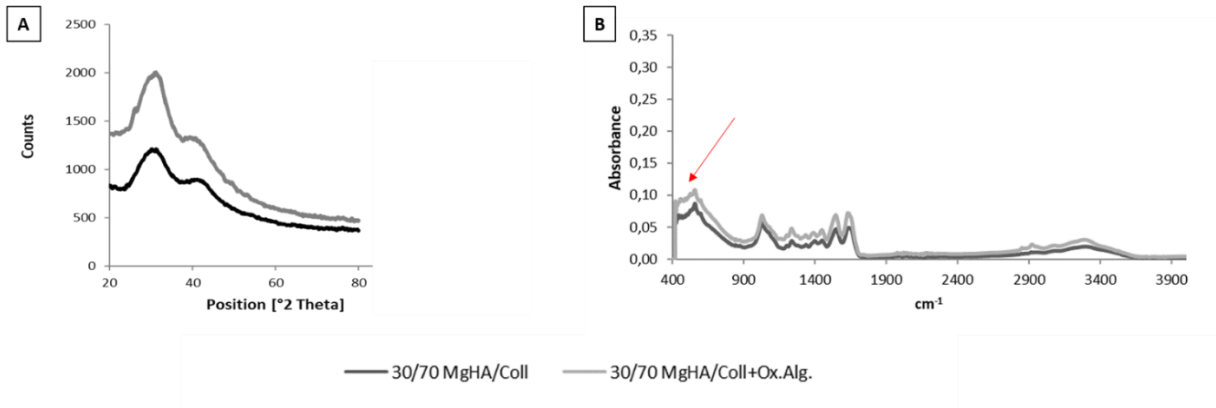

Figure 4.5: *A) XRD spectra of 30/70 MgHA/Coll and 30/70 MgHA/Coll+Ox.Alg. B) Comparation of FTIR between 30/70 MgHA/Coll, and 30/70 MgHA/Coll+Ox.Alg, in particular the red arrow highlighted the peak at 500 cm^{-1}, showing a difference shoulder between MgHA/Coll+Ox.Alg. and MgHA/Coll*

The scaffolds are characterized by FTIR and XRD (fig.4.5). XRD spectra (fig.4.5A) show the preservation of low crystalline order of mineral phase in both hybrid scaffolds, thereby the functionalization doesn't affect the low crystallinity and nanosized dimensions of hydroxyapatite. For all samples, XRD analyses did not reveal any further secondary phases. The low crystallinity of hydroxyapatite, due to the biomineralization process, in particular to the low temperature during synthesis and the chemical interaction between the mineral MgHA particles and collagen molecules, indicates the achievement of a high biomimetic mineral phase.

Collagen and alginate are biopolymers with common functional groups, such as carboxyl and hydroxyl groups, and therefore have overlapping peaks. The relevant difference and the estimation of the presence of alginate is found in the fingerprint area, at 500 cm^{-1} (fig.4.5B).

This peak is present in both scaffolds, but the functionalization behaves a wide peak in the MgHA/Coll+Ox.Alg. respect the sharp peak of MgHA/Coll.

The chemical interaction of mineral phase MgHA with collagen fibers are evidenced by the shift from 1340 cm^{-1} to 1337 cm^{-1} due to the chemical bond between carboxylic groups of collagen and Ca^{2+} ions of the apatite. The spectra revealed the characteristic peaks of phosphate ion PO_4^{3-} (474, 569, 602, 962, 1045 and 1091 cm^{-1}) and OH^- (633 and 3572 cm^{-1}) groups, corresponding to the typical hydroxyapatite peaks. While the bands at approximately 3497 and 1638 cm^{-1} indicate the presence of lattice water in the material. [31-32]

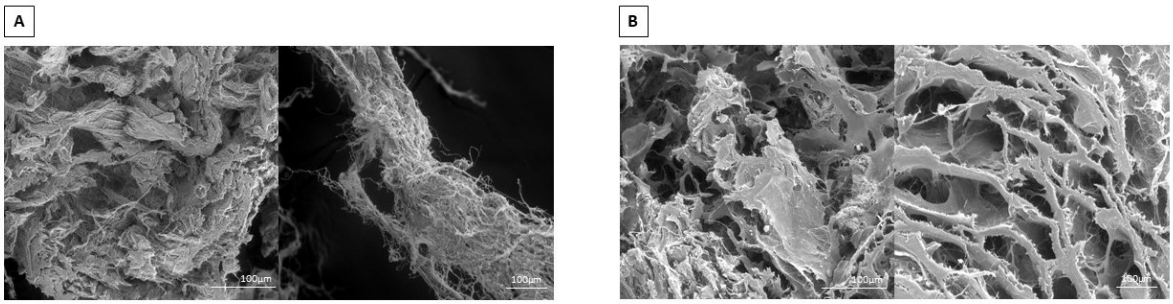

Figure 4.6 *MgHA/Coll 30/70 (A) and MgHA/Coll 30/70+ Ox. Alg (B): overview on the scaffold and detail of a fiber.: uniformly distribution of mineral MgHA nanoparticles for both scaffolds. In particular, the B images shows the oxidized alginate layer on collagen fibers*

The ESEM images (fig. 4.6) highlighted the different morphology in presence and absence of the oxidized alginate. For both scaffolds, the MgHA nanoparticles are homogeneously distributed on the collagen fibers matrix and are distinguishable on the wall of pores.

An isotropic structure with the presence of randomly distributed and interconnected macro- and micro-porosity is highlighted. This property has an important role in stimulating bone regeneration because facilitates cell adhesion, permeation and proliferation, as well as vascularization and extracellular matrix deposition in the whole scaffold. The permeation in the structure of oxygen, nutrients and metabolites is essential for a proper bone tissue growth and regeneration. At high magnification, on the wall of pores are distinguishable the MgHA nanoparticles that are completely embedded and homogeneously distributed on the collagen fibers matrix. Furthermore, oxidized alginate spreads over the collagen fiber, providing a smooth surface, improving the porosity and water uptake behavior, confirmed through swelling tests (fig.4.7). In fact, the addition of aldehyde increases the water absorption of the hybrid scaffold, thanks to the hydrophilic behavior of alginate.

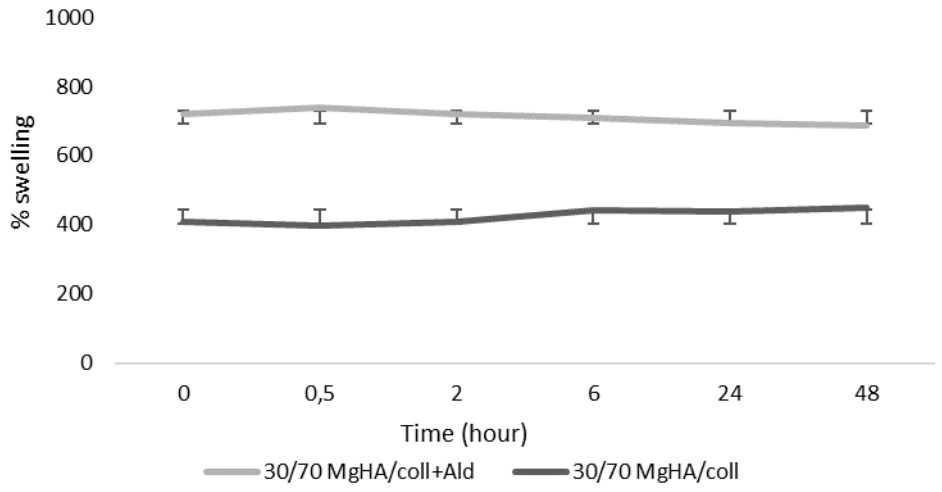

Figure 4.7: Swelling chart: *Evaluation of swelling capability, in PBS and 37°C, of all the developed dried materials.*

Samples	Ca/P	Std	Mg/Ca	Std	(Ca+Mg) /P	Std
30/70 MgHA/Coll	1,423	0,010	0,039	0,019	1,478	0,009
30/70MgHa/Coll+Ox.Alg	1,376	0,006	0,020	1,163	1,403	0,008

***Table 2**: ICP analysis of the inorganic component (MgHA) in dried materials*

The chemical composition of mineral components was quantitatively evaluated by ICP-OES. 30/70 MgHA/Coll samples present a (Mg+Ca)/P molar ratio above1.42-1.30, lower than the typical Ca/P = 1.67 of stoichiometric apatites, and distinctive of substituted and low crystalline phase (table 2). The Mg/Ca ratio decreases in the scaffolds functionalized with oxidized alginate, indicating that some Mg ions are lost during the covalent attachment of the carbohydrate process.

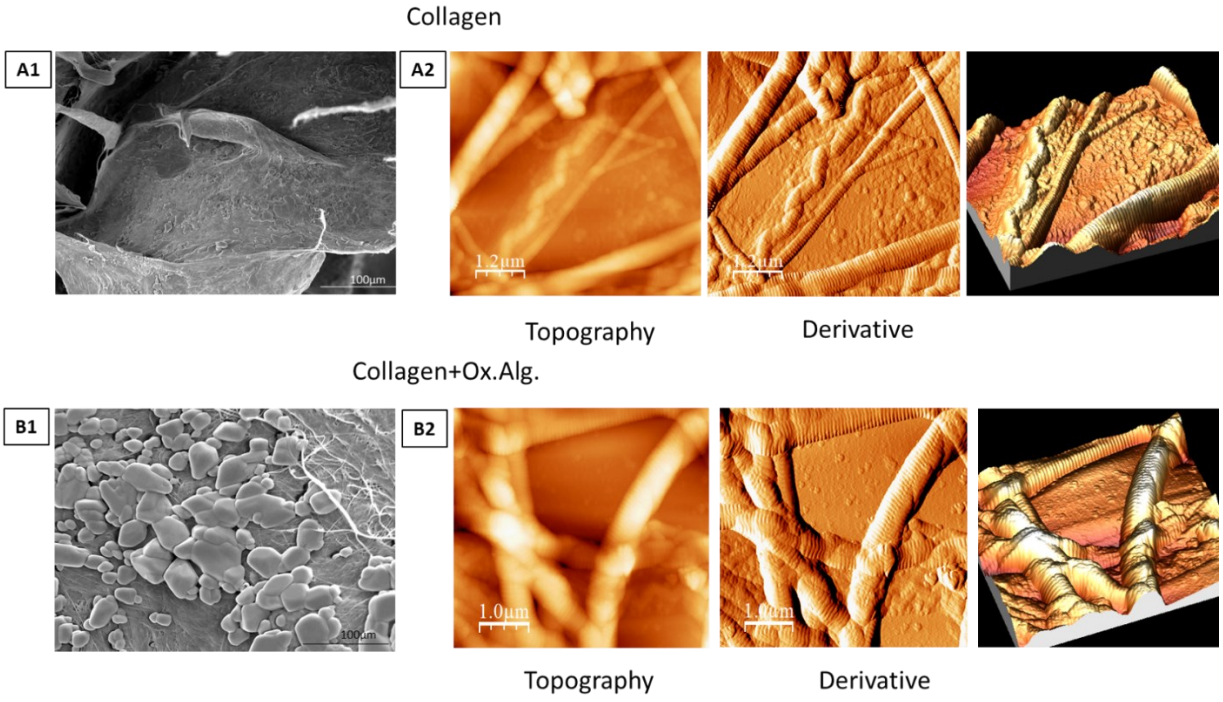

***Figure 4.8**: ESEM (A1 and A2) and AFM (B1 and B2) images of Collagen fibers and Collagen functionalized by oxidized alginate*

The functionalization of alginate on the collagen surface was studied, through ESEM and AFM characterization.

The oxidized alginate spreads on collagen fibers and involve in roughness structures, (fig. 4.8A). On AFM (fig. 4.8B) the alginate is barely detected, thereby doesn't affect the collagen fiber structure, totally. The distribution along the fibers is probably not homogeneous.

4.3.3 Functionalization with oxidized alginate: Increasing the amount of Hydroxyapatite

We were interested in functionalizing hybrid scaffolds containing higher hydroxyapatite ratios, similar to the ones present in bones. We validated and optimized the method to functionalize hybrid scaffolds containing MgHA/Coll ratio of 40/60, 60/40, 70/30, in which MgHA covers a larger area of the collagen fibers leaving less functional groups available. Results indicated that the coupling occurred even at high amounts of hydroxyapatite present, although the amount of oxidized alginate decreased. The characterization of all materials is shown below.

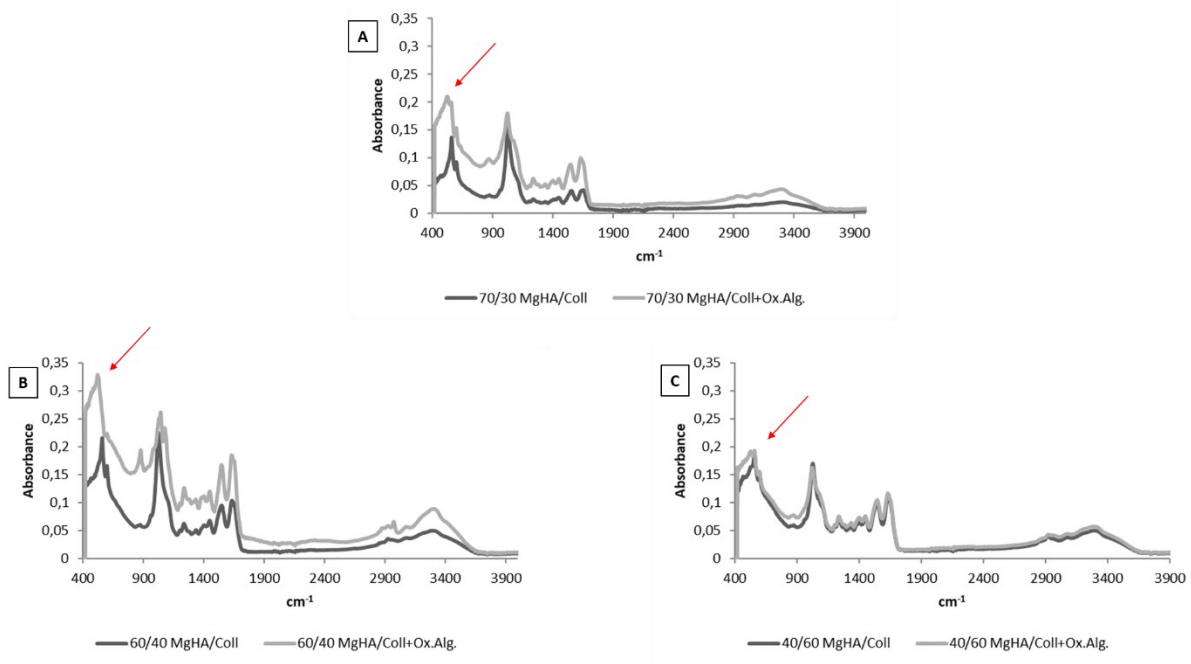

Figure 4.9: *FTIR, of functionalized and not functionalized scaffolds. In particular: A) 70/30 MgHA/Coll vs 70/30 MgHA/Coll+Ox.Alg., B) 60/40 MgHA/Coll vs 60/40 MgHA/Coll+Ox.Alg. and C) 40/60 MgHA/Coll vs 40/60 MgHA/Coll+Ox.Alg.*

FTIR (fig.4.9) and XRD (fig.4.10) characterization confirmed the previous study. The FTIR spectra indicate the chemical interaction of MgHA with collagen fibers and the peaks of phosphate, that we explained before in the paragraph 4.3.2 (Fig.4.5B). The relevant difference and the estimation of the presence of oxidized alginate in the scaffolds is found in the fingerprint area, at 500 cm^{-1}. Probably, the functionalization changes the morphology of the peak.[31-32]

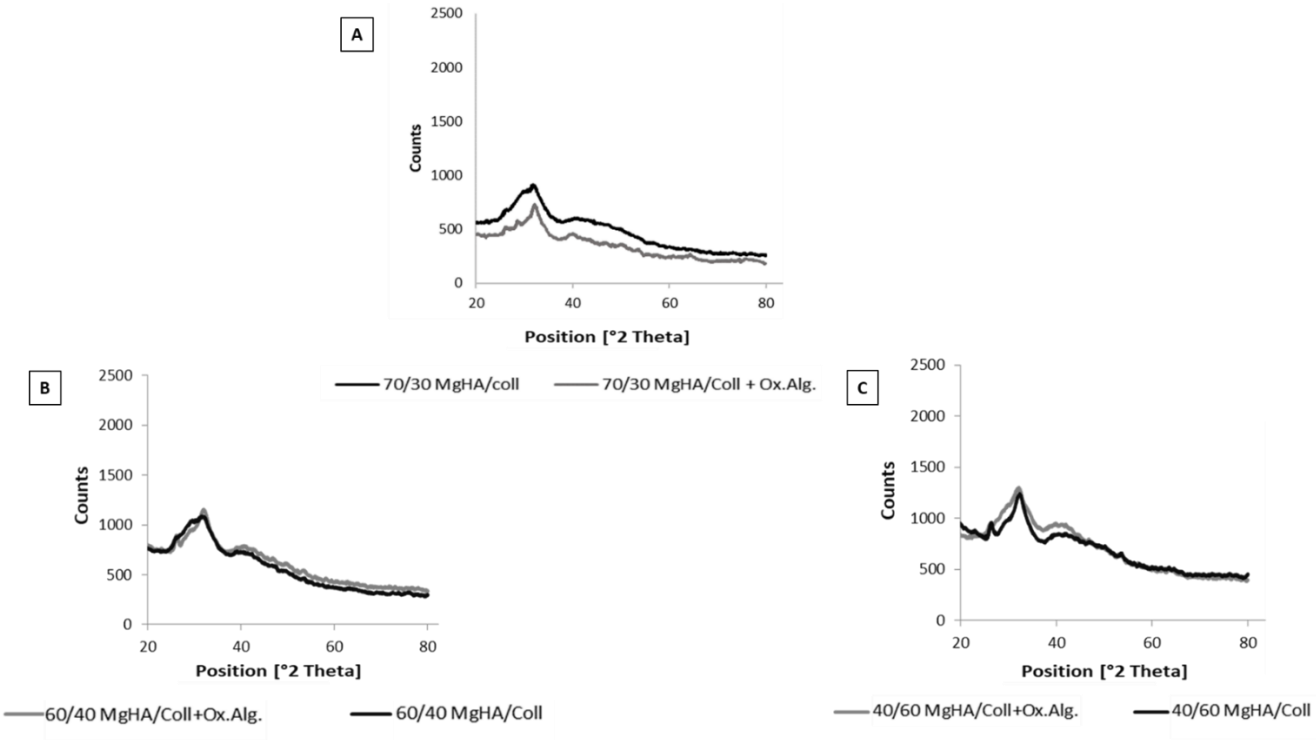

Figure 4.10: *XRD spectra of 70/30 (A), 60/40 (B), 40/60 (C) MgHA/coll compared with each hybrid scaffold link to oxidized alginate*

XRD spectra shows that the MgHA phase behaves as described above in the paragraph 4.3.2 (fig.4.5A), thereby we can confirm that the functionalization doesn't affect the low crystallinity and nanosized dimensions of hydroxyapatite.

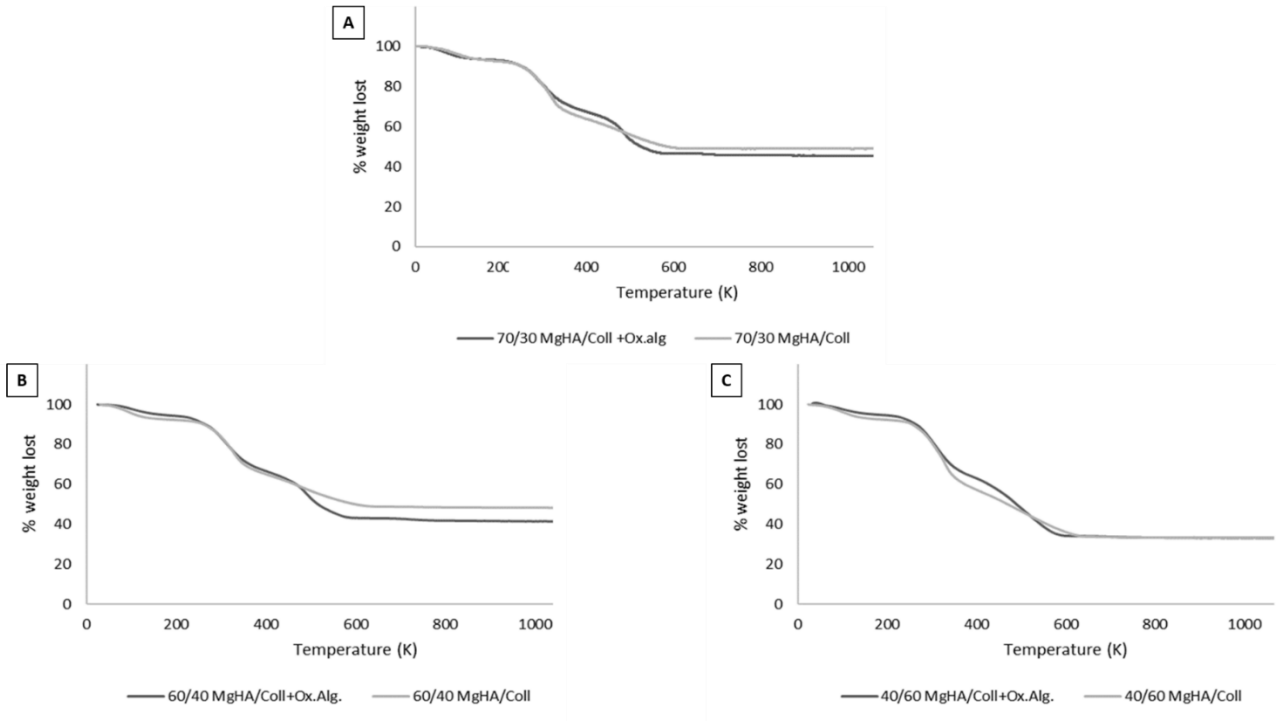

Figure 4.11: *TGA of MgHA/Coll and MgHA/Coll+ Ox. Alg. in different composition (A) 40/60, (B) 60/40, (C) 70/30)*

The effective mineral content in MgHA/Coll samples was assessed by thermogravimetric analysis (Fig. 4.11). TGA curves exhibit three main weight loss steps: the first from 25°C to 170°C due to the release of adsorbed and bound water (7-8 wt.%), the second loss from 170 °C to 360 °C due to degradation of Type I collagen and the last, from 360 °C to 660 °C, due to the complete combustion of organic residues. The residual weights correspond to the mineral phase content, which were 55 wt.% for MgHA/Coll (70/30), 52 wt.% for MgHA/Coll (60/40) and 34 wt.% for MgHA/Coll (40/60). For the functionalized scaffolds the mineral phase contents is 53% for 70/30 MgHA/Coll+Ox.Alg, 43,66 % of 60/40 MgHA/Coll+Ox.Alg and 34,78% for 40/60 MgHA/Coll.

Samples	Ca/P	std	Mg/Ca	std	(Ca+Mg) /P	std
70/30 MgHA/Coll	1,300	0,062	0,036	0,088	1,347	0,012
70/30 MgHA/Coll+Ox.Alg.	1,496	0,710	0,022	0,732	1,525	0,005
40/60 MgHA/Coll	1,419	0,009	0,0246	0,0003	1,454	0,011
40/60 MgHA/Coll+Ox.Alg.	1,059	0,049	0,010	0,001	1,070	0,008
60/40 MgHA/Coll	1,401	0,010	0,026	0,0003	1,437	0,010
60/40 MgHA/Coll+Ox.Alg.	1,080	0,011	0,013	0,0001	1,095	0,011

Table 3: *ICP analysis of inorganic component in dried materials*

ICP-OES highlights that MgHA/Coll samples (70/30, 60/40, 40/60) present a (Mg+Ca)/P molar ratio about 1,40. The ratio of (Mg+Ca)/P and Mg/Ca decrease in the functionalized scaffold cause of some Magnesium and Calcium ions are loose during the process.

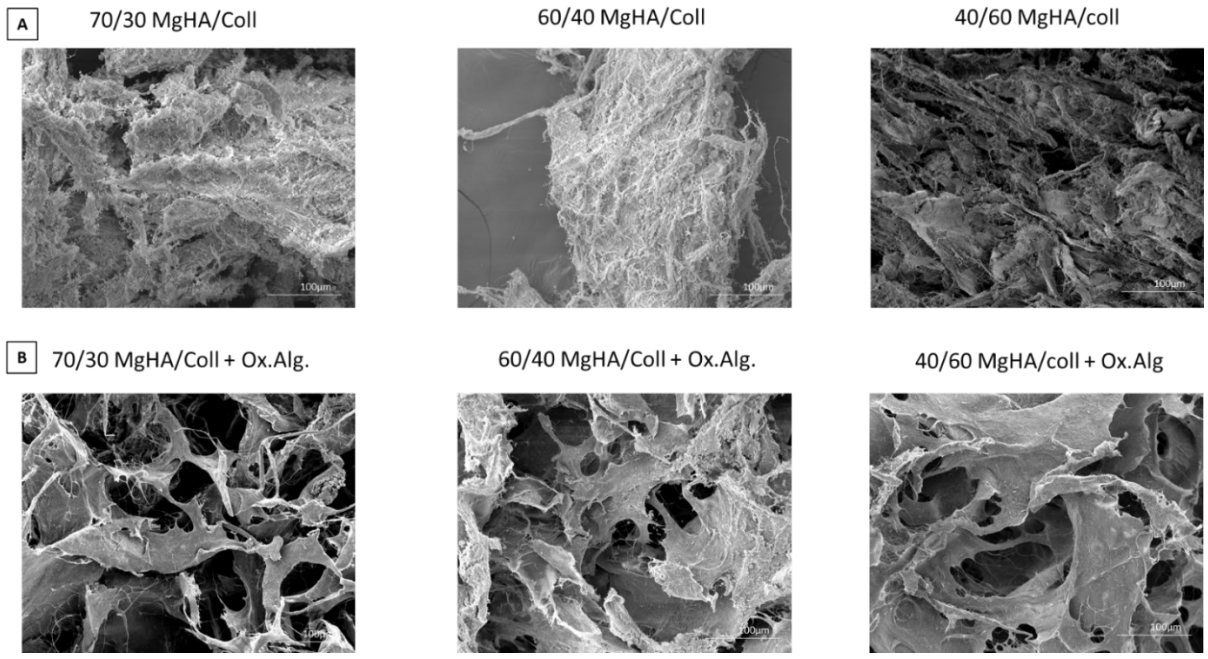

Figure 4.12: *ESEM of MgHA/Coll (A) and MgHA/Coll+Ox.Alg. (B) in different compositions (40/60, 60/40, 70/30). All the scaffolds show the uniform distribution of mineral MgHA nanoparticles. The panel B shows the functionalized scaffold: Alginate covering the fibers is observed.*

The ESEM images (fig. 4.12) don't present significant differences respect to the previously described samples (fig.4.6). In fact, the isotropic structure is maintained and the MgHA is homogenously distributed and cover the collagen fiber.

In the functionalized scaffold, the smooth surface of the collagen fiber is confirmed, due to the spread of oxidized alginate on the collagen. The smooth morphology improves the porosity and the water uptake behavior, confirmed by tests shown below.

MgHA/Coll Porosity	Density method	Water squeezing method
70/30 MgHA/Coll	85,41%	48,09%
70/30 MgHA/Coll+Ox.Alg	88,85%	65,49%
60/40 MgHA/Coll	86,12%	39,94%
60/40 MgHA/Coll+Ox.Alg	92,99%	68,02%
40/60 MgHA/Coll	80,95%	45,48%
40/60 MgHA/Coll+Ox.Alg	87,42%	62,03%

Table 4*: Porosity test: comparison of functionalized and unfunctionalized scaffolds*

The porosity test and water squeezing highlights the increase of the porosity in the scaffolds with the presence of aldehyde, also confirmed by the swelling test. In fact, the addition of oxidized alginate increases the water absorption of the hybrid scaffold, thanks to the hydrophilic behavior of the polymer (Table 4). The interaction of the scaffolds with water medium, at 37°C in PBS medium highlights the increase of the swelling property when the scaffolds is functionalized with Oxidized Alginate (fig.4.13).

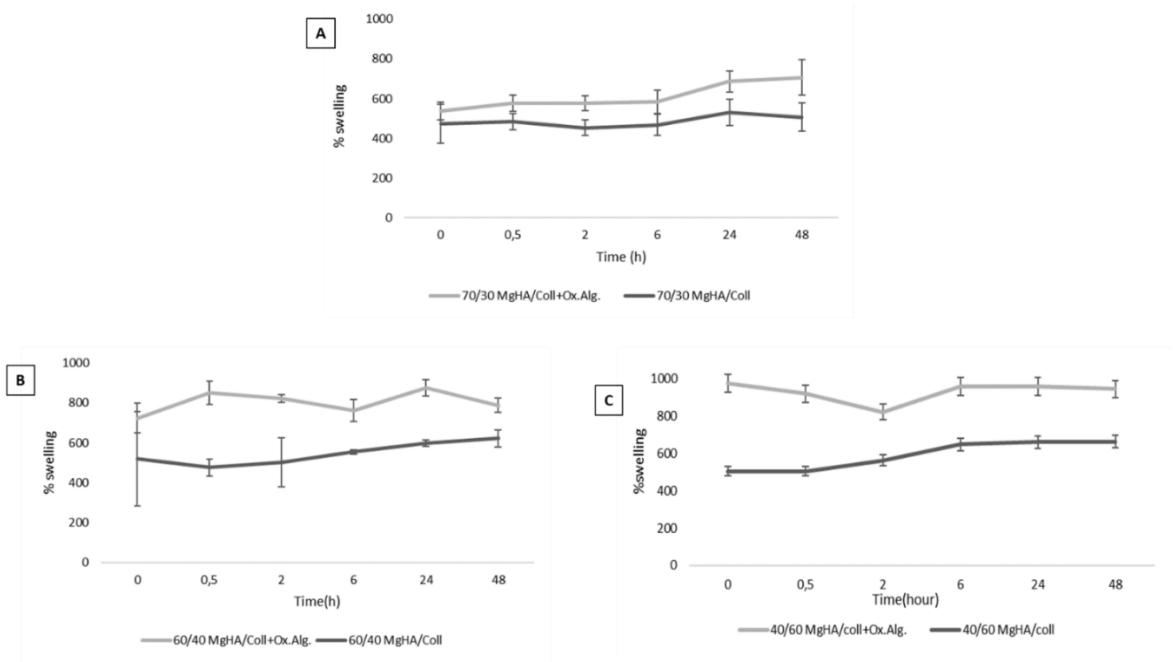

Figure 4.13: *Evaluation of swelling capability, in PBS and 37°C, of all the developed dried materials. In particular we compared A) 70/30 MgHA/Coll and 70/30 MgHA/Coll+Ox.Alg. B) 60/40 MgHA/Coll and 60/40 MgHA/Coll+Ox.Alg C) 40/60 MgHA/Coll and 40/60 MgHA/Coll+Ox.Alg*

Degradation tests (fig.4.14) indicate an increase of the degradation of functionalized scaffolds, caused by the loss of oxidized alginate during the 21 days, revealed by FTIR characterization (4.15) of the degraded scaffolds, after 7 days and 14 days.

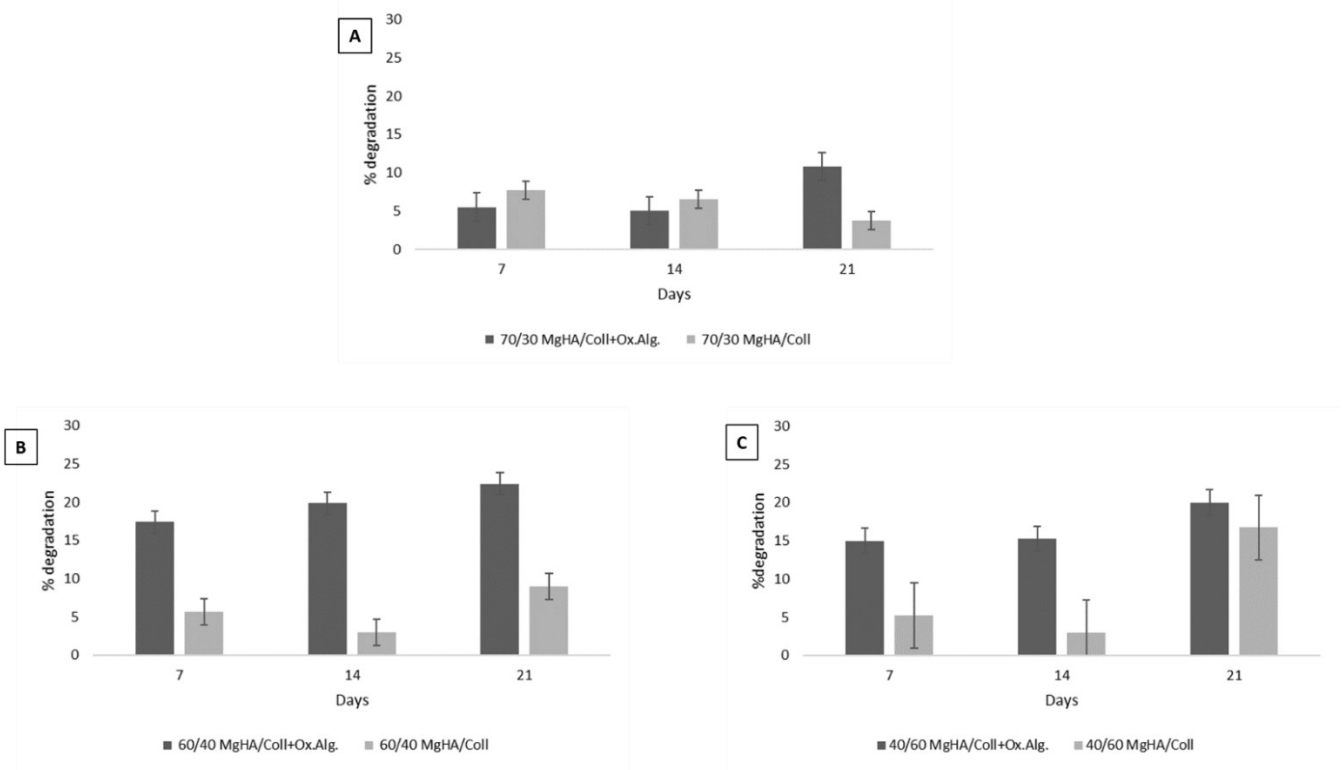

Figure 4.14: Degradation test *carried out in PBS and 37°C. on 70/30 (A), 60/40 (B), 40/60 (C) MgHA/coll compared with each hybrid scaffold link to oxidized alginate*

The major difference was found in 70/30 MgHA / Coll + Ox. Alg., the aldehyde component is completely lost after 7 days, confirming the amount of functionalization correlates with the availability of non-mineralized collagen. The biodegradation of Ox. Alg. increases because the formed aldehyde groups are susceptible to hydrolysis. [21] In fact, the hump of the peak at 500 cm^{-1}, indicating the presence of oxidized alginate, change its morphology in a sharp peak. On the other hand, when the presence of hydroxyapatite decreases, the oxidized alginate remains present after 2 weeks, confirming that its amount correlates with collagen availability. From these and previous FTIR, results we can deduce that oxidized alginate interacts preferentially with collagen, rather than with hydroxyapatite.

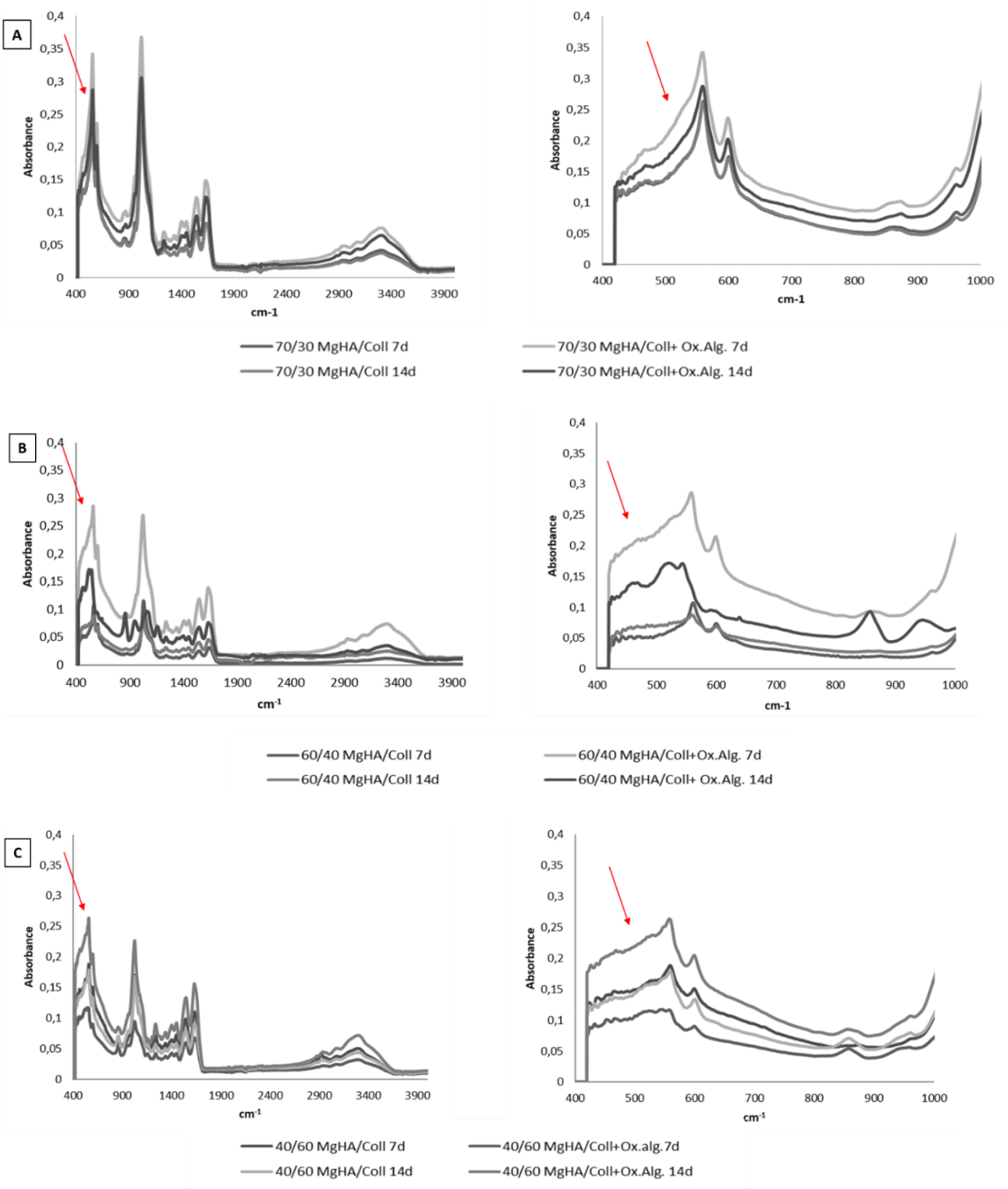

Figure 4.15: *FTIR of functionalized and not functionalized scaffold degraded in 7-14 days. Spectra and particular of Fingerprint that show the peak of oxidized alginate*

The synthesis aqueous phases were analyzed at HPSEC-ELSD in order to estimate the ratio of oxidized alginate not bound. The method helps to calculate indirectly the functionalized percentage in the sample.

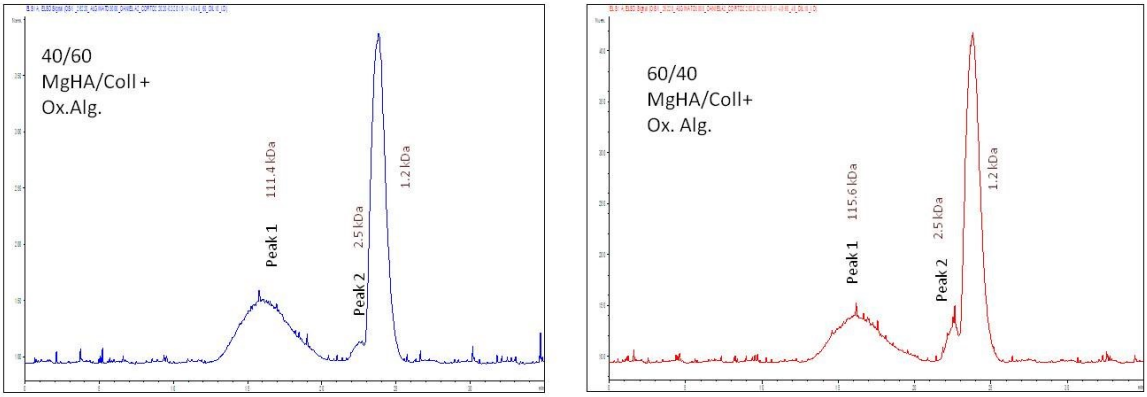

Figure 16: *HPSEC-ELSD spectra of Alginate (A) and Oxidized alginate (B), representative of decrease of Molecular weight in oxidized alginate samples, due to cleavage of carbon bonds*

Therefore, on the basis of the oxidized alginate yield (table 1) and the percentages of unbound oxidized alginate, table 5 shows that the greater presence of the apatite component leads to a lower bond of the oxidized alginate, because the functional groups of the collagen are covered and therefore less available. It can be deduced that 90% of oxidized alginate is bound to Coll+Ox.Alg., 69% to 40/60 MgHA / Coll+Ox.Alg. and 60% to 60/40 MgHA / Coll, confirming the dependent collagen functionality.

	Media Molecular weight kDa		% w/w (g compound / 100 g product)	
	Average	SD	Average	SD
60/40 MgHA/Coll+ Ox. Alg	111.4	7.0	39.8	3.1
40/60 MgHA/Coll+ Ox. Alg.	115.6	14.4	30.9	0.1
Coll+Ox.Alg.	115,9	7,9	8,8	0,1

Table 5:

Molecular weight and ratio of oxidized Alginate present in the synthesis aqueous phase analysed by HPSEC-ELSD: The peak 1 is considered oxidized Alginate and the other two peaks are impurities

4.4 CONCLUSION

The covalently functionalization of the alginate, with the devised method, induces changes in the morphology that are beneficial for its use as a bone scaffold, because increase porosity and water uptake properties, important for cell adhesion, permeation and proliferation to stimulate bone regeneration. The disadvantage encountered is the increase degradation, cause of the easy hydrolysis of oxidized alginate.

To overcome this problem, some crosslinking could be employed, such as heat treatment, which could decrease degradation.

Furthermore, the designed method will allow to be tested also on other sugar polymers, such as hyaluronic acid, so as to be able to implement the characteristic biocompatibility of MgHA / Coll.

This functionalization process will open several avenues for the formation of new reactive site to bind other molecules. The oxidation of alginate is not total and therefore some hydroxyl groups remain usable for a new oxidation, which can create other aldehyde groups. These groups have a well-known reactivity, particularly with amines, functional groups present in many pharmaceutical molecules or growth factors. So, this would allow:

1. To bind covalently drugs and release them in a controlled manner
2. Binding growth factors in order to create tumour niches and facilitate the recreation of tumor surrounding in cell culture.

Therefore, the future optimization of this method could be functional for many areas such as bone regeneration, drug-delivery and the creation of 3D tumor models.

---

(1) Nyga, A., Cheema, U. & Loizidou, M. 3D tumour models: novel in vitro approaches to cancer studies. J. Cell Commun. Signal. **5,** 239 (2011).

(2) Fischbach, C., Chen, R., Matsumoto, T. et al. Engineering tumors with 3D scaffolds. Nat Methods **4,** 855–860 (2007).

(3) Duval K., Grover H., Han L., Mou Y., Pegoraro A.F., Fredberg J., Chen Z., Modeling physiological events in 2D vs. 3D cell culture Phisiology 32, 266-277

(4) Dietmar W. H. Biomaterials offer cancer research the third dimension Nature Materials vol 9 february 2019

(5) Holliday DL, Brouilette KT, Markert A, Gordon LA, Jones JL (2009) Novel multicellular organotypic models of normal and malignant breast: tools for dissecting the role of the microenvironment in breast cancer progression. Breast Cancer Res

(6) Moreau J.E., Anderson K., Mauney R. J., Trang N., Kaplan D.L. and Rosenblatt M., Tissue-Engineered Bone serves as a Target for Metastasis of human breast cancer in a mouse model. Cancer Res 2007;

(7) Tampieri A., Celotti G., Lanedi E., Sandri M., Roveri N., fallini G., Biologically inspired synthesis of bone-like composite: Self-assembled collagen fibers/hydroxyapatite nanocrystals Journal of Biomedical Materials Research part A. 2003 619-625

(8) Tampieri A. Sandri M. Landi E., Pressato D., Francioni S., Quarto R., Martin I. Design Of graded biomimetic ostheocondral composite scaffolds Biomaterilas 29 (2008) 3539-3546

(9) Tampieri A., Landi E., Valentini F., Sandri M., D'Alessandro T., Dediu V., Marcacci M. A conceptually new type of bio-hybrid scaffold for bone regeneration Nanotechnology 22 (2011)

(10) Gopal Shankar Krishnakumar, Natalia Gostynska, Massimiliano Dapporto, Elisabetta Campodoni, Monica Montesi, Silvia Panseri, Anna Tampieri, Elizaveta Kon, Maurilio Marcacci, Simone Sprio, Monica Sandri, Evaluation of different crosslinking agents on hybrid biomimetic collagen-hydroxyapatite composites for regenerative medicine, International Journal of Biological Macromolecules, Volume 106,2018, Pages 739-748

(11) Madaghiele, M, Calò, E, Salvatore, L, Bonfrate, V, Pedone, D, Frigione, M, Sannino, A. 2016. Assessment of collagen crosslinking and denaturation for the design of regenerative scaffolds. J Biomed Mater Res Part A 2016: 104A: 186– 194.

(12) Roman A. Perez, Meeju Kim, Tae-Hyun Kim, Joong-Hyun Kim, Jae Ho Lee, Jeong-Hui Park, Jonathan C. Knowles, and Hae-Won Kim.Tissue Engineering Part A.Jan 2014.103-114.

(13) Jayachandran Venkatesan, Ira Bhatnagar, Panchanathan Manivasagan, Kyong-Hwa Kang, Se-Kwon Kim, Alginate composites for bone tissue engineering: A review, International Journal of Biological Macromolecules, Volume 72, 2015, Pages 269-281.

(14) David L, Dulong V, Le CD, Chauzy C, Norris V, Delpech B, Lamacz M, Vannier JP (2004) Reticulated hyaluronan hydrogels: a model for examining cancer cell invasion in 3D. Matrix Biol 23:183–193

(15) Tatiana Segura, Brian C Anderson, Peter H Chung, Rebecca E Webber, Kenneth R Shull, Lonnie D Shea, Crosslinked hyaluronic acid hydrogels: a strategy to functionalize and pattern, Biomaterials, Volume 26, Issue 4,2005,Pages 359-37,

(16) Palumbo, F.S., Agnello, S., Fiorica, C., Pitarresi, G., Puleio, R., Tamburello, A., Loria, R. and Giammona, G. (2016), Hyaluronic Acid Derivative with Improved Versatility for Processing and Biological Functionalization. Macromol. Biosci., 16: 1485-1496.

(17) Yang H., Lan L., Zhipeng G., Wihua D., Nianhua D, Xixun Y. Modification of collagen with a natural derived cross-linker, alginate dialdehyde Carbohydrate Polymers 1-9 2014

(18) Kuo CK, Ma PX. Maintaining dimensions and mechanical properties of ionically crosslinked alginate hydrogel scaffolds in vitro. J Biomed Mater Res A. 2008 Mar 15;84(4):899-907.

(19) Biji Balakrishnan, Nitin Joshi, Athipettah Jayakrishnan, Rinti Banerjee, Self-crosslinked oxidized alginate/gelatin hydrogel as injectable, adhesive biomimetic scaffolds for cartilage regeneration, Acta Biomaterialia, Volume 10, Issue 8, 2014, Pages 3650-3663.

(20) Zucca, P.; Fernandez-Lafuente, R.; Sanjust, E. Agarose and Its Derivatives as Supports for Enzyme Immobilization. Molecules **2016**, 21, 1577.

(21) Ji-Sheng Yang, Ying-Jian Xie, Wen He, Research progress on chemical modification of alginate: A review, Carbohydrate Polymers, Volume 84, Issue 1, 2011, Pages 33-39,

(22) Tanyarut Boontheekul, Hyun-Joon Kong, David J. Mooney, Controlling alginate gel degradation utilizing partial oxidation and bimodal molecular weight distribution, Biomaterials, Volume 26, Issue 15, 2005, Pages 2455-2465,

(23) Tavano O.L., Fernandez-LaFuente R., Goulart J.A., Mont R. Optimization of the immobilization of sweet potato amylase using glutharaldehyde- agarose support. Characterization of the immobilized enzyme. Process Biochemistry 48,7, 2013 pg 1054-1058

(24) Guadalupe Penzol, Pilar Armisén, Roberto Fernández-Lafuente, Lorenzo Rodés, José M. Guisán Use of dextrans as long and hydrophilic spacer arms to improve the performance of immobilized proteins acting on macromolecules Volume60, Issue4 2000 Pages 518-523

(25) Wang, Q., He, W., Huang, J., Liu, S., Wu, G., Teng, W., Wang, Q. and Dong, Y. (2011), Synthesis of Water Soluble, Biodegradable, and Electroactive Polysaccharide Crosslinker with Aldehyde and Carboxylic Groups for Biomedical Applications. Macromol. Biosci., 11: 362-372.

(26) Jejurikar, Aparna, et al. "Degradable alginate hydrogels crosslinked by the macromolecular crosslinker alginate dialdehyde." Journal of Materials Chemistry 22.19 (2012): 9751-9758.

(27) C.G. Gomez, M. Rinaudo, M.A. Villar, Oxidation of sodium alginate and characterization of the oxidized derivatives, Carbohydrate Polymers, Volume 67, Issue 3, 2007, Pages 296-304,

(28) Jianyun Wang, Weili Fu, Dongming Zhang, Xixun Yu, Jian Li, Changxiu Wan, Evaluation of novel alginate dialdehyde cross-linked chitosan/calcium

polyphosphate composite scaffolds for meniscus tissue engineering, Carbohydrate Polymers, Volume 79, Issue 3,2010, Pages 705-710,

(29) E. Boanini, K. Rubini, S. Panzavolta, A. Bigi, Chemico-physical characterization of gelatin films modified with oxidized alginate, Acta Biomaterialia, Volume 6, Issue 2, 2010, Pages 383-388,

(30) Kemal Baysal, Ayse Z. Aroguz, Zelal Adiguzel, Bahattin M. Baysal, Chitosan/alginate crosslinked hydrogels: Preparation, characterization and application for cell growth purposes, International Journal of Biological Macromolecules, Volume 59, 2013, Pages 342-348

(31) Cai, K., Zhang, J., Deng, L., Yang, L., Hu, Y., Chen, C., Xue, L. and Wang, L. (2007), Physical and Biological Properties of a Novel Hydrogel Composite Based on Oxidized Alginate, Gelatin and Tricalcium Phosphate for Bone Tissue Engineering. Adv. Eng. Mater., 9: 1082-1088.

(32) Jose C.S. dos Santos, Nazzoly Rueda, Oveimar Barbosa, Maria del Carmen Millán-Linares, Justo Pedroche, María del Mar Yuste, Luciana R.B. Gonçalves, Roberto Fernandez-Lafuente, Bovine trypsin immobilization on agarose activated with divinylsulfone: Improved activity and stability via multipoint covalent attachment, Journal of Molecular Catalysis B: Enzymatic, Volume 117, 2015, Pages 38-44

Conclusion and future perspectives

MgHA/Coll is a hybrid material formed by collagen and hydroxyapatite nanoparticles doped with Magnesium which present excellent properties such as high biomimicry, high biocompatibility, osteoinductivity, and bioresorbability. These scaffolds, used as bone substitute, have the ability to regenerate bone tissue thanks to their porosity and their chemical physical characteristics. However, bone infections are very common pathologies and their systemic treatment involves in side effects.

The challenge of my PhD is to develop antibiotic-loaded scaffolds through soaking method, to be reproducible even in the surgery room. Thanks to the interaction between the drug and the ceramic component (MgHA) of the scaffold, the release is partially controlled, highlighted when it's increased the amount of Hydroxyapatite.

It was demonstrated from the microbiological tests, the loaded antibiotics are effective against the bacteria, involved in infections. Therefore, at the same time, the biomaterials, implemented with antibiotics, presents regenerative and antibacterial features. Furthermore, as preliminary data in my PhD thesis demonstrated, the release profile could be improved studying the possibility to load drug into micro- and nano-beads encapsulated into the scaffold implementing the antibacterial efficacy to prevent osteomyelitis infection.

In my PhD work, also an antitumor drug was loaded into the scaffold to create a local therapy that could reduce chemotherapy and radiotherapy administration. After surgery, the biomaterial loaded with anticancer drugs could restore the bone tissue and eliminate the cancer cells that may have remained after the tumour removal. These studies allowed to demonstrate also that loading protocol developed

can be transversal for different drugs and hybrid devices in order to provide an adequate local therapy in many diseases.

Finally, the last part of my PhD thesis was focused on the implementation of the biomimetic properties of hybrid scaffold (MgHA/Coll), through covalent functionalization with alginate, composed of oxidation and reduction steps. Oxidation with periodate is typical of sugar groups and allows the formation of highly reactive aldehyde groups towards the amino groups present in collagen. Then, through a reduction reaction the bond between the sugar polymer and MgHA/Coll Scaffold was stabilized

Alginate was chosen because is the analogue of the hyaluronic acid, a polymer present in bone tissue and highly present in the malignant tumours. The development of this protocol opens the way to the creation of 3D tumour models, that mimics the *in vivo* environment. Scaffolds developed in this PhD research and functionalized not only with Alginate, but also with several sugar polymers, implemented with bioactive molecules and growth factors, could form tumour niches, in which cancer cells are able to grow.

In conclusion, my PhD activity has widely demonstrated the excellence of the hybrid material MgHA/Coll developed through a biomineralization process that confers high biomimicry, biocompatibility and osteoinductivity making it very similar to natural bone tissue. In spite of several studies already present about this material in the last decade, it is a material still under study since new functionalizations and interactions with other bioactive molecules can pave new ways in the field of the regenerative medicine thanks to its multifunctionality.